Terms and Conditions of Use of Digitised Theses from Trinity College Library Dublin

Copyright statement

All material supplied by Trinity College Library is protected by copyright (under the Copyright and Related Rights Act, 2000 as amended) and other relevant Intellectual Property Rights. By accessing and using a Digitised Thesis from Trinity College Library you acknowledge that all Intellectual Property Rights in any Works supplied are the sole and exclusive property of the copyright and/or other IPR holder. Specific copyright holders may not be explicitly identified. Use of materials from other sources within a thesis should not be construed as a claim over them.

A non-exclusive, non-transferable licence is hereby granted to those using or reproducing, in whole or in part, the material for valid purposes, providing the copyright owners are acknowledged using the normal conventions. Where specific permission to use material is required, this is identified and such permission must be sought from the copyright holder or agency cited.

Liability statement

By using a Digitised Thesis, I accept that Trinity College Dublin bears no legal responsibility for the accuracy, legality or comprehensiveness of materials contained within the thesis, and that Trinity College Dublin accepts no liability for indirect, consequential, or incidental, damages or losses arising from use of the thesis for whatever reason. Information located in a thesis may be subject to specific use constraints, details of which may not be explicitly described. It is the responsibility of potential and actual users to be aware of such constraints and to abide by them. By making use of material from a digitised thesis, you accept these copyright and disclaimer provisions. Where it is brought to the attention of Trinity College Library that there may be a breach of copyright or other restraint, it is the policy to withdraw or take down access to a thesis while the issue is being resolved.

Access Agreement

By using a Digitised Thesis from Trinity College Library you are bound by the following Terms & Conditions. Please read them carefully.

I have read and I understand the following statement: All material supplied via a Digitised Thesis from Trinity College Library is protected by copyright and other intellectual property rights, and duplication or sale of all or part of any of a thesis is not permitted, except that material may be duplicated by you for your research use or for educational purposes in electronic or print form providing the copyright owners are acknowledged using the normal conventions. You must obtain permission for any other use. Electronic or print copies may not be offered, whether for sale or otherwise to anyone. This copy has been supplied on the understanding that it is copyright material and that no quotation from the thesis may be published without proper acknowledgement.

Failure of cemented hip implants under complex loading: experimental and numerical analysis

John Robert Britton, B.E. (N.U.I.)

A thesis submitted to the University of Dublin in partial fulfilment of the requirements for the degree of

Doctor in Philosophy

Department of Mechanical Engineering

Trinity College

Ireland

March, 2004

Prof. P.J. Prendergast

Supervisor

Prof. J.F. Orr

External examiner

(The Queen's University of Belfast)

Mr. C.G. Lyons

Internal examiner

In memory of my father, Henry

Declaration

I declare that I am the sole author of this thesis and that all the work presented in it, unless otherwise referenced, is my own. I also declare that this work has not been submitted, in whole or in part, to any other university or college for any degree or other qualification.

I authorise the library of the University of Dublin to lend this thesis upon request.

John Britton

June 9, 2004

Acknowledgements

It is traditional to start by acknowledging the guidance and support of one's supervisor. In my case, it is very appropriate that Prof. Paddy Prendergast is the first to be acknowledged, as without him persuading me to return to college from industry, and providing the opportunity to read for a research degree, there would be no acknowledgements. So, Paddy, heartfelt thanks for the challenges, frustrations, and occasional moments of success. I look forward to continuing to work with you.

The importance of a friendly, dedicated, and inquisitive research group can not be overstated. To my fellow bio-engineering researchers and friends, I say thank you. It is always dangerous to name people for fear of offending those you inadvertently omit, but here goes anyhow: Suzanne, Damien, Alex, Bruce, Linda, Adriele, Seosamh, Danny, Triona, Laoise, John G., John V., Paul, Conor, Kevin, Matteo, Laura, James, and the two honorary bio-engineers, Mary and Richard. I hope in time to develop firm friendships with the 'baby bio-s', consisting of Louise, Niamh, Mary, and Melanie, and trust that they will enjoy themselves as much as I have done. Thanks to Peter P. for his help with several of the figures in this thesis.

Several individuals within the Department of Mechanical Engineering provided much appreciated assistance during the course of my work. Thanks to James for helping with the design of the experimental rig, Gabriel for fabricating the rig and helping with the test setups, Peter for explaining the intricacies of the antique Instron to me, and Paul for dealing with my strain-gauging needs, and helping with the temperature and voltage measurements. Thanks to John Gaynor for his I.T. help. A particular debt of gratitude is owed to Mr. Garrett Lyons, Senior Lecturer, for debating with me the potential sources of error in migration measurement and, for providing direction in determining the effect of those errors.

An especially enjoyable part of this thesis was the opportunity to collaborate with researchers throughout Europe. To the Berlin and Bologna groups, thanks for the stimulating debate. To Jan, Nico, and Rik, thanks, not only for the inquisitions, but for your help and providing the chance to sample a vast range of beers in Nijmegen.

Mere words are insufficient to express properly my thanks to my family. To my parents, Mary and Henry, what can I say, but thanks for everything. To my wife, Amanda, many thanks for your support and encouragement during the past 4 and a half years, and for your forbearance with my distraction during the last few months.

I acknowledge the funding of the European Commission under contract SMT4-CT96-2076 (PreClinTest project), and the funding of Enterprise Ireland under contract ATRP/02/411 (Patient Specific Prosthesis Analysis) project as part of the National Development Plan.

Publications and presentations resulting from this study

Papers

1. Britton, J.R., Walsh, L.A., Prendergast, P.J. Mechanical simulation of muscle loading on the proximal femur: Analysis of cemented femoral component migration with and without muscle loading, *Clinical Biomechanics*, 2003. 18:637-646

2. Britton, J.R., Prendergast, P.J. Migration measurement as a basis for a pre-clinical test of cemented hip implants: an investigation of four prostheses under simulated muscle loading, 2004. Submitted for publication.

3. Britton, J.R., Lyons, C.G., Prendergast, P.J. Measurement of the relative motion between an implant and bone under cyclic loading, *Strain*, 2004. Submitted for publication.

4. Verdonschot, N., Bergmann, G., Britton, J.R., Cristofolini, L., Deuretzbacher, H., Duda, G.N., Heller, M., Lennon, A.B., Maher, S.A., Malchau, H., Morlock, M., Murphy, B.P., Stolk, J., Waide, V., Prendergast, P.J., Huiskes, R. A European proposal for pre-clinical testing methods of cemented femoral hip prosthesis implants, *Journal of Arthroplasty*, 2004. Submitted for publication.

Presentations

1. Britton, J.R., Prendergast, P.J., Egan, J.P. Design of a system for application of muscle loading to an implanted femur in a preclinical test. In Prendergast, P.J., Lee, T.C., and Carr, A.J., eds., *Proc. 12th Conf. of the European Society of Biomechanics*, Dublin, Ireland, p.131, 2000

2. Britton, J.R., Maher, S.A., Lyons, C.G., Egan, J.P., Prendergast, P.J. Relative motion of hip prostheses and bone under simulated physiological loading conditions. In FitzPatrick, D.P., and Carr, A.J., eds., *Proc. 7th Annual Conf. Section of Bioengineering*, Royal Academy of Medicine in Ireland, Arklow, Ireland, p.9, 2001

3. Britton, J.R., Maher, S.A., Prendergast, P.J. Design of a system for applying complex muscle loading during dynamic experimental testing of implanted femurs, *Proc. American Society of Mechanical Engineers Summer Bioengineering Meeting*, Salt Lake City, USA, Vol. 50, pp. 907-908, 2001

4. Britton, J.R., Maher, S.A., Prendergast, P.J. Development of a pre-clinical test for cemented femoral hip implants, *Proc. of the joint meeting of the British Orthopaedic Research Society and the Northern Ireland Biomedical Engineering Society*, Belfast, Northern Ireland. Published in *Journal of Bone and Joint Surgery*, Vol.83B, Suppl. III, p.350, 2001

5. Britton, J.R., Walsh, L.A., Prendergast, P.J. Different migration rates and inducible displacements quantified for four cemented hip prosthesis designs in an in vitro test. In FitzPatrick, D.P., McCormack, B.A.O., and Dickson, G.R., eds., *Proc. Bioengineering in Ireland (8)*, Royal Academy of Medicine in Ireland and the 16th Meeting of the Northern Ireland Biomedical Engineering Society, Sligo, Ireland, p.80, 2002

6. Britton, J.R., Walsh, L.A., Prendergast, P.J. In vitro measurement of migration and inducible displacement of four cemented hip femoral components - results include cyclic muscle forces. In Bedzinski, R., Pezowicz, C., and Sci-

gala, K., eds., *Proc. 13th Conf. European Society of Biomechanics, Acta Bioengineering and Biomechanics*, Wrocław, Poland, p.290, Vol.4(Suppl.1), 2003

7. Britton, J.R., Walsh, L.A., Prendergast, P.J. In vitro measurement of migration and inducible displacement of four cemented femoral component designs in long term cyclic tests, *Proc. 13th Annual Meeting European Orthopaedic Research Society*, Helsinki, Finland, p.26, 2003

8. Britton, J.R, and Prendergast, P.J., Detection of differences in migration between cemented femoral component designs under long term cyclic loading in vitro, *50th Annual Meeting of the Orthopaedic Research Society*, San Francisco, USA, p.98, 2004.

Contents

Abstract

A new generation of experimental pre-clinical testing methods for cemented hip replacement femoral components have been proposed, and preliminarily validated by comparing a 'good' prosthesis design with a 'bad' prosthesis design. The basis for these new tests is the measurement of relative motion between implant and bone over time while loading is applied. However, it is yet to be proven whether these next generation tests can satisfactorily distinguish between the performance of several prosthesis designs. Additionally, opinions vary widely as to the necessary loading conditions required, particularly over whether or not muscle loading should be simulated.

A novel experimental rig which mimicked physiological loading of the implanted proximal femur was developed. Using this rig, the influence of simulated muscle loading on the migration of a femoral component was investigated. Numerical simulations were performed to ascertain possible reasons for differences between migration patterns. Experimental tests consisting of one million loading cycles with muscle loading were performed using four different prosthesis designs; the Charnley Extra Small, the Exeter Polished, the Lubinus SPII, and the Müller Curved.

Muscle loading was found to reduce the migration of the femoral component within the medullary canal of the femur. Differences in migration and inducible displacement (recoverable cyclic motion) were detected between the four prosthesis designs, although not at a significant level. A performance ranking of the designs based on migration did not agree with observed clinical performance as measured by revision rate. However, ranking the prostheses based on whether their inducible displacements were increasing or decreasing did correlate with their clinical revision rates.

In conclusion, the experimental test can distinguish between the performance of several prosthesis designs. However, the sample size required to achieve statistical significance is prohibitive. Muscle loading should be included in experimental tests.

List of Figures

List of Tables

Nomenclature

a, horizontal distance from line of action of F_R to centre of pin joint

b, horizontal distance from line of action of F_V to centre of pin joint

c, vertical distance from line of action of F_R to centre of pin joint

d, horizontal distance from line of action of F_C to centre of femoral component head

e, horizontal distance from line of action of F_L to centre of femoral component head, unknown

f, vertical distance from line of action of F_C and F_L to centre of femoral component head

F_C, force required to statically balance F_V and F_R, unknown magnitude and direction, assumed to act through P

F_H, hip joint reaction force, known magnitude

F_L, required loading force, unknown magnitude, acts vertically downwards due to roller bearing

F_R, force of resolved abductor and tensor fasciae latae muscles, known magnitude and direction

F_V, force due to the vastus lateralis, assumed to be acting vertically downward, known magnitude and direction

MMD, migration measurement device

P, probability value

P_f, probability of failure

P_s, probability of survival

Q, femoral component head centre, about which moments are summed for the primary lever, line of action of F_H passes through this point

S, centre of pin joint of secondary lever, about which moments are summed

α, angle of direction of F_C

β, angle of direction of F_R

γ, angle of direction of F_H

Chapter 1

INTRODUCTION

Contents

1.1 Total Hip Replacement

According to the theory of natural selection proposed by Darwin (1859), the human body has evolved through a process of continual adaptation over a period of many millions of years. Each component of the human body is largely optimised in form and function, though the evolutionary process continues unabated with minute changes undetectable in an individual lifetime. As an example, the joints in our body that allow movement, known as diarthrodial joints (Mow et al., 1992), have evolved as a complex structure consisting of hard tissue (bone), soft tissue (cartilage), and fluids. Each constituent part in turn is composed of several other materials. Breakdown of these structures can occur through sudden injury or degenerative diseases, and result in failure of the joint, often manifested as impaired joint mobility and pain.

The hip joint is the largest diarthrodial joint in the body and experiences repetitive loads of high magnitudes from daily activities. As least partially due to the

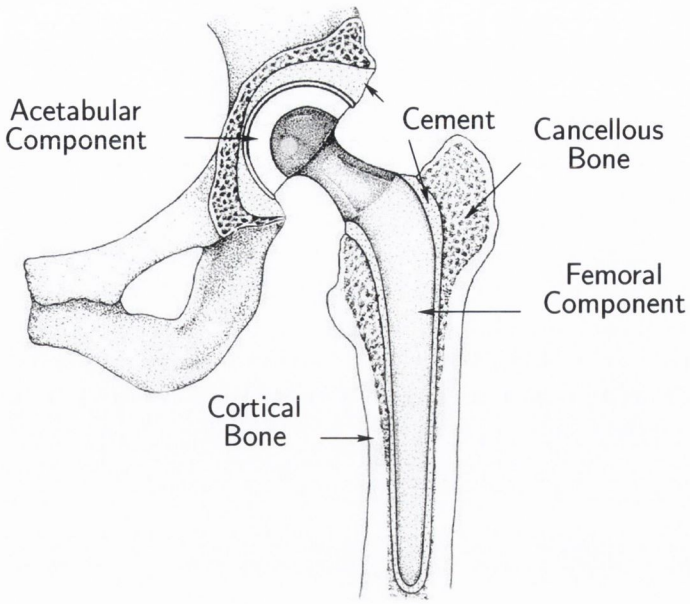

Figure 1.1: Schematic of a cemented total hip replacement. Adapted from Hardinge (1983)

large loads, the hip joint is particularly prone to failure. Any such failure is typically treated through surgical intervention. Generally, the surgical procedure used is the operation commonly referred to as either total hip replacement (THR) or total hip arthroplasty (THA), see Figure 1.1. This operation involves using artificial materials to replace the bearing surfaces of the femur (the femoral component) and pelvis (the acetabular component). An estimated one million hip replacements are carried out worldwide per annum (for example, 289,000 hip replacements were performed in the United States in 1997 (AAOS, 2000)), with demand for the procedure predicted to increase significantly in the developed world over the next 25 years (Ostendorf et al., 2002). The great majority of the operations are very successful with most patients satisfied with the pain reduction and increased mobility achieved (Lieberman et al., 2003).

Some long established and widely used hip replacement prostheses have given survival rates of greater than 90% after ten years (Malchau et al., 2002). However, there have also been widely reported cases where significant numbers of patients had to endure a revision operation within two to three years of the primary operation, e.g. the Müller Curved prosthesis (Sutherland et al., 1982), and more recently, the

Capital hip prosthesis (Massoud et al., 1997; McGrath et al., 2001). Such cases serve to highlight the fact that, although the number of THR prosthesis designs continues to grow, the benefits associated with many of the new designs remain to be proven (Huiskes, 1993; Faulkner et al., 1998).

In recent decades a considerable body of legalisation has been enacted to govern the medical device industry, including the Medical Device Amendment Acts (initially introduced in 1976, and subsequently amended in 1990, 1992, 1997, and 2002) in the United States of America, and the Medical Device Directives from 1993 onwards by the member states of the European Union. While the wording varies between different amendments and directives, the primary purpose of these laws and regulations is to ensure the safety and effectiveness of any device intended for human usage.

One of the methods by which the aforementioned laws attempt to achieve their objective is through testing of the medical devices. The various stages of device testing are summarised in Figure 1.2.

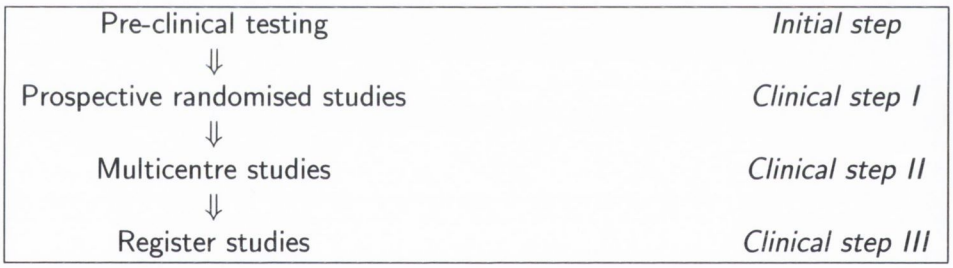

Figure 1.2: Stages of medical device testing. Once the device has performed satisfactorily in the pre-clinical testing stage, it progresses to studies involving increasing numbers of patients in the clinical stages. Adapted from Malchau et al. (1995).

Of particular interest for this thesis is the pre-clinical stage, which can consist of laboratory bench tests, numerical analysis, and animal experiments (Faro and Husikes, 1992; Prendergast and Maher, 2001). The purpose of pre-clinical testing is to (Prendergast, 2001a,b):

- ensure the bio-functionality of the new device,
- prove the mechanical strength of new designs,

- eliminate inferior designs prior to clinical trials,
- demonstrate the superiority of new designs over existing devices.

Animal experiments are frequently criticised as being unrealistic because of the differences between human and animal anatomies, and are regarded as ethically unacceptable by many. The development of a laboratory bench test, or numerical simulation, or indeed some combination of both which proves effective in attaining the pre-clinical testing objectives listed above, would result in a reduction in the number of animal experiments performed. However noble this outcome would be, it is more important that patients are not exposed to novel prosthesis designs which subsequently prove to have a sub-standard performance.

1.2 Aims of thesis

Can an *in vitro* experimental test be devised which can differentiate the performances of several hip replacement prostheses? Recent research suggests that the answer might be in the affirmative; that it is possible to develop an experimental test which can discriminate the performances of different cemented hip femoral components. The initial steps towards such a pre-clinical test were the subject of a previous Ph.D. thesis of the University of Dublin (Maher, 2000). Both Maher and Prendergast (2002) and Cristofolini et al. (2003) demonstrated that laboratory tests, based on measures which are observed clinically to predict the failure of a hip replacement, could distinguish between a 'good' prosthesis design (one which has a low revision rate) and a 'poor' prosthesis design (a design which has a high revision rate). However it was not established whether or not these tests could discriminate between several prosthesis designs, in particular if the implants had similar clinical performances or widely differing design objectives.

An issue of much contention in pre-clinical experimental testing of hip prostheses is whether or not the forces which result from muscle action *in vivo* should be simulated *in vitro*. Some authors contend that it is necessary to simulate all the muscle forces acting on the femur to achieve realistic loading conditions (Polgar

et al., 2003). Other authors, while supporting the above assertion in principle, recognise that achieving it is not always practicable, and recommend the application of a small subset of the active muscles in experimental tests (Duda et al., 1997; Kassi et al., 2002). Yet more authors find that the application of a single muscle force is sufficient (Stolk et al., 2001). However, the most commonly reported experimental set-up applies no muscle forces but only the hip joint contact force (Cristofolini, 1997).

Hence, in this thesis the following questions are asked:

(i) is simulated muscle loading required for experimental comparative tests of prosthesis designs, and

(ii) can an experimental test be devised which can adequately distinguish between the performances of four cemented hip replacement femoral component designs?

Chapter 2

LITERATURE REVIEW

Contents

2.1 The implanted hip

2.1.1 Historical development

Although operations to increase motion in diseased and injured hips were occurring as early as the 1820s the operation remained unsatisfactory until 1923 when Smith-Peterson introduced cup arthroplasty (Fielding and Stillwell, 1987), a procedure in which a cup was used to replace the damaged surface of the femoral head, see Figure 2.1. Much of the focus of improvement efforts in the following years was on appropriate choice of materials for the components used during the procedure. In 1961 Charnley, after a series of animal experiments investigating joint lubrication, introduced the idea of low-friction arthroplasty which consisted of a small prosthesis stem head articulating in a thick-walled polytetrafluoroethylene (PTFE) socket (Charnley, 1961). It was found that the PTFE wore too rapidly and it was replaced by polyethylene (PE). This design has been refined over time but the fundamental principle of operation remains the same.

Figure 2.1: Radiograph of a Smith-Peterson cup arthroplasty. Adapted from Fielding and Stillwell (1987)

2.1.2 Types of hip implants

Two distinct types of hip implants are in common usage today; cemented hip implants and cementless hip implants. These are differentiated by their fixation method: (i) cemented, which consists of a layer of polymethylmethacrylate (PMMA), commonly known as bone cement, imposed between the prosthesis and the bone as a mechanical grout (see Figure 1.1) first introduced by Charnley, and (ii) cementless, which rely on a press-fit of the prosthesis to the bone for fixation. Cementless designs are usually used in younger patients with the assumption that these prostheses will simplify a later revision operation (Huiskes and Verdonschot, 1997). Combinations of the two types are also used, i.e. a cemented acetabular component may be used with an uncemented femoral component or vice versa.

In the last decade, partially cemented femoral components have greatly increased their surgical usage (582 implanted in Sweden during the period 1979 and 1989, 5,905 implanted between 1990 and 2000 (Malchau et al., 2002)). This design attempts to combine the initial stability of a cemented femoral component with osseointegration by encouraging bony ingrowth on the uncemented portion of the stem surface (Baleani et al., 2000). The design has at least partially succeeded in its objective, with several studies demonstrating initial stability comparable to fully cemented implants (Baleani et al., 2000; Claes et al., 2000).

However, cemented hip implants remain the most widely used type of implants (Lucht, 2000; Puolakka et al., 2001; Malchau et al., 2002). They are commonly implanted into elderly patients (mean age in Sweden of 70 years (Malchau et al., 2000)) with the expectation that the lifetime of the prosthesis will exceed the remaining life expectancy of the patient. Huiskes et al. (1998) sub-divided cemented femoral components into two categories:

(i) shape closed designs, which are designed to provide immediate stability of the femoral component through geometrically matching the stem with the femur. Typical features include a collar and a matte surface finish.

(ii) force closed designs, which obtain their stability by migration within the femur until force equilibrium is achieved. Such designs usually have no collar and

have a highly polished surface finish.

2.2 The mechanical environment of the implanted hip

2.2.1 Loading of the hip joint

Rydell (1966) was the first to directly measure the forces acting on implanted hips in a living person through use of a strain-gauged prosthesis. He found that for normal walking (normal defined as the patient's natural gait pattern and speed) two force peaks were experienced by the hip joint, with the peak force magnitudes equal to approximately twice the person's body weight. English and Kilvington (1979) implanted a prosthesis containing a single axis load cell into one patient, and made telemetric measurements during gait after 42 days of post-operative recovery. They found a peak load during gait of approximately three times bodyweight. Davy et al. (1988) also implanted a telemeterised prosthesis into a patient, and measured an average peak load of 2.6 times bodyweight during gait. They also noted that the resultant joint force had a relatively small range of motion during gait, and was bounded by a cone angle between 30° and 35° off the stem neck axis, and by a polar angle of between 15° and 25° anterior to the sagittal plane of the prosthesis, as shown in Figure 2.2. Subsequent work by Bergmann et al. (1993) and Taylor et al. (1997), again for normal gait, confirmed the presence of two force peaks, but in both cases the force magnitude was approximately thrice body weight. Both these studies used telemeterised prostheses. Further research by Bergmann et al. (2001) investigating the hip joint loading during typical daily activities revised the peak hip joint force magnitude during gait downwards to approximately 2.3 times bodyweight, as shown in Figure 2.3. Similarly to Davy et al. (1988), Bergmann et al. (2001) also determined that the hip joint resultant force acted anteriorly and superiorly on the femoral component head within a small range.

Other daily activities which load the hip joint were also examined. Rydell (1966) studied the force generated while standing on one leg (up to 2.8 times bodyweight),

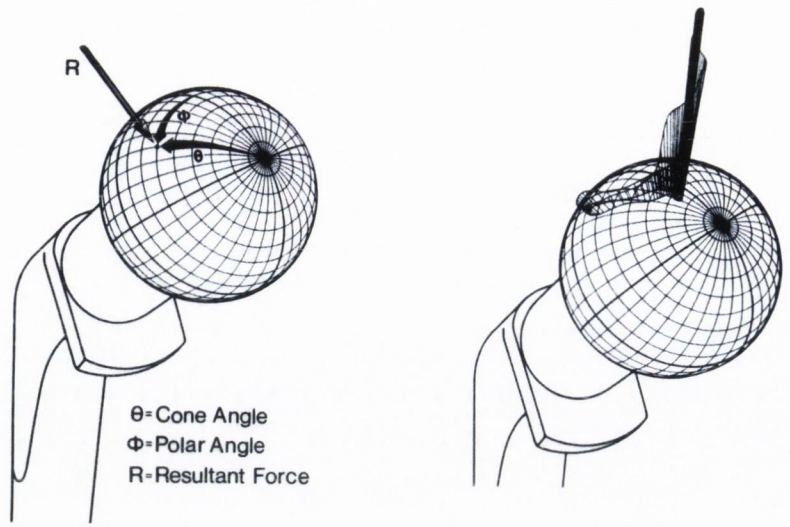

(a) (b)

Figure 2.2: Plot of (a) force-orientation angles used to describe motion of hip joint resultant force, and (b) three-dimensional plot of hip joint resultant force during gait. The lengths of the lines indicate the magnitude of the force. Adapted from Davy et al. (1988).

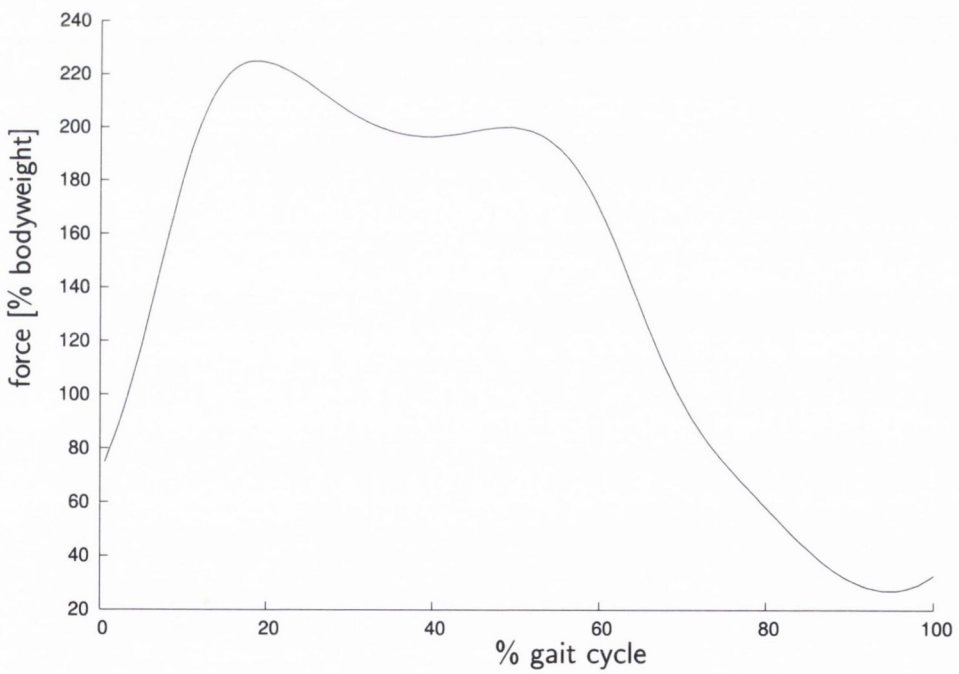

Figure 2.3: Plot of the hip joint contact force during a complete gait cycle (from heel-strike to heel-strike). The double peak nature of the curve is visible. Adapted from Bergmann (2001).

walking upstairs (up to 3.5 times bodyweight), walking downstairs (approximately 2.5 times bodyweight), and running (approximately four times bodyweight). Davy et al. (1988) found a force of 1.5 times bodyweight was generated when their patient was getting into and out of bed. In a series of papers, Bergmann et al. (1993, 1995, 2001) examined the loading applied to the hip from other activities such as running (up to 5.2 times bodyweight), stair climbing (approximately 3.5 times bodyweight), and stumbling. They found that stumbling generated the largest forces (nine times bodyweight) and moments (16 times bodyweight metres). However stair climbing produce torsional moments almost as high as those produced by stumbling on a more regular basis. Bergmann et al. (2001) found that on average the torsion experienced by the implant during stair climbing is 23% greater than that of normal walking.

2.2.2 Muscle loading of the proximal femur

The effect of muscle forces on the skeleton has been investigated since Borelli (1680) determined that the lever arms available to muscle forces are often considerably smaller than those of the applied external loads, and hence, the muscles must exert substantial forces on the skeleton. A large number of muscles act on the femur, some of which are shown in Figure 2.4.

The functions of the femoral muscles shown in Figure 2.4 are summarised in Table 2.1. It is apparent that the muscles have specialised functions, sometimes shared with other muscles, and are not necessarily used during every activity which loads the femur. It is common practise to group muscles together by their primary function, e.g. the gluteus maximus, gluteus medius, and gluteus minimus are often collectively referred to as the abductors.

Pauwels (1965), in his now classic work, proposed that muscles act to reduce the bending moments and hence reduce the stresses experienced by the long bones. He confirmed his hypothesis with photoelastic analysis using a series of ingenious two dimensional models representing the lower limb. Further *in vivo* confirmation of Pauwels hypothesis can be found in Lu et al. (1997) who used implanted instrumented proximal femoral prostheses to show that muscles act to safeguard bones

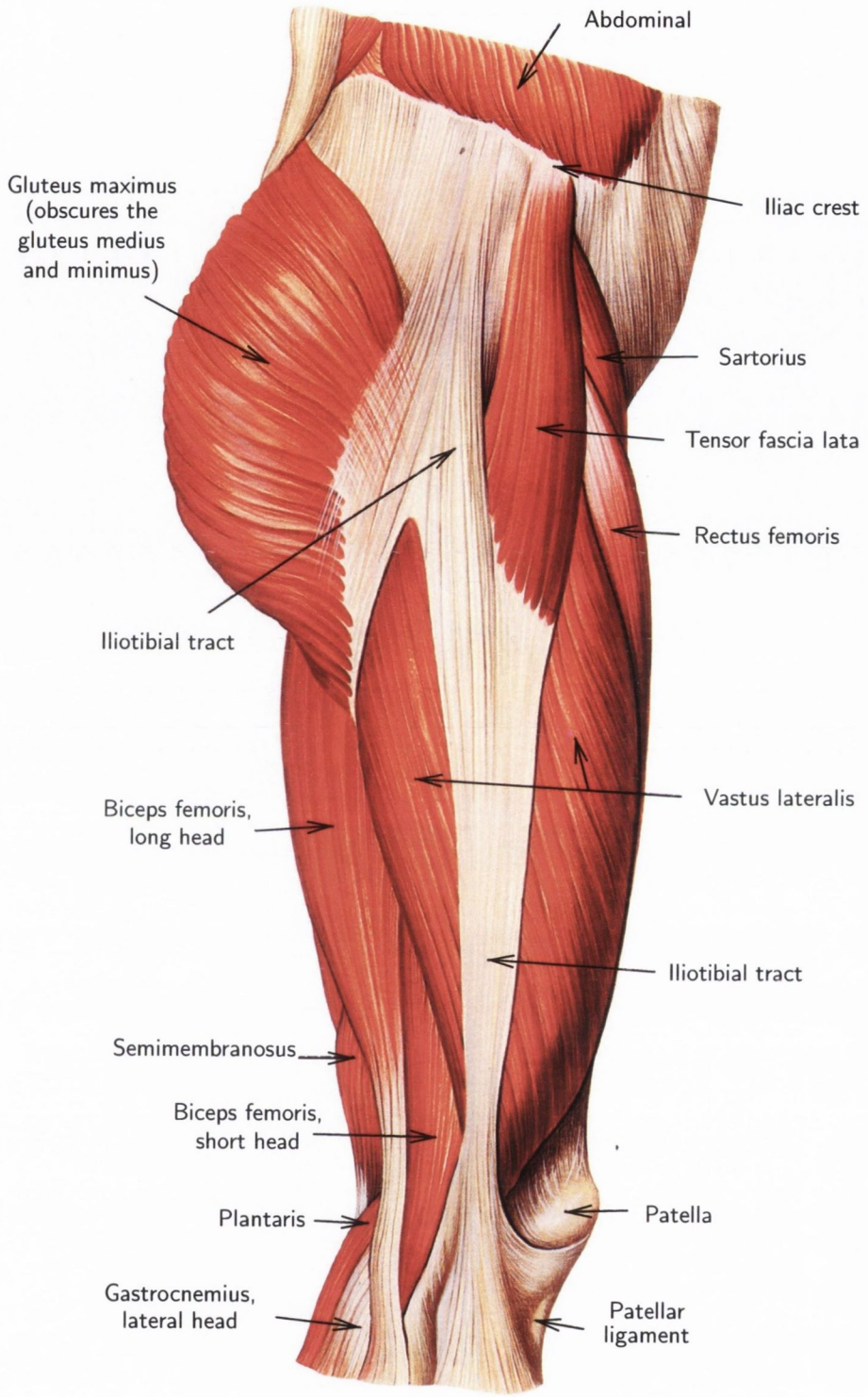

Figure 2.4: Lateral view of the superficial layer of the right gluteal and thigh muscles. Adapted from Sobotta (1988)

Table 2.1: Muscles of the femur and their primary functions. Adapted from Sobotta (1988)

Muscle	Function
Sartorius	flexes, laterally rotates, and abducts the thigh at the knee joint
Rectus femoris	extends the leg at the knee joint
Vastus medialis	extends the leg at the knee joint
Vastus lateralis	extends the leg at the knee joint
Vastus intermedius	extends the leg at the knee joint
Iliacus	flexion and lateral rotation of the thigh
Psoas	flexion and lateral rotation of the thigh
Pectineus	adducts, rotates, and flexes the thigh at the hip joint
Adductor longus	adducts and flexes the thigh
Adductor brevis	adducts and flexes the thigh
Adductor magmus	powerful adduction of the thigh
Gracilis	adducts the thigh
Obturator externus	rotates the thigh laterally
Gluteus maximus	abducts, extends, and laterally rotates the thigh
Gluteus medius	abducts and medially rotates the thigh
Gluteus minimus	abducts and medially rotates the thigh
Tensor fascia lata	flexes and abducts the thigh
Piriformis	laterally rotates the extended thigh
Obturator internus	rotates the extended thigh laterally
Gemellus	rotates the extended thigh laterally
Quadratus femoris	rotates the thigh laterally
Biceps femoris	flexes the leg at the knee joint
Semitendinosus	flexes the leg at the knee joint
Semimembranosus	flexes the leg at the knee joint

from excessive bending moments. They concluded that experimental studies investigating loads in bone should appropriately mimic muscle forces. Cristofolini et al. (1995) examined the effects of ten muscles on the axial strains of the proximal femur. They discovered that including the three glutei muscles (the abductors) along with the hip joint reaction force gave similar strain in the bone compared to a model which included all ten muscles. Additionally they found that combining the abductors with the hip joint contact force into a single resultant force applied to the head of the femur did not adequately simulate physiological strain patterns. In a comprehensive examination of the literature Cristofolini (1997) concluded that it was necessary to apply the same bending moments to the test femur as the intact femur in order to produce similar loading, and devised an experimental device which tried to achieve this (Cristofolini et al., 1997), see Figure 2.5.

Duda et al. (1997), using a mathematical model of the lower limb with free body analysis, also found that muscles act to reduce bending moments in the femur and create a state of axial compression in the diaphysis of the femur. With regard to the proximal femur, they determined that inclusion of the abductors and vastii in their model gave results within 10% of their physiological loadcase which included 24 muscle forces. Duda et al. (1998) also investigated the influence of muscles on the strain distribution within the femur. They found that inclusion of the adductors, the abductors, the iliotibial tract, and the hip joint contact force in a finite element model of the femur gave peak surface strains within 5% of a finite element model including all the thigh muscles. Stolk et al. (2001) found that inclusion of the abductor muscles reduced the peak tensile cement stress in cemented hip replacements. They concluded that simulating the abductor forces as well as the hip joint reaction force can reasonably simulate the stress/strain distributions in cemented reconstructions. The additional inclusion of the adductors, the vastii, and the iliotibial tract had only a small effect. This view is apparently contradicted by Szivek et al. (2000) who found, using an experimental model of an intact composite femur, that including the abductors, the vastus lateralis and the iliotibial band reduced the peak strains across the bone transverse section compared with a model which only

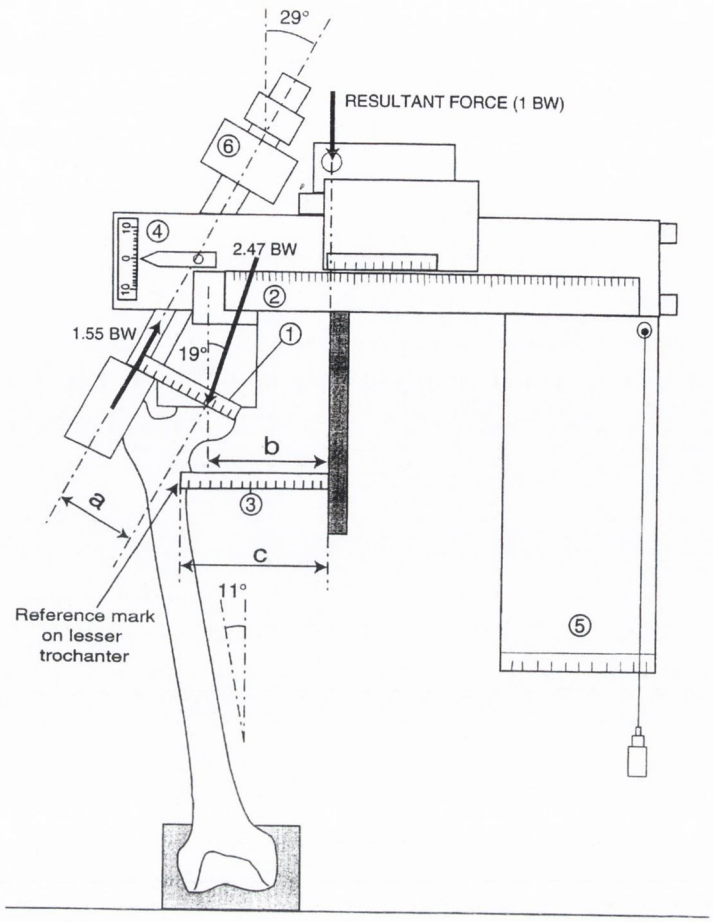

Figure 2.5: Schematic of the device used by Cristofolini et al. (1997) to apply the hip joint and abducting force to a femur. The numbers indicate: rulers to measure distance between head centre and abducting force (1), head centre and resultant force (2), reference point on the diaphysis and resultant force (3); goniometers to measure angle of abducting force (4) and check horizontality of device (5); the load cell measuring the magnitude of the abducting force (6). Distances a, b, and c were measured for every test.

included the abductors. However there is considerable experimental scatter in their results. Polgar et al. (2003) using finite element analysis found that reducing the number of muscles included in a model of the femur resulted in unrealistic femoral head displacements and strain magnitudes which exceeded those measured in vivo.

The determination of the magnitude of muscle forces during typical activities has proven to be a complex problem requiring the selection of various optimisation criteria for an inverse dynamic solution (An et al., 1997). Electromyography can provide indirect estimates of muscle force; however, it is unable to determine

the contraction strength of individual muscles and it is difficult to obtain readings from a moving subject (Whittle, 2001). *In vivo* measurement of the muscle forces is presently impossible using non-invasive means and ethical barriers to invasive measurement techniques exist. However mathematical modelling combined with gait analysis has provided quantitative information on the magnitudes and directions of muscle forces. One such study is that of Heller et al. (2001) who calculated the muscle forces which contribute to loading of the hip joint during walking and stair climbing. On the companion cd-rom (Bergmann, 2001) to their publication, they presented the magnitude and direction of action of 25 muscle forces active during the various stages of a gait cycle. The peak muscle force (due to the abductors) was approximately one times body weight and occurred at the first hip joint reaction force peak, see Table 2.2.

Table 2.2: Magnitude of muscle forces acting on femur at instant of the first peak of the hip joint force. Adapted from Bergmann (2001).

Muscle	Force magnitude [times bodyweight]
Abductors	1.05
Biceps femoris long head	0.04
Semimembranosus	0.60
Tensor fascia lata	0.19
Vastus lateralis	0.95

2.2.3 Activity levels of total hip replacement patients

One million gait cycles per leg per year appears to be a commonly accepted figure in the literature (Huiskes and Verdonschot, 1997). This figure was reinforced by Zahiri et al. (1998) who surveyed 100 hip replacement patients and found a mean of approximately one million walking cycles. However Schmalzried et al. (1998) found a range from 144,175 to 6,467,070 steps per year in their study, but again the average figure was close to one million. More recently, Morlock et al. (2001), using a custom designed portable monitoring system, investigated the daily activities of 42 hip replacement patients. They found that patients typically spent most of their

time awake sitting (44.3%), followed by standing (24.5%), then walking (10.2%), lying (5.8%), and finally stair climbing (0.4%). The median daily ratio of gait cycles to stair climbing steps was 6048:227, which extrapolates to a yearly total of approximately 2.2 million gait cycles (1.1 million per leg) and 80,000 stair steps (40,000 per leg).

2.3 Failure scenarios of total hip replacements

Failure of a hip replacement ultimately results in a revision operation. Malchau et al. (2002) analysed the details of 14,081 revision operations contained in the Swedish Hip Register between 1979 and 2000 to determine the reasons for revision operations. It is clear from their findings that aseptic loosening is the dominant reason for revision operations, see Table 2.3. Aseptic loosening will be examined in detail later, see Section 2.3.1, but first some of the other causes of failure are briefly described.

Table 2.3: Reasons for initial revision operation taken from the Swedish Hip Register, adapted from Malchau et al. (2002)

Reason	Share [%]
Aseptic loosening	75.4
Primary deep infection	6.7
Dislocation	5.7
Fracture only	5.1
Technical error	3.0
Implant fracture	1.5
Secondary infection	0.9
Polyethylene wear	0.9
Miscellaneous	0.8

Primary deep infection and secondary infection, taken together, constituent 7.6% of revision operations. There are a number of causes of infection (Petty, 1991; Bauer and Schils, 1999) mainly related to the operating theatre environment, with the risk of infection occurring during a revision operation markedly higher (Petty, 1991). Advances in operating theatre technology, such as ultraviolet lighting and 'clean room' environments, combined with the availability of more effective antibiotics

have contributed to lowering the risk of infection.

Fracture of the femur may occur intra-operatively or postoperatively due to the trauma of the operation (Petty, 1991). One possible cause of these fractures is increased hoop stress in the femur due to incorrectly sized press-fitted prostheses. Dislocation refers to dislocation of the femoral component head from the acetabular component socket. Lack of physical coordination (mental impairment, drunkenness, disease) appears to be the primary cause of dislocation.

Implant fracture, once a common cause of failure, is now much reduced, largely due to the adoption of international standards, such as the ISO 7206-3, 'Determination of endurance properties of stemmed femoral components without application of torsion' standard. Technical error in the above table refers, presumably, to surgeon error during the procedure. Whether any of the other reasons for revision originate with the surgeon is unclear. Polyethylene wear (also known as Mode-1 wear (Schmalzried and Callaghan, 1999)) occurs due to friction of the prosthesis head (often metallic) and the polyethylene lined acetabular socket. Excessive wear reduces the stability of the reconstruction. This failure mechanism is sometimes referred to as the *destructive wear* failure scenario (Huiskes, 1993).

2.3.1 Aseptic loosening of cemented implants

Table 2.3 reveals the dominant cause of failure of hip implants as aseptic loosening. Aseptic loosening can be defined as long-term loosening of the prosthesis components unrelated to infection, which occurs gradually (Huiskes and Verdonschot, 1997). Slightly more femoral components (26.6%) than acetabular components (23.8%) were revised because of aseptic loosening according to the Swedish Hip Register, though in the remainder (49.6%) of revision operations both components were replaced (Malchau et al., 2002). An earlier study based on the Norwegian Arthroplasty Register found that 65% of revision operations necessitated by aseptic loosening were due to loosening of the femoral component alone (Espehaug et al., 1995).

Aseptic loosening of an implanted prosthesis is commonly measured using roent-

gen stereophotogrammetric analysis (RSA) (Mjoberg et al., 1986; Kiss et al., 1995; Kärrholm et al., 2000). This technique involves the implantation of radiopaque markers into well-defined positions in the pelvis and proximal femur. Radiographs taken of the pelvic area, with respect to a known reference system, over time allow the migration of the markers to be computed (Kärrholm et al., 2000). It is worth noting that Brand et al. (1986) found that differing definitions of loosening based on radiographic evidence can influence the reported loosening rate by a factor of two.

There are several possible causes of aseptic loosening, with the dominant mechanism still unknown, though mechanical failure of the prosthesis/cement interface is regarded as the most likely initiator of aseptic loosening (Jasty et al., 1991; Harris, 1992), with the other causes secondary to and, in cases, induced by the mechanical failure. Indeed, it is possible that the various causes may act in concert with one another (Humphreys et al., 1991). The possible causes are outlined below:

(i) Wear particles generated by relative motion between two contacting surfaces of the THR reconstruction, particularly debris due to friction between the femoral component head and acetabular socket, cause an inflammatory response which results in bone resorption (Harris, 1994; Huiskes and Verdonschot, 1997; Bauer and Schils, 1999; Schmalzried and Callaghan, 1999). This is referred to as the *particulate reaction* failure scenario (Huiskes, 1993), see Figure 2.6.

(ii) Trauma during the surgical procedure interface can cause bone death. This trauma may result from rasping of the medullary canal, cell-toxic effects of residual monomer in the cement, or from thermal injury during polymerisation of the cement (Mjoberg et al., 1986).

(iii) Implantation of a femoral component alters the stress distributions in the femur (Huiskes, 1990; Hua and Walker, 1995). The femur reacts to this altered distribution by depositing bone in areas of high stress, and resorbing bone in under-stressed locations. This adaptive bone remodelling can lead to aseptic loosening through removal of bone stock, see Figure 2.7. Huiskes (1993) identifies this phenomenon as the *stress shielding* failure scenario.

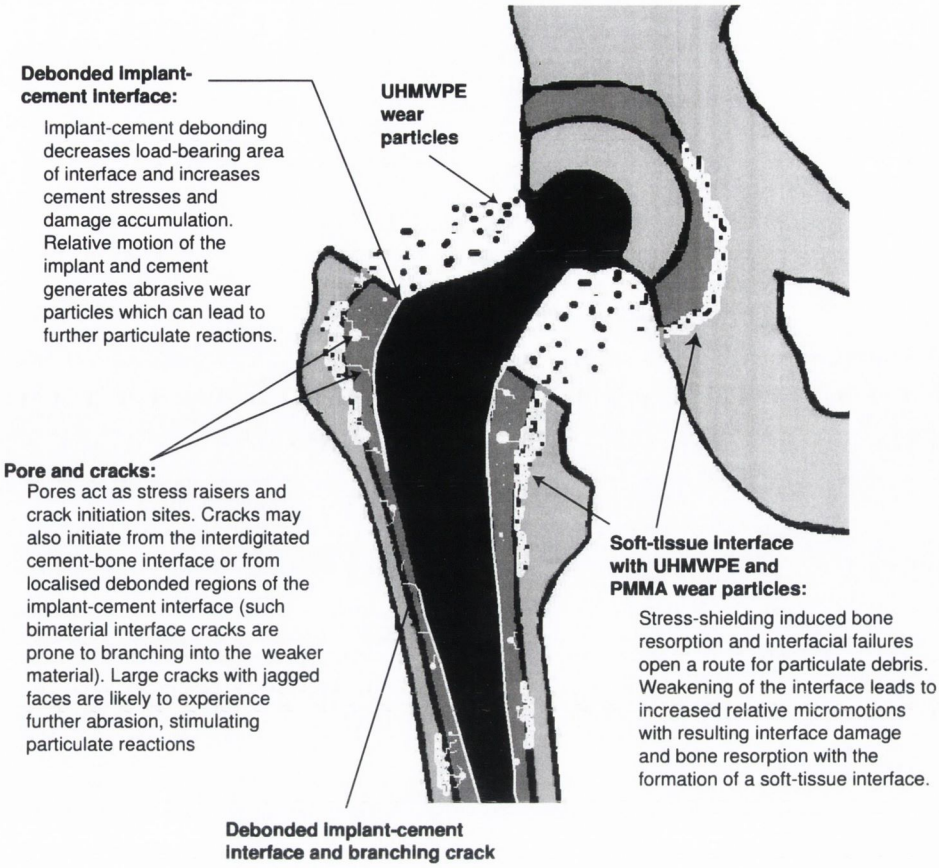

Figure 2.6: Illustration of causes of and interaction of the particulate reaction and damage accumulation failure scenarios. After Lennon (2002).

(iv) The *stress bypassing* failure scenario occurs when proximal load transfer is bypassed and load is preferentially transferred distally (Huiskes, 1993). It can result from localised osseointegration, which induces bone resorption in some locations and bone deposition in other locations (Bauer and Schils, 1999).

(v) The repeated mechanical loading experienced by the THR reconstruction may result in fatigue failure of the prosthesis/cement interface in a process commonly referred to as the *damage accumulation* failure scenario (Huiskes, 1993), see Figure 2.6. Maloney et al. (1989) examined cross-sections of retrieved implanted femora under a scanning electron microscope and saw cement fractures in the cement mantle. Tide marks were observed around voids from which some of the fractures originated. Jasty et al. (1991) examined 16 post-mortem retrieved implanted femora to determine the loosening mechanisms

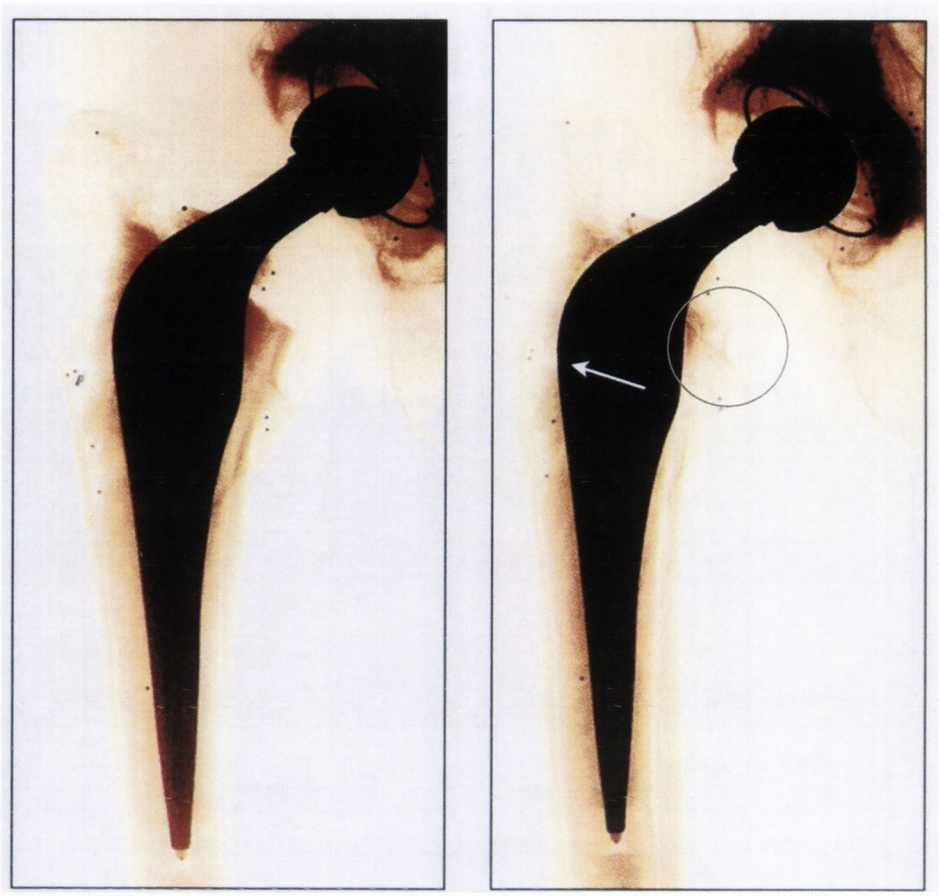

(a) (b)

Figure 2.7: Radiographs of implanted SHP prosthesis (a) immediately post-operative, and (b) after five years. Some bone resorption has occurred proximally medially (grey circle) and a cement fracture is visible (white arrow). Adapted from Kärrholm et al. (2000).

(duration of implantation ranged from two weeks to 17 years). They found that the initial loosening step was debonding of the stem/cement interface, followed by fracture growth in the cement mantle, and concluded that the primary aseptic loosening mechanism was mechanical in nature. Additionally they postulated that cracks in the cement mantle allowed PMMA particles to cause the localised osteolysis observed in several of the retrieved femora. Further support is provided by Verdonschot and Huiskes (1997) who modelled the debonding process of a cemented femoral component using finite element analysis. They found that debonding proceeds slowly and creates localised stress peaks at the edges of debonded regions which could initiate fracture of

the cement mantle. However, Humphreys et al. (1991) conducted cyclic *in vitro* tests of implanted cemented femoral components for five million cycles and concluded that loosening does not occur solely as a result of fatigue failure of the cement mantle. They suggested that a combination of biological and mechanical factors initiate loosening.

(vi) Implant micromotion as a direct result of inadequate initial fixation (the *failed bonding* failure scenario, (Huiskes, 1993)) can cause resorption of adjacent bone (Bauer and Schils, 1999). Micromotion can also result in the formation of a soft tissue layer at the bone/cement interface (Huiskes, 1993; Boss et al., 1994), which can thicken and eventually result in aseptic loosening. High fluid pressures in the soft tissue layer surrounding an implanted femur have been proven to result in bone resorption in animal models (Asperberg and der Vis, 1998a,b). (Formation of the soft tissue layer may also result from an inflammatory response to wear debris).

Clinical indicators of aseptic loosening include thick radiolucent lines at the prosthesis/cement or cement/bone interfaces (Gruen et al., 1979; Strömberg et al., 1996), and excessive migration of the prosthesis relative to the bone. Rapid early migration of the femoral component has been positively correlated with aseptic loosening (Pellicci et al., 1979; Chafetz et al., 1985; Kobayashi and Terayama, 1992; Freeman and Plante-Bordeneuve, 1994; Kärrholm et al., 1994; Berry et al., 1998; Alfaro-Adrian et al., 2001). In a study of Lubinus SP femoral components, Kärrholm et al. (1994) examined several factors, such as patient age, weight, type of operation, and concluded that subsidence (distal migration) of the prosthesis was the best predictor of need for a revision operation due to aseptic loosening. However, Alfaro-Adrian et al. (2001) examined Charnley Elite and Exeter femoral components in a radiostereometric study and concluded that internal rotation of the femoral components associated with posterior head migration was more deleterious than distal migration.

2.4 Pre-clinical testing of cemented femoral components

The current standard tests for pre-clinical testing of cemented femoral components, e.g. the ISO 7206 series first established in 1985, were developed to ensure that the femoral component would have sufficient fatigue strength to protect against stem fracture *in vivo* (Paul, 1997a). These normative tests have proven very successful, with the Swedish Hip Register reporting that only 1.5% of revision operations are due to implant fracture, see Table 2.3. However, given that the current dominant reason for revision is aseptic loosening (Section 2.3), and that its primary mechanism is most likely mechanical in nature (Section 2.3.1) considerable clinical and economical benefits are possible if a pre-clinical test could be devised which would prove as effective in the reducing the incidence of revision surgery due to aseptic loosening as the ISO 7206 Part 3 test has done for stem fracture.

Prendergast (2001a) provides an algorithm to establish a pre-clinical test, as shown in Figure 2.8. This algorithm provides a logical, sequential approach which, if followed should result in a valid test.

Generic methodology	*application to cemented hip prostheses*
Determine failure scenarios	*mechanical failure of the femoral component/cement interface*
⇓	
Design a method to measure failure	*excessive migration or micromotion*
⇓	
Design a method to apply *in vivo* loading and environmental conditions	*some simplification may be necessary*
⇓	
Protocol for pre-clinical test	*subject to extensive validation*

Figure 2.8: A flowchart outlining the necessary steps in designing an effective pre-clinical test. Adapted from Prendergast (2001a)

2.4.1 Experimental methods

Several studies have attempted to determine the migration and micromotion of femoral components by applying a number of loading cycles. Burke et al. (1991) ex-

amined the initial stability of cemented femoral components for simulated single leg stance (hip joint reaction and abductor forces applied) and simulated stair climbing (hip joint reaction, abductor and extensor forces applied) for a sequence of three repeated measurements. As already mentioned, Humphreys et al. (1991) applied loads of up to 4.1 kN to the head of the implanted prosthesis for five million cycles. Doehring et al. (1999) developed a rig to apply abductor, extensor, and adductor muscle forces, and the hip joint reaction force to uncemented femoral components but the rig was only used to apply quasi-static loading for 75 cycles at 0.05 Hz, see Figure 2.9. Similarly, Kassi et al. (2002) developed an apparatus that applied forces at a frequency of 0.25 Hz for testing the primary stability of uncemented femoral components. Speirs et al. (2000) used a biaxial fatigue testing machine to load the heads of two types of cemented femoral component for 3000 loading cycles. Liu et al. (2003) measured the migration of a cemented femoral component over three million loading cycles, applying the hip joint reaction force only. Race et al. (2003) developed a rig to simulate stair climbing and used it to load implanted cemented femoral components for 300,000 cycles at 2 Hz. The rig applied a moment to the femoral component head which was 'balanced by rods representing the abductors and the hamstrings'.

An experimental apparatus for dynamic testing of femoral components which includes muscle loading for testing a stemless hip prosthesis was presented by Munting and Verhelpen (1993, 1995). This apparatus consists of two actuators and a lever mechanism, as shown in Figure 2.10. It is designed to apply the hip joint contact force and three muscle forces; the abductor, iliotibial band, and vastus lateralis. However an issue of concern with this apparatus is that the lever mechanism may be dynamically indeterminate or over-constrained because two cables were located after the fulcrum to attach the lever to the test specimen making it impossible to resolve individual muscle forces.

Maher (2000) developed a testing method which proved capable of detecting significant differences in the migration patterns of two designs of cemented femoral components (the Lubinus SPII and Müller Curved) during fatigue tests. An inser-

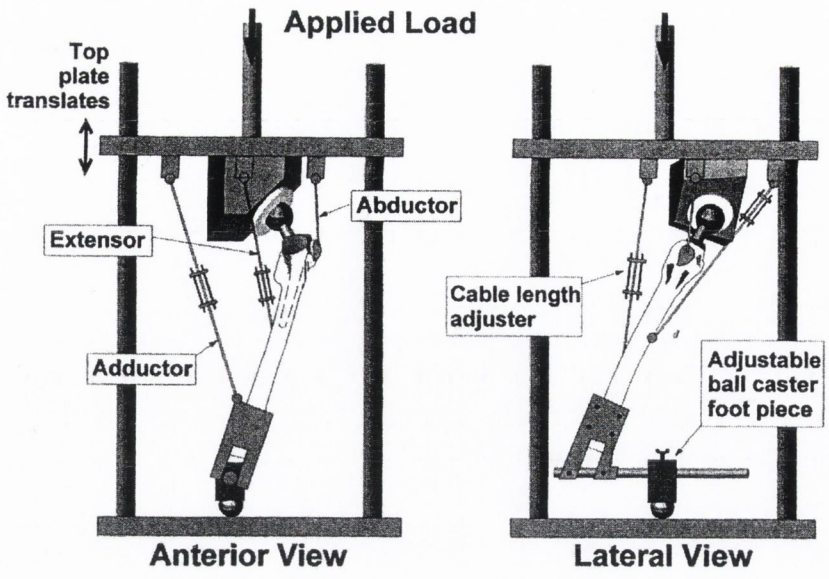

Figure 2.9: Schematic showing two views of the experimental rig that Doehring et al. (1999) used to simulate stair-climbing. Loading is applied to the top plate using a materials testing machine. The position of the femur is maintained solely by the cables representing the muscle groups.

tion machine capable of accurately and reproducibly implanting a prosthesis into a composite femur was designed and fabricated (Maher et al., 2000). A migration measurement device was developed (Maher et al., 2001), of which further details are given in Section 2.4.2 and Section 3.2.6. The experiment setup consisted of applying a cyclic force of peak 2.3 kN to the implanted femur at a frequency of 5 Hz for two million loading cycles, see Figure 2.11. Using this test procedure, significant differences in the migration patterns of two prosthesis designs were detected after one million and two million loading cycles (Maher and Prendergast, 2002). Additionally, the inducible displacement (recoverable deformation during a single loading cycle) was quantified, and correlated to the migration rates of the implants. The implants with decreasing inducible displacement usually had a decreasing migration rate, and vice-versa. However muscle loading was not included in these tests, and only two prosthesis designs with very different clinical performances were tested.

Cristofolini et al. (2003) examined the same two prosthesis designs, applying

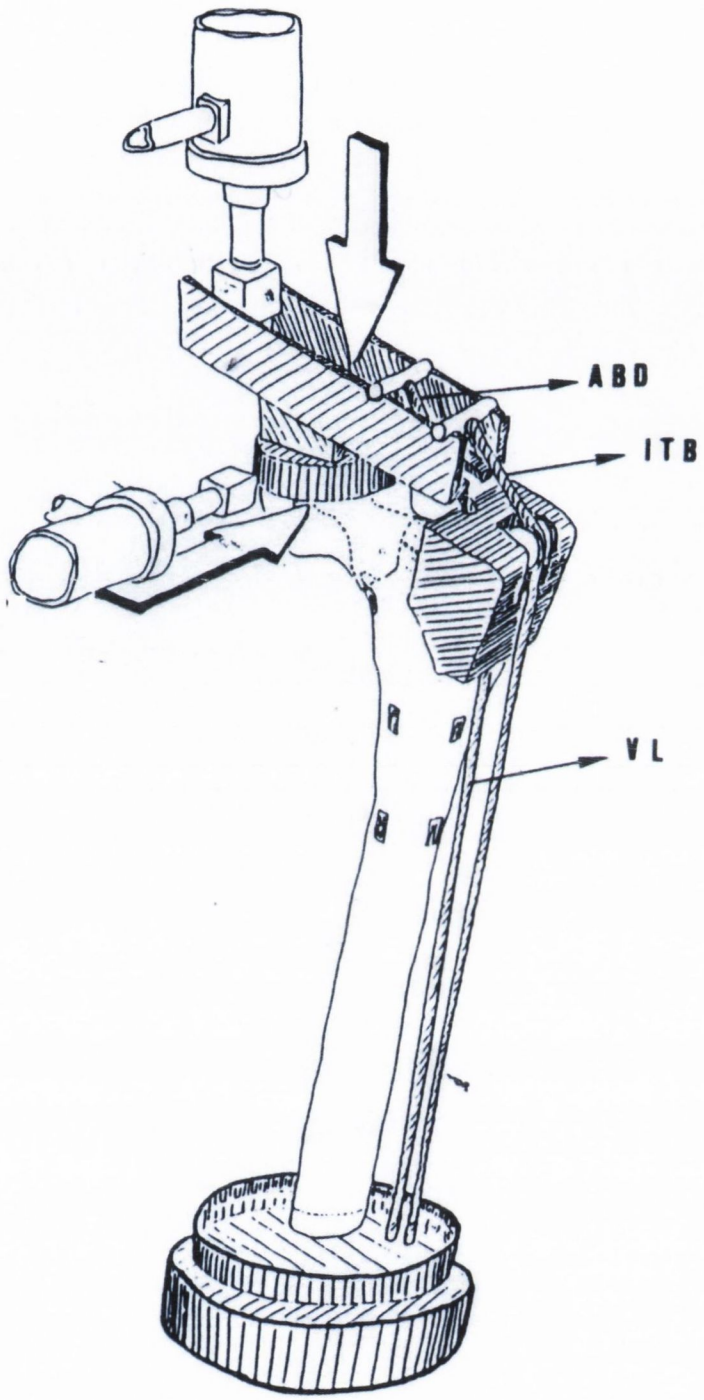

Figure 2.10: View of the walking simulator developed by Munting and Varhelpen. The abductor muscles are represented by cable ABD, the ili-otibial band by cable ITB, and the vastus lateralis by cable VL. Adapted from Munting and Verhelpen (1995).

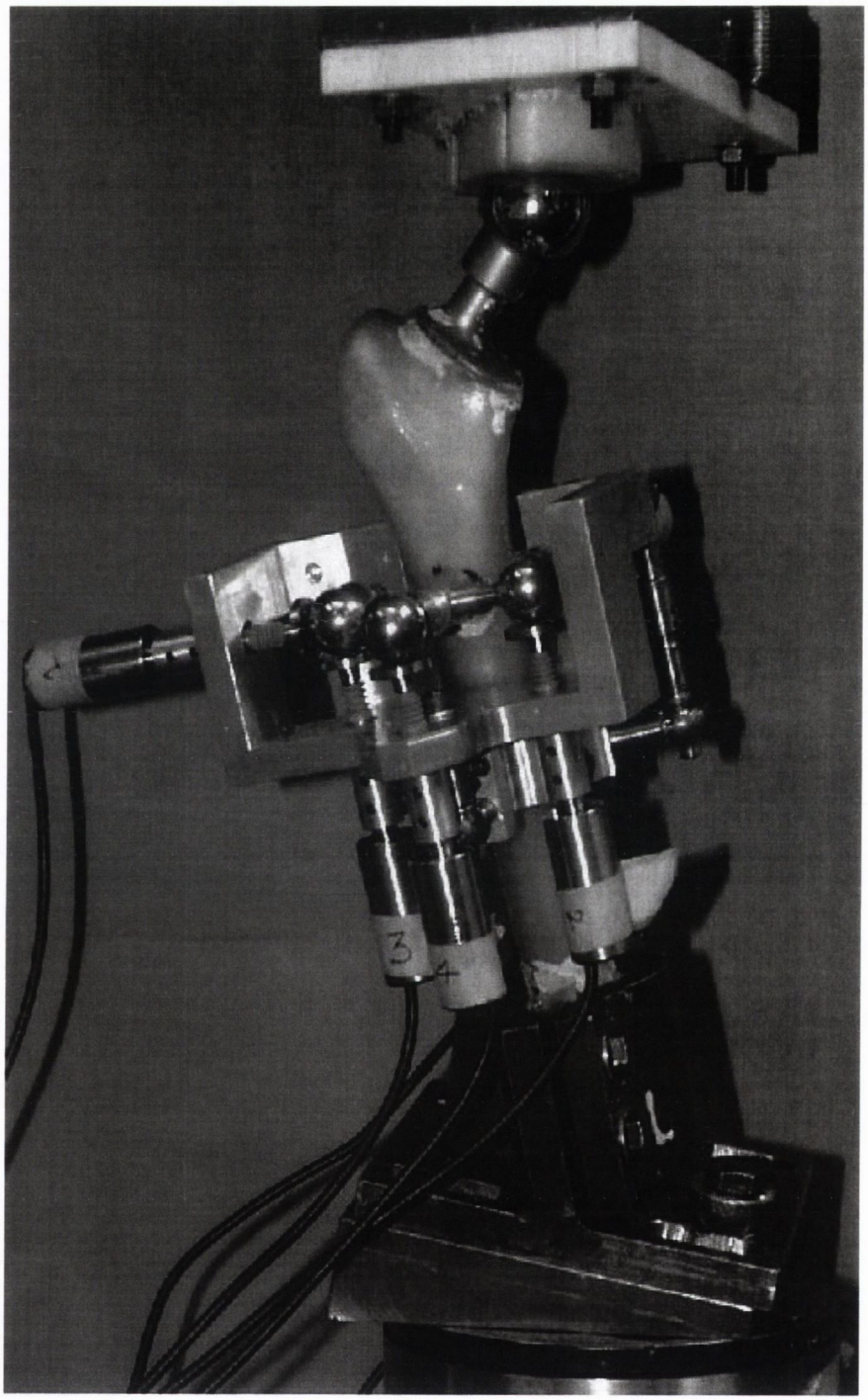

Figure 2.11: View of the experimental setup used by Maher showing an implanted Lubinus SPII prosthesis with the migration measurement device attached. The femur is oriented in 10° adduction and 9° flexion as per the recommendations of ISO 7206 Part 3. Adapted from Maher (2000).

a cyclic load for one million cycles. The load was intended to represent the force and moments generated in the proximal femur during stair-climbing. Similarly to Maher and Prendergast (2002), they found differences in migration and inducible displacement. Additionally, they reported significantly more cracks in the cement mantle of the Müller Curved prostheses compared to the Lubinus SPII prostheses.

2.4.2 Measurement of migration

There are certain obstacles to be overcome in measuring migration. The magnitude of the motion tends to range from tens of microns to a millimetre (Kärrholm et al., 2000), and hence is commonly referred to as micromotion. Both permanent migration and recoverable elastic deformation (inducible displacement) can take place, as shown in Figure 2.12. Long-term tests require measurement over an extended duration, which poses robustness and reliability issues for the measurement technique, and which also must accommodate random fluctuations in environmental conditions while testing. The chosen measurement technique should also be capable of continuous output during the course of the test.

In clinical studies, radiostereometric analysis (RSA) is commonly used to assess the migration of the implant relative to the femur. According to Kärrholm et al. (1997) when used in total hip arthroplasty, RSA has a precision of 0.15 mm in translation and 0.3° in rotation at the 99% significance level. In an *in vitro* study of prosthesis migration Verdonschot et al. (2002) used RSA as the measurement technique with an overall reproducibility error of 40 μm. However, even this error level could potentially confound the outcomes of experimental tests, and additionally, continuous RSA measurements are impracticable in most mechanical testing laboratories.

Several approaches to measuring relative femoral component/bone motion in vitro are found in the literature:

- Charnley and Kettlewell (1965) measured the 'slip' between the distal tip of a femoral component and bone with an one ten-thousandth inch dial gauge mounted on the bone and in indirect contact with the stem by means of a

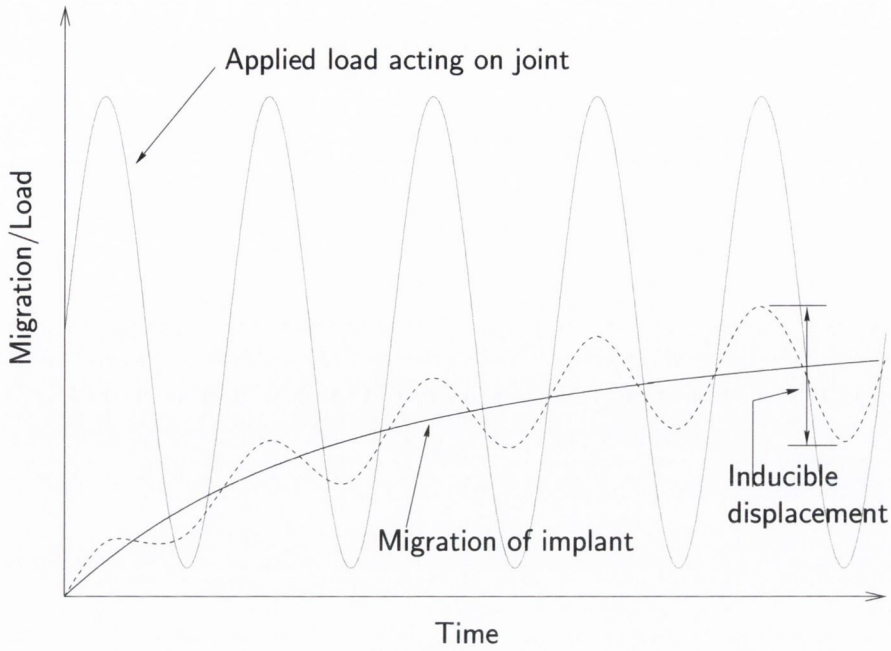

Figure 2.12: Schematic showing development of migration and inducible displacement with respect to time. As loading is applied to the joint (represented by a sinusoidal wave), the position of the implant, relative to a defined reference frame such as anatomical landmarks, changes with time. This permanent change in position is referred to as the "migration" of the implant. However during the course of a single loading cycle the implant can undergo reversible motion which is called inducible displacement.

pivoted lever. Whiteside and Easley (1989) measured relative motion using dial gauges with a sensitivity of 5 μm mounted on the femur. The dial gauge probes touched the implant's surface through holes drilled in the bone. A dial gauge together with a vernier height gauge were used by Humphreys et al. (1991) to measure movement of the femoral component in their study.

- Markolf et al. (1980) used an extensometer to measure the relative motion between implant and bone in two locations, stem tip and stem collar. Similarly, Manley et al. (1987) used an extensometer to measure stem subsidence, based on stem neck displacement relative to the proximal femur. Verdonschot and Huiskes (1998) also measured the motion of geometrically simplified femoral component stems relative to the cement mantle using an extensometer with a resolution of 0.5 μm.

- Walker et al. (1987) press-fitted a rod to the implanted femoral component

through a clearance hole drilled in the bone. Six non-contact eddy current displacement transducers monitored the motion of a steel target fitted to the free end on the rod. It was not possible to determine rotation about the medial-lateral axis with this device.

- Nunn et al. (1989) used a cantilever attached to the bone, with a pointer on the opposite end on the cantilever in contact with the prosthesis surface, to measure displacement under application of a maximum load of 800 N.

- Schneider et al. (1989), in a study examining the initial stability of cementless femoral components, used five transducers and an x-y table to determine the relative motion.

- Burke et al. (1991) used an extensometer, attached to the femoral component by a pin inserted through a clearance hole in the bone, and attached to the bone with a metallic cylinder lining the clearance hole, to alternatively measure axial and transverse motions in simulated single-leg stance. No indication of measurement precision is given. Callaghan et al. (1992) used two extensometers and Engh et al. (1992) used three extensometers in the same fashion as Burke et al. (1991) with a claimed precision of 1 μm.

- McKellop et al. (1991) used a rigid frame attached to the proximal femur. Three strain-gauge displacement transducers, mounted on the rigid frame, were brought into contact with the prosthesis to monitor its motion. The transducers had a precision of $\pm$ 2 μm over a range of 3 mm. Distal and medial displacement together with anterior rotation were recorded.

- Gilbert et al. (1992) measured displacement of the femoral component relative to the femur with seven linear variable differential transducers (LVDTs), four attached superiorly, three attached distally. The LVDTs measured the motion of two aluminium cubes which were rigidly attached to the prosthesis through rods.

- Munting and Verhelpen (1993, 1995) used a pair of LVDTs, with one LVDT

located on either side of the femoral component. The orientation of the LVDTs was altered depending on the measurement being made, with a cited accuracy of $\pm$ 2 μm.

- Berzins et al. (1993) used a cruciform target device consisting of three steel spheres rigidly press-fitted to the lateral aspect of the femoral component. Six LVDTs were in contact with the spheres, orientated to measure all six degrees-of-freedom. This concept was adapted by Maher et al. (2001) for use in long-term tests (two million loading cycles) of cemented femoral components, and subsequently used in comparative tests by Maher and Prendergast (2002), Britton et al. (2003), and Britton and Prendergast (2004). Migration and inducible displacement of the femoral component head centre were reported for the six degrees of freedom. Liu et al. (2003) made a further adaptation of the original concept, and used a target device attached to the implant and a reference frame attached to the femur. Displacement of the target device relative to the reference frame was measured using a depth micrometer with a nominal resolution of 1 μm.

- Hua and Walker (1994) used a total of six LVDTs mounted at three levels. The LVDTs monitored the migration of plastic targets attached to pins inserted through the femoral component during the course of 2500 loading cycles.

- A linear extensometer was used by Harman et al. (1995) to measure the rotational displacement. This was further developed by Monti et al. (1999), Baleani et al. (2000), Viceconti et al. (2001), and Cristofolini et al. (2003) to incorporate four LVDTs to measure shear micromotion at various locations. Monti et al. (1999) provides an overall measurement error of the entire system of 2.3 μm between loading cycles, and 5 μm between different tests.

- Buhler et al. (1997b) developed a novel optoelectronic sensor based on silicon position-sensitive detectors. They used three of these sensors in an *in vitro* test with a claimed precision of approximately 5 μm in a range of 1.5 mm. Further *in vitro* tests using the optoelectronic sensors are described by Buhler

et al. (1997a) and Speirs et al. (2000).

- Bachus et al. (1999) measured relative micromotion with ten differential variable reluctance transducers before and after dynamic testing was performed. Continuous measurement was not possible with their experimental setup.

- In a series of *in vitro* experiments to determine the influence of femoral component and hip centre alterations on micromotion, Doehring et al. (1999) used 12 LVDTs to measure the displacement of six target spheres mounted on two triads inserted proximally and distally respectively into the implant. Each pair of LVDTs mounted on a bracket were calibrated to a resolution of 3 μm over a range of 750 μm.

- Claes et al. (2000) measured relative implant/bone motion with six LVDTs, two mounted proximally, two mounted approximately one-third along the length of the stem, and two mounted distally. The LVDTs' tips were in direct contact with the implant surface. Resolution of the LVDTs used varied from 0.5 μm to 1 μm.

This extensive list of research publications shows for hip prostheses alone, the need to assess the performance of prostheses has led engineers to devise a host of techniques for measuring migration and micromotion relative to the underlying bone. However, issues that have not been fully addressed with such tests are that environmental changes during the course of testing and between tests create errors, and the assumption of rigid body motion of the implant in some techniques makes measurement of inducible displacement, or more importantly its rate of change, rather problematic. These issues will be further addressed in this thesis.

2.5 Summary

Hip replacement operations are successful for the great number of patients in restoring mobility and relieving pain. The majority of the procedures use cemented components. At present, the dominant failure mode of hip replacements is aseptic

loosening. Whilst standard pre-clinical tests have succeeded in their objective of reducing the incidence of stem fracture *in vivo*, they do not test for aseptic loosening. Aseptic loosening of the femoral component is often initiated by mechanical failure of the stem/cement interface, and is clinically correlated with early rapid migration of the femoral component within the femur for several prosthesis designs.

Previous experimental studies have measured the migration of cemented femoral components in vitro. However these studies did not set out to recreate the *in vivo* mechanical loading of the implanted proximal femur or to emulate the typical activity levels of a hip replacement patient. Recent research has shown that it is possible to detect migration differences between two prosthesis designs. An experimental test which could discriminate several different prosthesis designs in accordance with their clinical performances based on migration measurement could provide a basis for a new generation of standardised tests.

Chapter 3

METHODS

Contents

3.1 Introduction

Two investigative techniques were used: i) *in vitro* fatigue testing with cyclic loads, and ii) numerical simulation using the finite element method. The experimental tests constitute the majority of the investigative work, while the finite element (FE) analysis was used to explore possible reasons for the behaviour observed in the experimental tests, i.e. to complement the experimental work. The first hypothesis to be tested was to determine whether or not a loadprofile which included muscle forces was necessary. Two approaches were taken to test this hypothesis; experimental testing was carried out with and without muscle loading, and a FE model of an implanted femur was solved with and without muscle loading. Next the comparative experimental tests of different prosthesis designs were executed. Additionally, the influence of temperature variation on the migration measurement device, and the validity of assuming rigid body motion of the prosthesis were investigated.

3.2 Experimental procedure

This section describes the experimental methods used in this thesis, including the loading applied, the design and validation of the experimental rig, the test methodology, and the measurement technique used.

3.2.1 Details of the test loadprofiles

The muscle loading profile was developed based on the work of Bergmann (2001), which also appeared as Bergmann et al. (2001), and Heller et al. (2001). It consists of three distinct cyclic forces, see Table 3.1, having been deduced from a profile which originally consisted of 25 muscle forces (Bergmann, 2001). This loadprofile is intended to mimic the forces acting on the implanted proximal femur of a fully recovered THR patient weighing 750 N during a gait cycle. It includes the muscle forces which are active at the first hip joint reaction force peak. As the tensor fascia lata and the abductor forces act at the same location (Bergmann, 2001), these forces were combined to generate the applied loading profile. The muscle forces are applied

Table 3.1: Simplified muscloskeletal loadcase used for experimental tests. A protocol was developed to apply the coordinate system developed by Bergmann et al. (1993) to the synthetic composite femora used in this study, to allow accurate location of the muscle attachment locations. See Section 3.2.2

Force	x [N]	y [N]	z [N]	Acts at point (see Figure 3.2)
Hip joint reaction	-405	-246	-1719	femoral component head centre
Resolved abductor and tensor fascia lata	485	114	605	P1 (greater trochanter)
Vastus lateralis	-7	139	-697	P2 (anterior and inferior to greater trochanter)

in phase with the hip joint reaction force. Although the tensor fascia lata does not attach to the femur (Paul, 1997b), it does wrap around the greater trochanter and hence must exert a force on the femur. A second loading profile consisted of the hip joint reaction force *without* any muscle loading. It was used to investigate the influence of muscle loading to determine whether or not muscle loading should be included in the comparative tests.

3.2.2 Method for determining location of muscle insertion points on a composite femur

The loadprofile defined in Table 3.1 is associated with a coordinate system for the femur defined by Bergmann et al. (1993), as shown in Figure 3.1. It was necessary to be able to reproduce this coordinate system to allow accurate location of the muscle forces origin and insertion locations on a composite femur, these points are given as P1, and P2 in Figure 3.2. The protocol developed for determining these locations consisted of two stages; (i) the definition of coordinate axes, and (ii) the determination of the muscles origin and insertion points, as described in Sections 3.2.2.1 and 3.2.2.2 below.

Once the protocol was successfully applied to a composite femur, that particular femur was retained as a 'reference' femur for locating the muscle origin and insertion points on the implanted composite femurs being prepared for experimental testing.

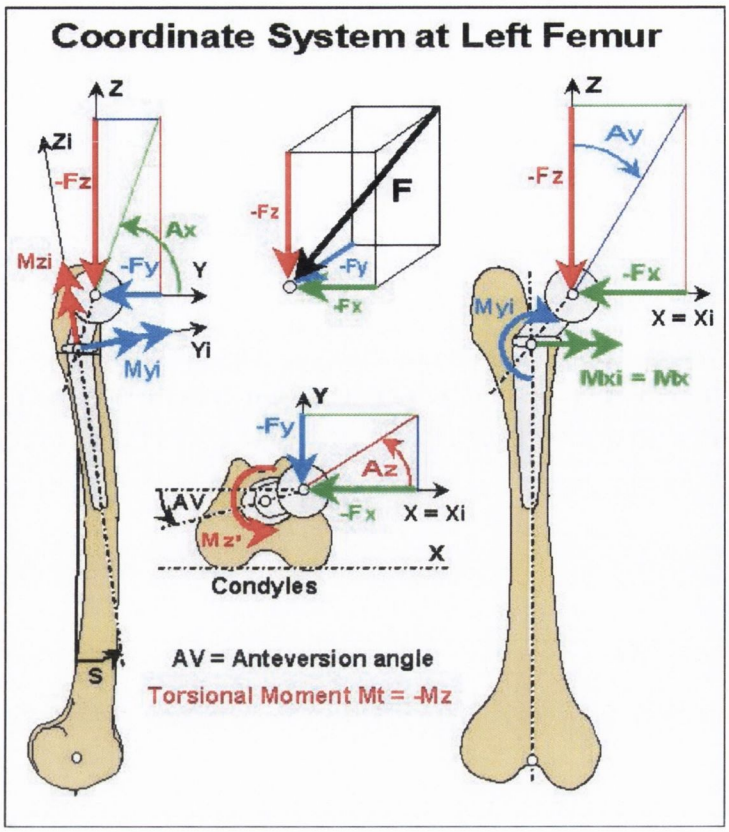

Figure 3.1: Coordinate system used by Bergmann et al. (1993) to describe the forces and moments acting on the left femur. The coordinate system origin is located at the head centre of the implant. The x axis points medially, the y axis points anteriorly, and the z axis is vertical. Adapted from Bergmann (2001).

3.2.2.1 Procedure to define the coordinate axes

1. Taking the composite femur, on the medial surface, mark the point where the curved femoral mid-line crosses the neck axis (call this point RP1, i.e. reference point 1), and mark the point where the curved femoral mid-line intersects the cortical bone of the intercondylar notch (call this point RP2), based on a visual assessment.

2. Approximate the dorsal aspects of the condyles of the femur in a lateral view as semicircles. Mark the centres of these semicircles as RP3 and RP4.

3. Clamp a rigid steel metre rule to an angle block using a G-clamp in a vertical orientation. This will be used as a straight edge. Place the assembly and an universal vice on a machine table or another flat surface.

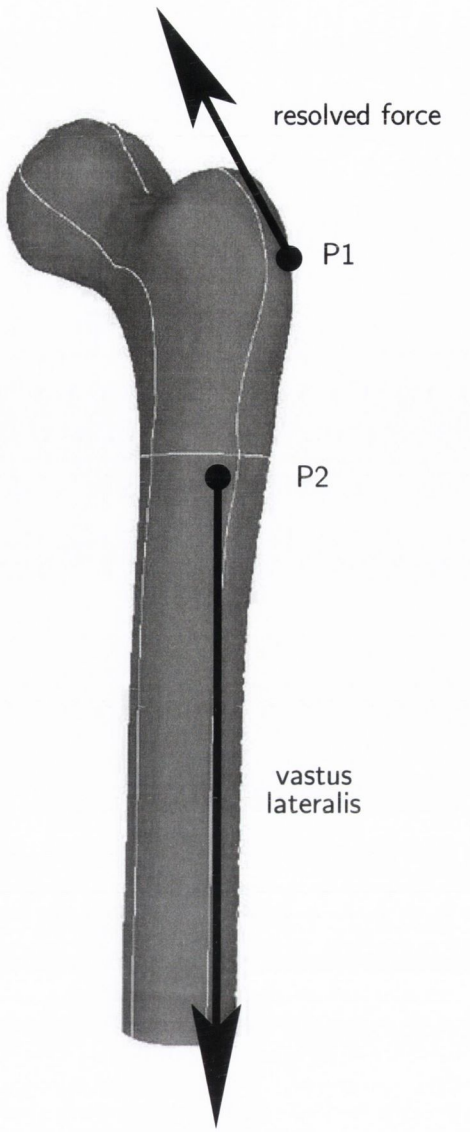

Figure 3.2: Location of muscle insertion locations points as listed in Table 3.1. Adapted from Bergmann (2001).

4. Using the universal vice, grip the condyles of the composite femur. (Firstly ensure that the degree of rotation of each axis of the vice is zero). The vice jaws should be in contact with the anterior and posterior faces of the condyles.

5. Using the straight edge align points RP1 and RP2 vertically. Tighten the vice jaws so that the femur is rigidly held. Re-check the alignment of the reference points. Outline the positions of the vice and angle block, using chalk.

6. Move the straight edge to the anterior face of the femur, align the femoral

long axis vertically (defined as the line connecting the points of inflection of the intercondylar notch and the superior curve between the greater trochanter and the femoral head, RP5 and RP6). Tighten the vice firmly in this position. Outline the position of the angle block.

7. Approximate the femoral head as a sphere, and measure its diameter in each of the superior to inferior (S-I), anterior to posterior (A-P), and medial to lateral (M-L) planes. Half these distances and mark them on the femoral head. This can be achieved by using the right angle square and the metre rule.

8. The point of intersection of the M-L and A-P lines on the superior aspect of the femoral head is now taken to be the exit point of the positive z axis, which will be exactly vertical.

9. Glue a thin straw/stick (e.g. a toothpick) to each of points RP3 and RP4, ensuring that the straw is aligned vertically with the z axis.

10. Rotate the vice on its vertical axis until the two straws are collinear. This is taken to be the direction of the knee axis. Note the angle and direction of rotation from the base of the vice. (Observer should adopt the same position as step 5).

11. Applying Pythagoras' theorem to the S-I plane of the femoral head, calculate the distance of the exit point of the x axis from the point of intersection of the A-P and S-I lines on the medial aspect of the femoral head. The x axis is now defined.

12. The same procedure is then used to define the y axis, ensuring a right hand coordinate system is formed.

3.2.2.2 Procedure to locate the muscles origin and insertion points

1. Align a large retort stand with the x-z plane of the femur, with the femur still located in the universal vice.

2. Grasp the femur securely in the clamp(s) of the retort stand, and then release the femur from the vice.

3. Turn the femur through 90° (i.e. long axis vertical to long axis horizontal), using the angle block.

4. Lower the femur until it is touching a large sheet of graph paper. Align the long axis of the femur with the graph paper and mark its position.

5. Mark the exit points of the x and z axes on the graph paper. Remove the femur and draw the x and z axes on the graph paper. Compensate for orientation of y axis by applying Pythagoras' theorem.

6. Mark the individual muscle insertion points on the graph paper (x, z coordinates) and re-align the femur with the graph paper.

7. The muscle insertion locations can now be marked in on the femur, with the y coordinates being measured vertically from the surface of the graph paper, allowing for the distance from the y axis exit point to the centre of the femoral head.

3.2.3 Design calculations for application of muscle forces

The experimental device was based on two linked levers acting in series, as shown in Figure 3.3. The hydraulic fatigue testing machine applied the required load to the primary lever (F_L in Figure 3.3), and the femoral component head acted as the fulcrum for the primary lever. The design calculations were based on the x-z plane, neglecting out of plane forces as these were generally relatively small, see Table 3.1. The secondary lever distributed the muscle forces F_R and F_V in the appropriate ratios. Referring to Figure 3.4 the known design variables were F_H, F_R, F_C, and β. The unknown design variables were b, e, F_C, F_L, α, and γ. The variables a, c, d, and f were set by the geometric constraints of the experimental device. It was assumed that the pin-joint at S, and the pin-joint on which the rollers were mounted, were frictionless, allowing the equilibrium equations to be written as:

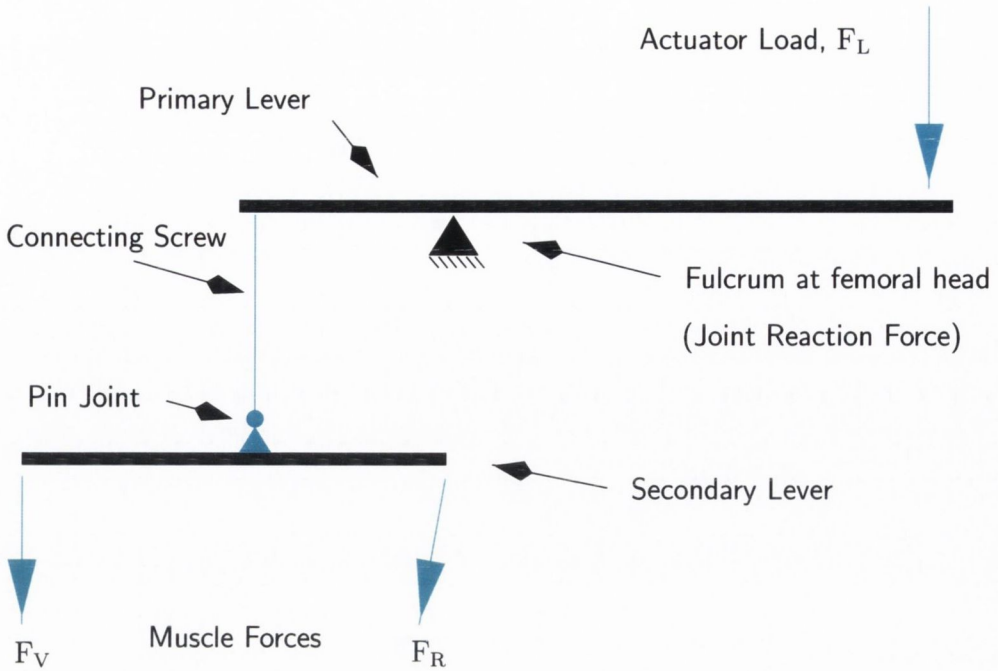

Figure 3.3: Simplified two-dimensional schematic of experimental rig showing basis of operation

For the secondary lever;

$$\sum F_x = 0: \quad \Rightarrow \quad F_C = \frac{F_R \sin\beta}{\sin\alpha} \tag{3.1}$$

$$\sum F_z = 0: \quad \Rightarrow \quad F_C = \frac{F_V + F_R \cos\beta}{\cos\alpha} \tag{3.2}$$

$$\sum M_S = 0: \quad \Rightarrow \quad F_V b = (F_R \sin\beta)c + (F_R \cos\beta)a \tag{3.3}$$

Therefore, from eqns. 3.1, 3.2, and 3.3;

$$\alpha = \arctan\left(\frac{F_R \sin\beta}{F_V + F_R \cos\beta}\right) \tag{3.4}$$

$$b = \frac{(F_R \sin\beta)c + (F_R \cos\beta)a}{F_V} \tag{3.5}$$

F_C can then be solved from either eqn. 3.1 or eqn. 3.2

For the primary lever;

$$\sum F_x = 0: \quad \Rightarrow \quad F_C = \frac{F_H \sin\gamma}{\sin\alpha} \tag{3.6}$$

$$\sum F_z = 0: \quad \Rightarrow \quad F_H = \frac{F_L + F_C \cos\alpha}{\cos\gamma} \tag{3.7}$$

$$\sum M_Q = 0: \quad \Rightarrow \quad F_L e = (F_C \cos\alpha)d + (F_C \sin\alpha)f \tag{3.8}$$

Therefore, from eqns. 3.6, 3.7, and 3.8;

$$\gamma = \arcsin\left(\frac{F_C \sin\alpha}{F_H}\right) \tag{3.9}$$

$$F_L = F_H \cos\gamma - F_C \cos\alpha \tag{3.10}$$

$$e = \frac{(F_C \cos\alpha)d + (F_C \sin\alpha)f}{F_L} \tag{3.11}$$

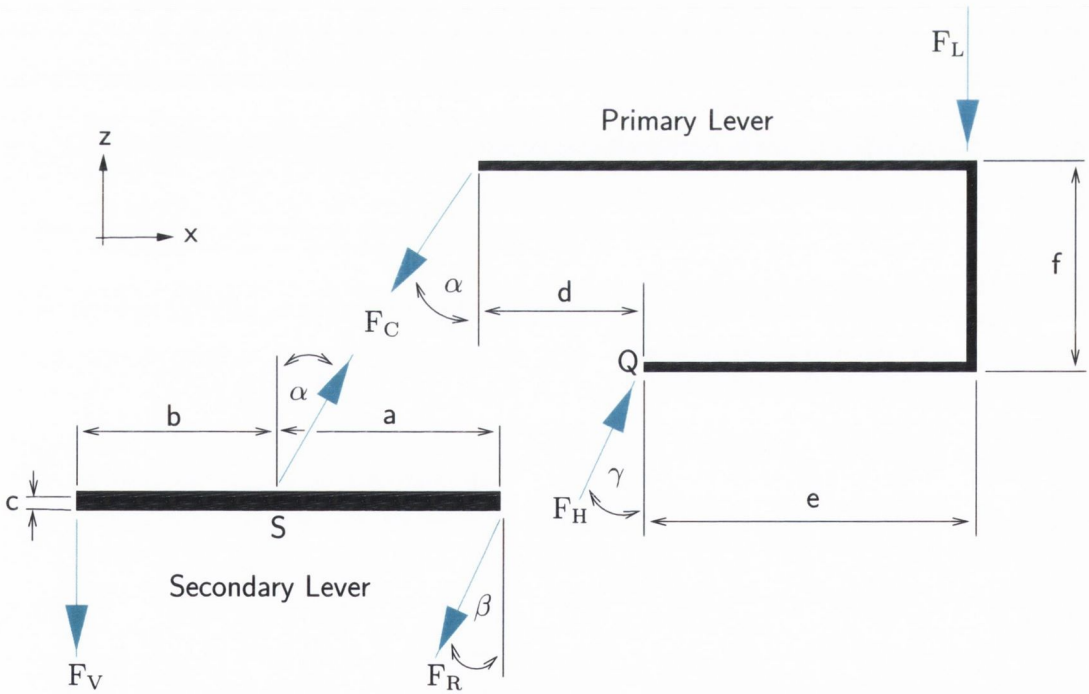

Figure 3.4: Schematic of experimental rig showing variables used in the design calculations

3.2.4 Physical embodiment of the design

The primary lever could translate within limits in the transverse and coronal planes on polytetrafluoroethylene (Teflon™, DuPont Co., USA) pads, i.e. the head of the femoral component was not constrained in the horizontal plane. This was to avoid creating a statically indeterminate system. The secondary lever was free to pivot on a pin joint; this ensured that the experimental device was not over-constrained. The heads of the femoral components were free to articulate within a polytetrafluoroethylene cup, contained within the primary lever. Two cup sizes were necessary to accommodate different head diameters. Both cups maintained the geometric ratios of the primary lever to ensure equal hip joint reaction forces were applied in all tests. No adjustment was made for different femoral component neck lengths. A complete set of technical drawings for the experimental rig is contained in Appendix B.

Both ends of the secondary lever were attached to the implanted femur by woven ultra-high strength polyethylene straps (Dyneema™, Toyobo Ltd., Japan). These were bonded to the femur using a high strength epoxy adhesive (Araldite™ Precision, Bostick Findley Ltd., UK) [note: several trials of various material/adhesive combinations were carried out to find one with suitable bond strength and fatigue properties]. The bonds were compressed while curing over a period of three days to enhance their shear strength. Adhesion of straps was chosen as the method of attachment, rather than wires, as it better mimics the non-localised attachment of muscle tissue to bone. The three-dimensional position and orientation of the bonded area of the strap was intended to replicate the attachment area of each muscle and its line of action. A pulley was used to ensure that the vastus lateralis acted downwards, as depicted in Figure 3.5.

To tension the straps prior to the commencement of testing, they were clamped to the secondary lever and the screw connecting the secondary lever to the primary lever was advanced until the primary lever was brought into contact with the testing machine. A spirit level was used to ensure the primary lever was aligned vertically and horizontally. All surfaces which experienced relative motion during testing were lubricated with a silicon oil containing PTFE particles to minimise friction.

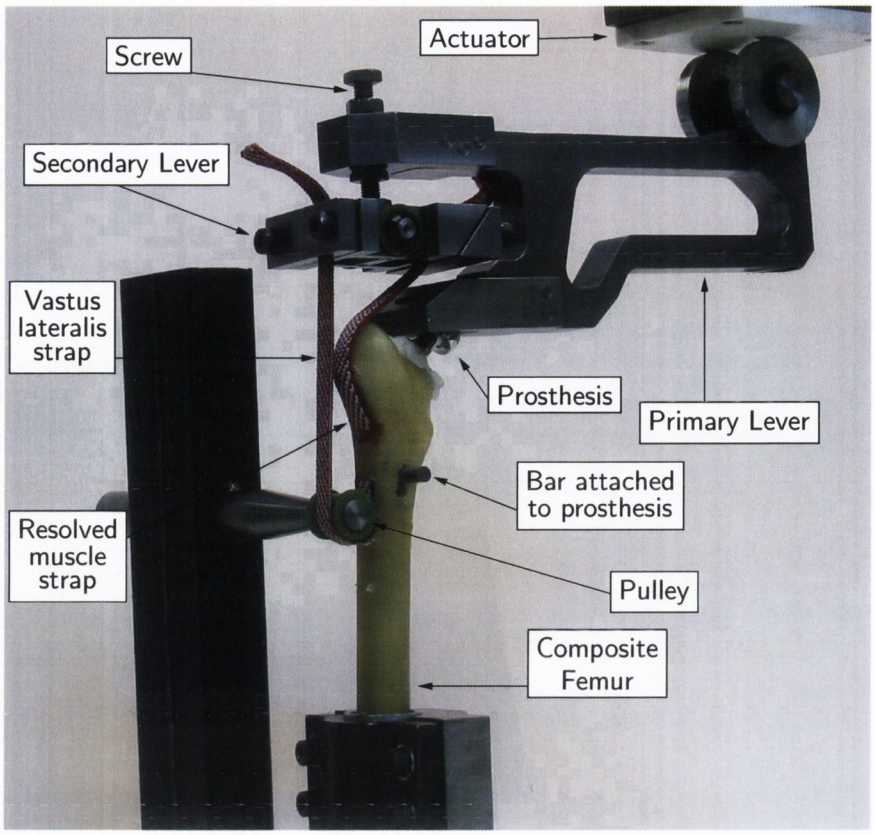

Figure 3.5: Lateral-posterior view of experimental rig with the migration measurement device removed for clarity. Rig consists of two linked levers

3.2.4.1 Verification of muscle application device

Foil strain gauges (FLG-02-11, Tokyo Sokki Kenkyujo Co., Japan) were attached to the screw connecting the secondary lever to the primary lever (this screw is visible in Figure 3.5). A femur implanted with a femoral component was loaded statically and strain measurements taken. This process was repeated several times. A mean axial force of 1.32 kN (standard deviation of 0.49 kN) was measured compared to the desired force of 1.49 kN from the design calculations. Possible reasons for this discrepancy include: (i) two people (the author and Theo Boogaard) alternatively assembled and re-assembled the experimental setup for each measurement and it was possible that different tensions where applied to the muscle straps by each person, (ii) after the experiment was completed it was noted that one of the strain gauges was loose, however it was not possible to determine when exactly the loosening started.

To ensure that the secondary lever functioned as intended, a dial gauge was mounted on the primary lever, and its probe brought into contact with the secondary lever. We measured relative motion of several microns between the two levers during cyclic loading, indicating that the secondary lever was rotating on its pin joint, maintaining the required distribution ratio of F_V and F_R.

3.2.5 Experimental test details

Proximal synthetic composite femora (Model #3103 Sawbones™, Pacific Research Laboratories, USA) were implanted with either Charnley Extra Small (DePuy International Ltd., UK), polished Exeter (Stryker Osteonics Howmedica, France), Lubinus SPII Co-Cr (Waldemar-Link GmbH., Germany), or Müller Curved (JRI Ltd, UK) femoral components. These femoral components were chosen because comprehensive data on their *in vivo* performances has been reported by various researchers (Sutherland et al., 1982; Malchau et al., 1993; Kärrholm et al., 2000; Alfaro-Adrian et al., 2001). The similar structural behaviour of the composite femora to human femora has been confirmed by other researchers (Szivek et al., 1990; Cristofolini et al., 1996).

A purpose-built insertion machine (Maher et al., 2000) was used to ensure repeatability and accuracy of stem placement for the Charnley, Lubinus, and Müller femoral components. The insertion path differed for each of these femoral component designs, and was achieved through the design and fabrication of a specific guide plate for each type. The Exeter femoral components were inserted using a custom-designed jig fitted to a radial arm drill; this approach was necessitated by their vertical, linear insertion path. (Note: a distal centraliser was used for each Exeter implantation). Vacuum mixed bone cement (Cemex™ RX low viscosity, Tecres S.p.a., Italy) was used for all tests. After a seven day curing period, the stems were sinusoidally loaded with either (a) the loadprofile which included muscle forces or (b) the loadprofile without muscle forces, at a frequency of 5 Hz, for one million cycles. Note that Humphreys et al. (1989) found only small temperature increases in bone cement during cyclic tests at a frequency of 6 Hz. The duration of one mil-

lion cycles was chosen because Maher and Prendergast (2002) found that differences in the migration of two different prosthesis designs were apparent after one million cycles of a fatigue test.

Five tests were carried out for each femoral component type ($n_{type} = 5$), giving a total of 20 tests ($n_{with\ muscles} = 20$) with the loadprofile which included muscle forces. Five tests were also executed using femurs implanted with the Lubinus femoral component applying the hip joint reaction force only, for an overall total of 25 tests ($n_{total} = 25$). Initially two femoral components of each type were tested in sequence: Lubinus, then Müller, followed by the Charnley, the Exeter, and the Lubinus without applied muscle forces. Once this first test sequence was completed then the remaining three femoral components of each type were tested in the following order: Lubinus, Lubinus without applied muscle forces, Exeter, Müller and Charnley. The purpose of this was to lessen the effect of any 'learning curve' associated with the test procedure on the test results.

3.2.6 Migration measurement and calculation

The migration of the femoral components was measured using the method described in detail by Maher et al. (2001). The operation of the migration measurement device can be briefly described as follows: a target device consisting of three spheres mounted on a cruciform structure was rigidly press-fitted to the femoral component, see Figure 3.6. Six linear variable differential transformers (LVDTs) were in contact with the spheres, and the changes in voltages of the LVDTs as the femoral component migrated were recorded using a data acquisition card (AT-MIO-16XE-50, National Instruments Corp., USA) and software package (LabVIEW 5.1, National Instruments Corp., USA), which sampled the LVDT readings every 10,000 cycles at a frequency of 100 Hz for three seconds.

It was necessary to modify the migration measurement device slightly to accommodate the pulley used to direct the vastus lateralis force downwards, see Figure 3.5. This involved altering the position of LVDT 5 through 180° relative to its original position as designed by Maher (2000), see Figure 3.7.

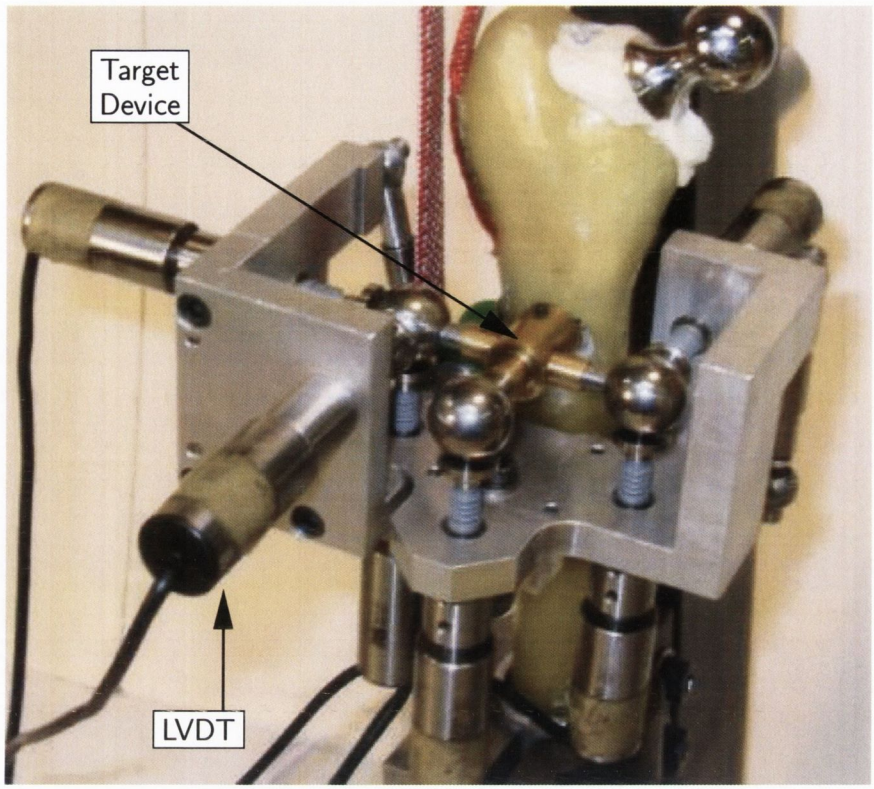

Figure 3.6: Detailed view of the migration measurement device attached to an implanted composite femur

After logging of the raw displacements, a locally weighted robust regression smoothing procedure, LOESS (Cleveland and Devlin, 1988), as implemented in MathCAD™ Professional 2000, MathSoft Inc., USA., was performed to remove any random noise. The basis of operation of the LOESS smoothing scheme is that, at each point in the data set a low-degree polynomial is fitted to a sub-set of the data with values near the point whose response is being estimated. The polynomial is fitted using weighted least squares, with more weight being given to those points near the point of interest. The value of the regression function is obtained by evaluating the polynomial for the point of interest. This procedure is repeated for all data points. The degree of the fitted polynomial, the weights used, and the size of the data sub-set are flexible and can be set by the user. The measured migrations were used to compute the migration (permanent change of position) of the femoral component head centre and inducible displacement (elastic deflection) at the point of attachment of the migration measurement device.

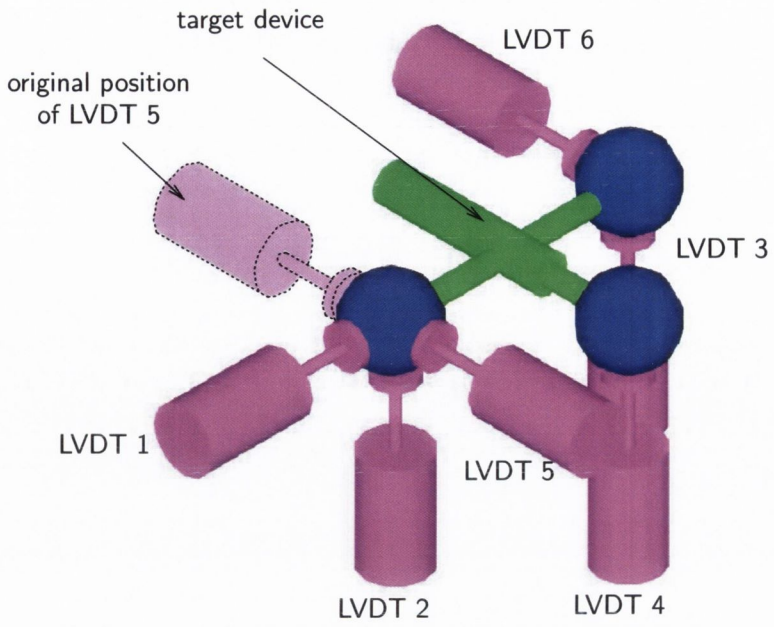

Figure 3.7: Illustration of the alteration to the position of LVDT 5 required to accommodate muscle loading. The dashed outline represents the position of LVDT 5 as designed by Maher (2000).

3.2.6.1 Quantification of error associated with use of the migration measurement device over extended time periods

Maher (2000) and Maher et al. (2001) have previously confirmed the response of the migration measurement device to gross movement using a materials testing machine. However, the question remained as to the influence of environmental changes during the course of an extended experimental test. The source of greatest variability in the testing environment was readily apparent as laboratory temperature. Repeated measurements using a platinum resistance thermometer (HP 2802A, Hewlett Packard, USA) revealed that a temperature change of up to 2.5°C could occur during the course of a test (as part of the diurnal cycle). Among the aspects this variation in temperature could influence were expansion and contraction of experimental materials (e.g., the target device, the synthetic femurs used), and electrical inputs and

outputs, such as the output voltages from the LVDTs. Therefore, we conducted a series of calibrations of the migration measurement device to estimate the influence of a 2.5°C change in temperature on its operation. Static tests (i.e. no loading was applied) were carried out using (i) the migration measurement device mounted on an implanted proximal composite femur, and (ii) the migration measurement device mounted on a steel bar with similar dimensions to the composite femur. Additionally the drift in the LVDTs' output voltage and power supply was monitored. The tests ran for several 24 hour periods over a period of two weeks. Temperature was continuously measured. It was assumed that the influence of temperature variations on the 16bit data acquisition card was negligible.

3.2.6.2 Effect of the assumption of rigid body motion

In previous studies,(Maher and Prendergast, 2002; Britton et al., 2003) the measured inducible displacement was transformed to the femoral component head centre to aid the comparison of different prosthesis designs; thus it was implicitly assumed that the relative movement between the implant and the bone was one where the bodies remained rigid. To investigate the effect of this assumption we created a finite element model of an implanted femur and solved for the displacements experienced over a loading cycle.

A model of a Lubinus SPII femoral component stem implanted in a proximal composite femur was created. Typical isotropic material properties were assigned to each element set, see Table 3.2 in Section 3.3.2. The FE model was constrained distally to emulate the experimental setup, and the hip joint reaction force only was applied. To model the migration measurement device, nodes at various locations of the femoral component were selected, see Figure 3.8. For each of these nodes, four new nodes were created in the same horizontal plane to represent the centres of the spheres of the target device. These nodes were joined with rigid beam elements, and constrained to three degrees of translation at the node on the femoral component surface. These four newly created nodes were then duplicated, and the duplicate nodes joined with rigid beam elements to a node on the bone surface. This process

was repeated four times to create four target device models.

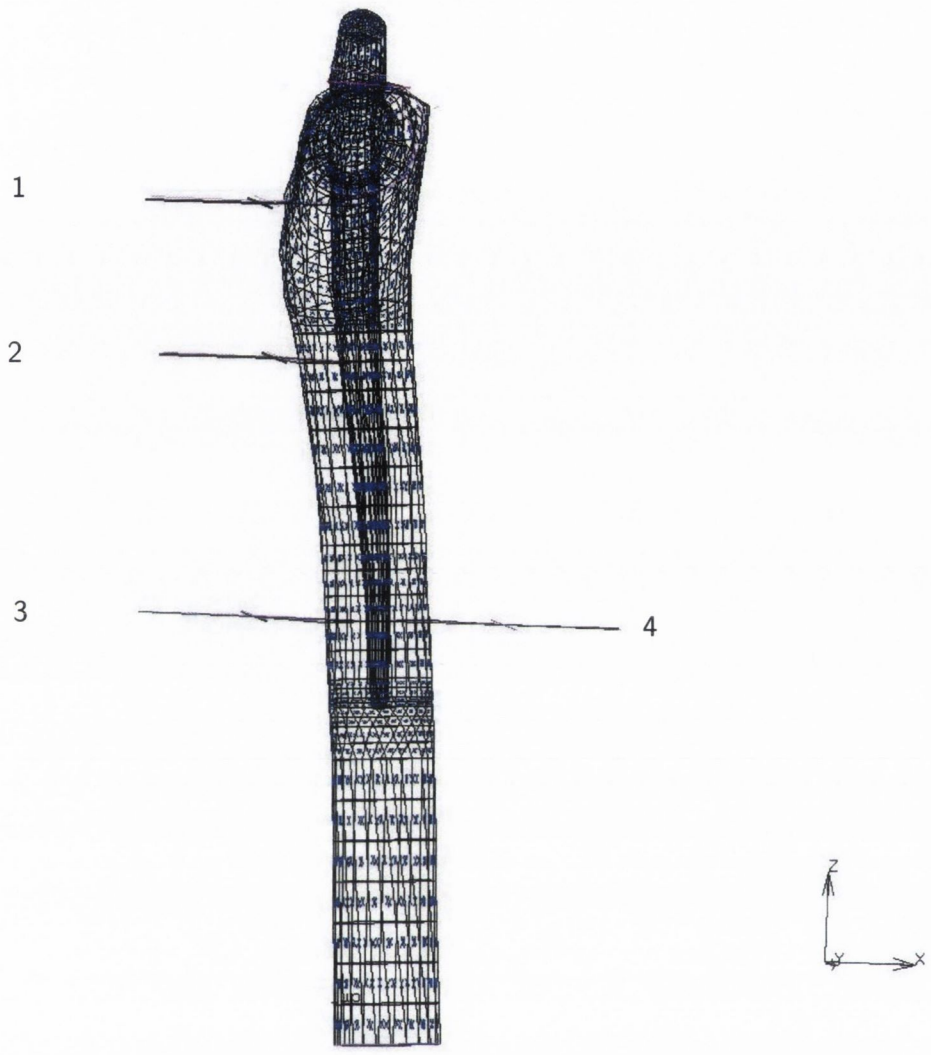

Figure 3.8: View of finite element model used to validate rigid body assumption, showing locations of simulated migration measurement devices

Two loading cycles were simulated, and the difference in position between the start of the second cycle (point of minimum loading) and the midpoint of the second cycle (point of maximum loading) was calculated for each MMD model, i.e. the inducible displacement experienced by each target device model, see Figure 3.9.

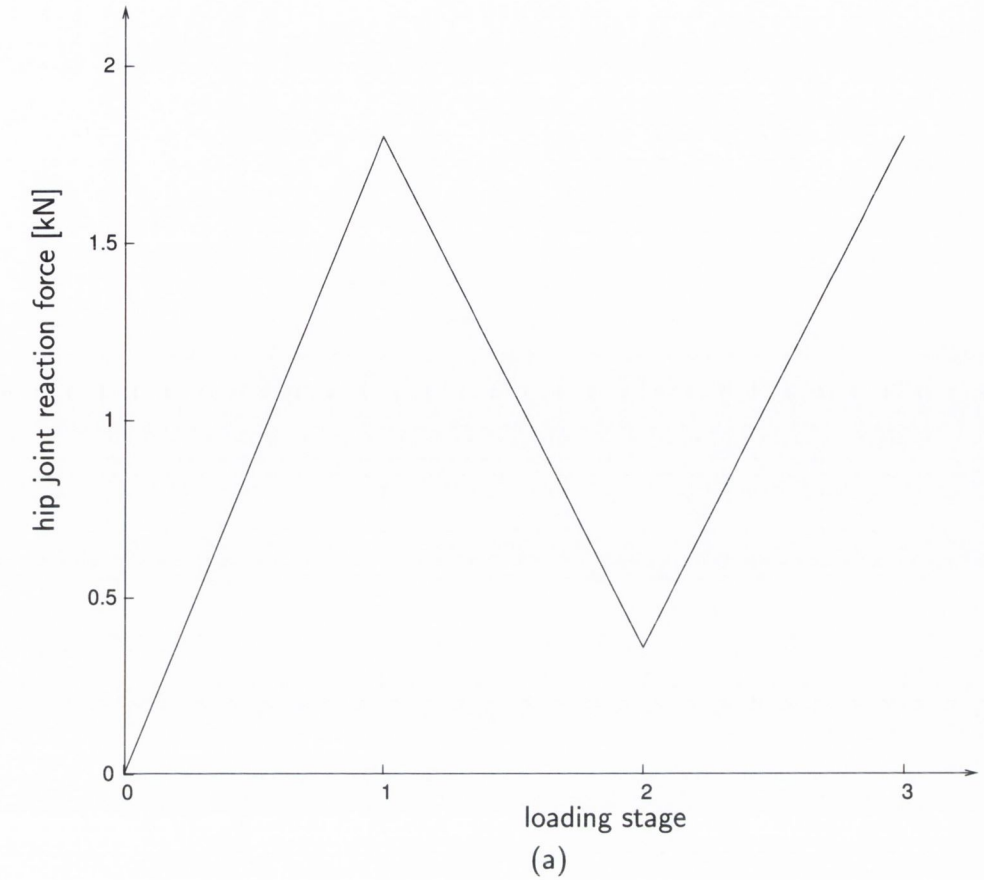

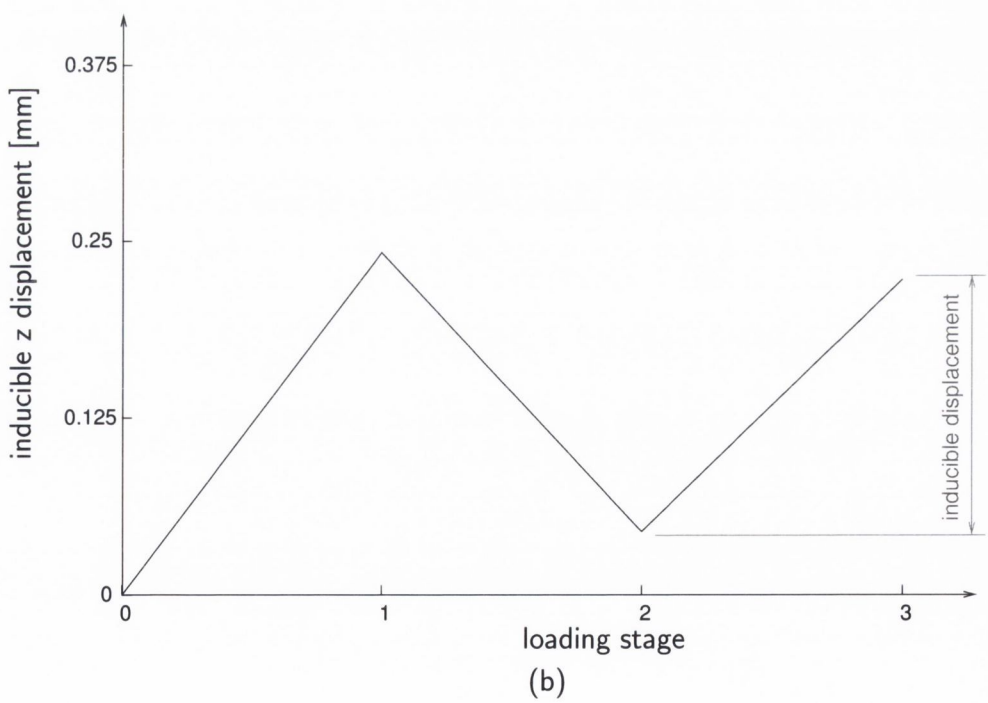

Figure 3.9: Graph of (a) loading applied to finite element model and (b) resulting inducible displacement

3.3 Finite element modelling of an implanted proximal femur

In this section the methods pertaining to the finite element analysis are outlined.

3.3.1 Development of finite element model

A virtual solid model of a Lubinus SPII femoral component was obtained (courtesy of Jan Stolk, University of Nijmegen, The Netherlands). After "geometrical healing" of the model to remove extraneous features (performed using GAMBIT 2.0.4, Fluent Inc, USA.) the model was imported into Ansys 7.0, (Ansys Inc., USA) along with a virtual solid model of the 'Standardized Femur' (version 2.3, Viceconti et al. (1996)), which is based on the model 3103 Sawbones™ composite femur. The Lubinus model was positioned within the femur model. Anterior-posterior and medial-lateral x-rays of the Lubinus femoral component (courtesy of Mr. Paul Connolly, Specialist Orthopaedic Registrar, Cappagh Orthopaedic Hospital, Dublin) which had the most typical migration characteristics were used to guide the placement of the femoral component.

Once satisfactorily positioned the combined model was sliced perpendicular to the longitudinal axis of the femur to create cross-sectional splines. The distance between the slices varied depending on the rate of change of the geometric features of the combined model, i.e. locations of rapid change, e.g. the distal tip of the femoral component, had multiple closely-packed slices taken, whereas those regions with slow change had fewer, widely-spaced slices. The original volumes were then deleted, and re-created from the cross-sectional splines. The newly created volumes were meshed with an eight-node hexahedral element, see Figure 3.10. The finite element mesh was then exported from Ansys to a text file. A FORTRAN program converted the text file to a format suitable for importation into Marc™ release 2003r2 (MSC Software Corp., USA). Mentat™ 2003 (MSC Software Corp., USA) was used as the graphical user interface to Marc. Marc was chosen to be the finite element solver because of its specialisation in non-linear analyses, and ability to interface

with subroutines written in a variety of programming languages.

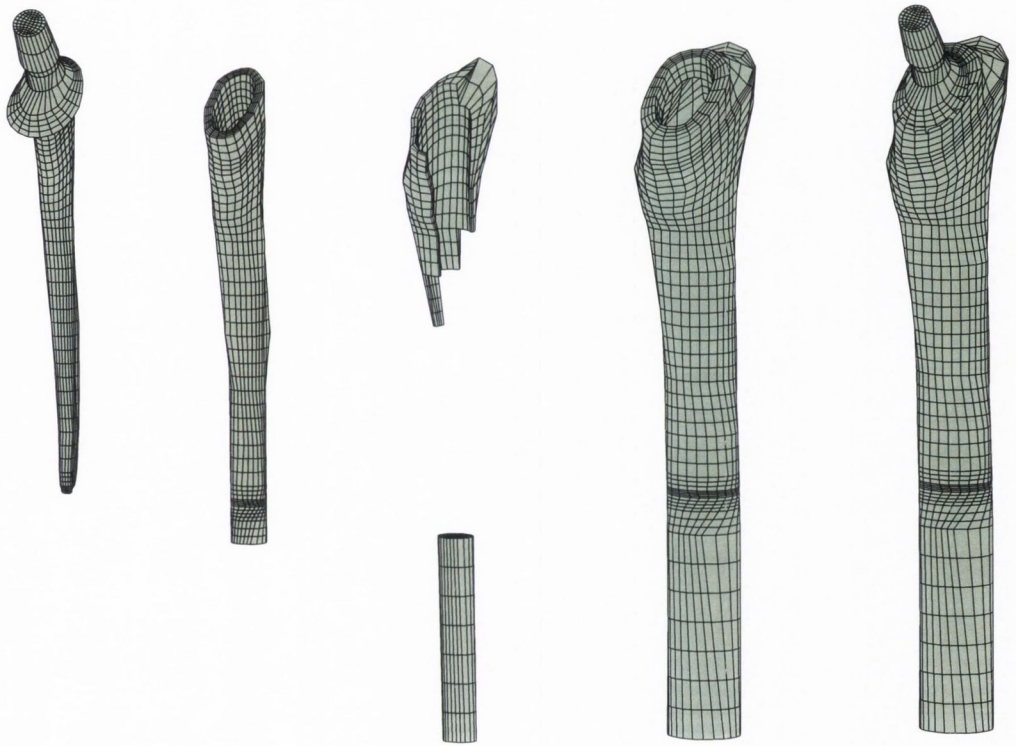

Figure 3.10: Finite element meshes of (a) the femoral component, (b) the cement mantle, (c) the cancellous bone, (d) the cortical bone, and (e) the complete assembly

3.3.2 Boundary conditions, loading, and material properties

The finite element model was constrained distally to represent the distal restraint of the experimental test. Two loadprofiles, analogous to the experimental tests, were applied in the analyses: i) hip joint reaction force only, and ii) the hip joint reaction force plus muscles (the resolved abductor and tensor fasciae latae force and the vastus lateralis force) as per Table 3.1.

The material properties from Lennon and Prendergast (2001) were used, see Table 3.2. All materials were considered to be homogeneous. The femoral component/cement interface was modelled as initially in contact (bonded) but free to separate and undergo relative motion (debonded), with friction. A Coulomb friction model was used with a friction coefficient of 0.3 (Lennon and Prendergast, 2001) for the femoral component/cement interface. The cement/bone interface was fully bonded.

Table 3.2: Material properties used in the finite element model. Taken from Lennon and Prendergast (2001).

Item *Material*	Number of elements	Elastic modulus, E [GPa]	Poisson's ratio, ν
Femoral component *Co-Cr steel*	4208	210	0.3
Bone cement *PMMA*	4688	2.28	0.3
Cancellous bone *Polyurethane foam*	1024	0.413	0.3
Cortical bone *Glass fibre reinforced epoxy composite*	4720	11.5	0.4

3.3.2.1 Simulation of creep

Bone cement creeps when exposed to physiological loads (Verdonschot and Huiskes, 1994). The creep law formulation used was taken from Verdonschot and Huiskes (1995). After each iteration of the finite element solver, an equivalent creep strain increment, $\Delta\varepsilon^c_{eq}$, is calculated:

$$\Delta\varepsilon^c_{eq} = 7.985 \cdot 10^{-7} \cdot (\mathrm{n}^c + \Delta\mathrm{n})^{0.4113 - 0.116 \cdot log_{10}\,\sigma} \cdot \sigma^{1.9063} - \varepsilon^c_{eq} \qquad (3.12)$$

where n^c is the current time, Δn the time increment, σ is the current total equivalent stress, and ε^c_{eq} is the total equivalent creep strain. This equivalent creep strain increment is then used to update the strain tensor and hence the stiffness matrix. The creep simulations were run for a duration equivalent to one million loading cycles.

3.3.3 Analyses performed

Two analyses were run in total, consisting of the two loadprofiles described in Section 3.3.2. Creep was simulated in both analyses. The applied loading increased linearly from 0% to 100% full value during the first loading cycle; thereafter, the loading was quasi-static. During each analysis, subroutines were executed to calculate additional output measures, such as those described by Lennon and Prendergast (2001). These include reporting the volume of cement stressed above a certain level to minimise the influence of singularities in the finite element mesh, and the probability of failure, P_f, of the cement mantle after ten million loading cycles using a regression polynomial based on the experimental data of Murphy and Prendergast (2000). The polynomial has the form:

$$P_f = 1 - P_s \tag{3.13}$$

where,

$$P_s = -0.0005\sigma^3 + 0.0202\sigma^2 - 0.3304\sigma + 1.8365 \tag{3.14}$$

P_s is the probability of survival of the cement mantle after ten million loading cycles. Post-processing was automated in so far as possible using computer scripts coded in Python (freely available from www.python.org) as a Python interface module (py_post.so) was available for Mentat from MSC Software.

3.4 Summary

The author's thesis is that pre-clinical testing of hip prostheses can be carried out using *in vitro* methods. In this chapter, the methods that will be used to produce data to test this thesis have been described. An experimental procedure for measuring the relative micromotion of a prosthesis and bone under cyclic loading with and without simulated muscle forces has been described. From this, the importance of loading *vis-à-vis* prosthesis/bone relative motion can be discerned. Next, finite element modelling can be used to quantify the effect of muscle loading on the cement mantle and to investigate whether or not the amount of the relative motion is due to creep.

Chapter 4

RESULTS

Contents

4.1 Introduction

The results of the experimental tests and numerical simulations are presented in this chapter. All migration data reported is for the head centres of the femoral components (to aid comparison of different designs). All inducible displacement data is reported for the point where the target device is press-fitted to the femoral component. Θ_x denotes rotation about the medial-lateral axis (for Θ_x, the head of the femoral component translates posteriorly and the tip anteriorly), Θ_y denotes rotation about the posterior-anterior axis (rotation into valgus is positive), and Θ_z rotation about the longitudinal axis (rotation into retroversion is positive, i.e. where the medial face translates posteriorly and lateral face translates anteriorly),

see Figure 4.1. All migration and inducible displacement rates are calculated by applying a linear least-squares fit to the data. *Early* rates are taken to occur between 0 and 500,000 loading cycles, whereas *steady state* rates are those from 500,000 to one million loading cycles.

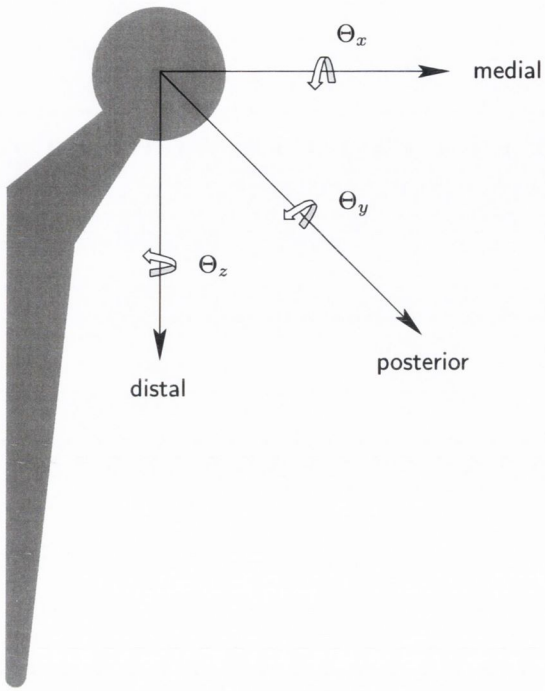

Figure 4.1: Schematic of a typical femoral component showing coordinate system used for presentation of migration results

A brief explanation of the statistical measures which are reported is necessary. P values and 90% confidence intervals are calculated for the results. The P values indicate the outcomes of the hypothesis tests, and the confidence intervals provide the precision of estimation of the mean values (Gardner and Altman, 1986; Sterne and Smith, 2001). When a comparison is made between two samples, a one-sided P value is reported where the null hypothesis is that there is no difference between means and the alternative hypothesis is that one mean is greater than the other mean ($H_0 : \mu_a = \mu_b, \quad H_A : \mu_a > \mu_b$), based on the Student t distribution. Two-sided P values can be obtained by doubling the one-sided P values. One-way analyses of variance (ANOVA) are performed for multiple comparisons (one-way because the only treatment examined is prosthesis type), as implemented in Mathematica™ 4.2, (Wolfram Research Inc., USA). The ANOVA technique is used when performing

multiple comparisons because the use of multiple two sample t tests increases the probability of falsely concluding that significant differences exist (Zar, 1999). As an example, in this thesis four prosthesis designs are compared. This would require a total of six t tests for comparison of, say, mean distal translation at one million loading cycles - the number of combinations of n different things, taken k at a time, without repetitions is n!/(k!(n-k)! (Kreyszig, 1999). If each t test was performed at a significance level of 0.05, the probability of incorrectly concluding that a significant difference exists is $1 - 0.95^6 = 0.26$ or 26%. When an ANOVA is performed, and a P value less than 0.05 is obtained, this implies that all the tested means are not equal (at a significance level of 0.05). To determine where any differences in the means are located an 'a posteriori' test is performed. The 'a posteriori' test employed in this thesis is the Newman-Keuls test. This test is very similar to the Tukey test (also known as the honest significant difference test) but is regarded as being more powerful, i.e. more likely to detect significant differences (Zar, 1999). The Newman-Keuls test is performed only when an ANOVA has detected differences. As is common practice, a significance level of 0.05 will be used throughout this thesis.

Three underlying assumptions of the ANOVA technique are: (i) that the samples are drawn independently and randomly from the source population, (ii) the source population can reasonably be expected to have a normal distribution, and (iii) the samples have approximately equal variance. These assumptions are justified in this thesis by virtue of equal sample size (Zar, 1999). Additionally, ANOVA results were compared to those obtained from the non-parametric Kruskal-Wallis test, and found to be similar.

4.2 Clarification of certain aspects of the operation of the migration measurement device

In this section the error associated with usage of the migration measurement device for extended durations is reported. Additionally, because of the elastic deflection

of the femoral component, the attachment location of the migration measurement device determines the inducible displacement; this is also quantified.

4.2.1 Quantification of error associated with extended usage of migration measurement device

The laboratory temperature was recorded for several 24 hour periods and over a weekend (for approximately 67 hours). The typical variation in laboratory temperature is shown in Figure 4.2(a), and the resulting errors in measurement of translation for an implanted composite femur shown in Figure 4.2(b).

The maximum variation in laboratory temperature found was 2.5° Celsius due to the diurnal cycle. It was found that a temperature increase of 2.5°C resulted in a systematic error of 5 μm for medial and posterior translation, 4 μm for distal translation, 0.004° for Θ_x and Θ_y rotations, and 0.003° for Θ_z rotation when the MMD was mounted on an implanted composite femur, see Table 4.1. The relationship between temperature variation and measurement errors was non-linear. Approximately half of the magnitude of these errors were due to hysteresis of the fabrication materials of the composite femur (determined through comparison of the two test setups as shown in Table 4.1). This hysteresis is also evident in Figure 4.2(c). The remainder of the error was due to voltage fluctuations and different rates of thermal expansion of the materials of the MMD.

Table 4.1: Effect of a 2.5° C temperature variation on measurements recorded by the migration measurement device

setup	medial [mm]	posterior [mm]	distal [mm]	Θ_x [degree]	Θ_y [degree]	Θ_z [degree]
composite femur	0.005	0.005	0.004	0.004	0.004	0.003
steel cylinder	0.003	0.002	0.002	0.002	0.002	0.001

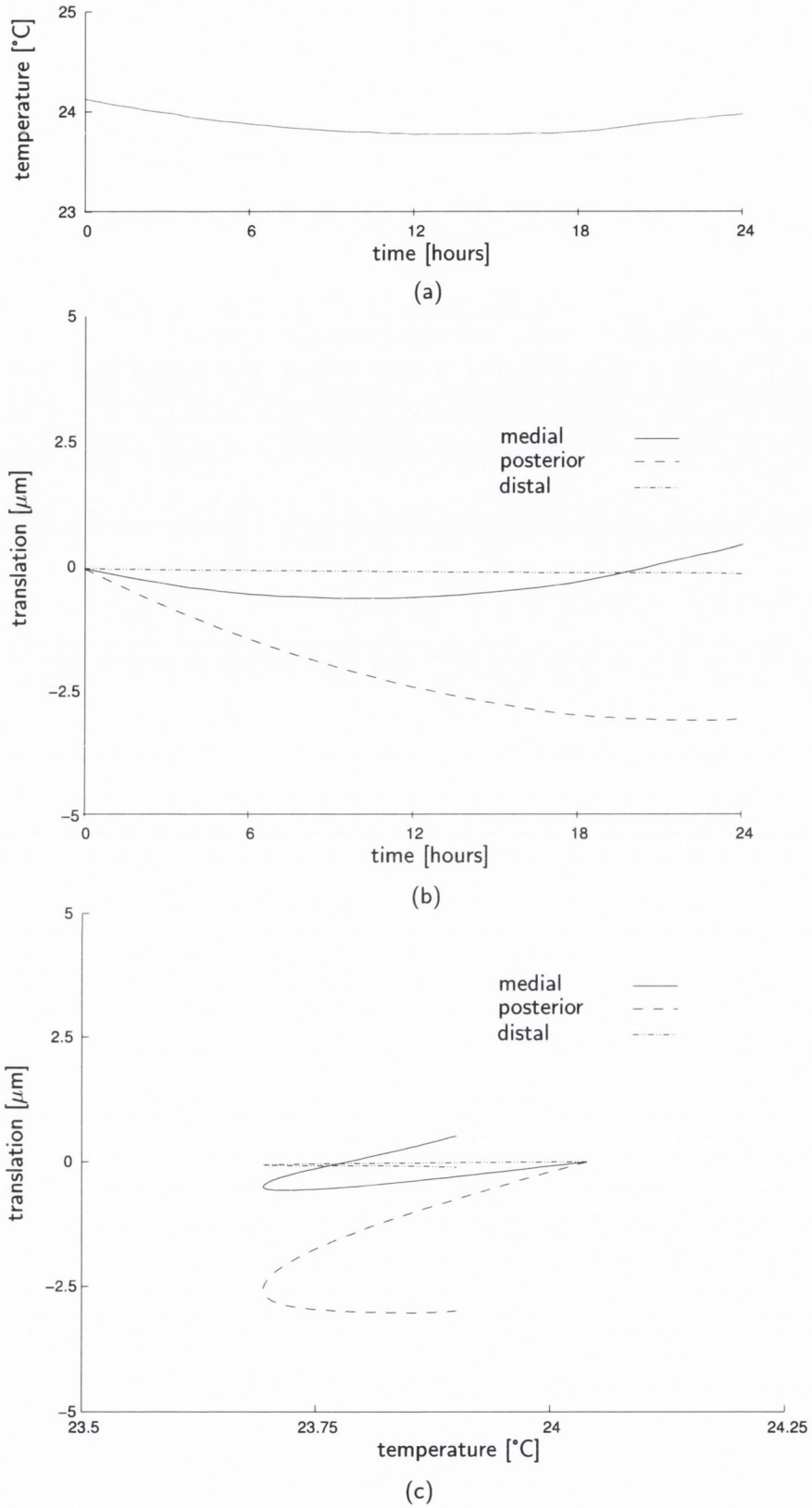

Figure 4.2: Graphs of (a) typically observed temperature variation over a 24 hour period, (b) measurement variation with respect to time over a 24 hour period, and (c) measured translation versus temperature for that same 24 hour period. Hysteresis is apparent in (c) (for a temperature value of 23.75°C there are two values for each of the translations).

4.2.2 Influence of target device location on inducible displacement magnitude

The inducible displacements calculated at the locations of the simulated target devices are listed in Table 4.2. As expected, the target devices which are located closest to the rigid constraints of the finite element model (equivalent to the distal clamping of the experimental setup) have the lowest inducible displacements. This result highlights that there is an issue (potential error) associated with the location of the attachment of the target device to the prosthesis when comparing the performances of different prostheses.

Table 4.2: Inducible displacements for each migration measurement device location (Locations and coordinate system are shown in Figure 3.8)

location	change in x [mm]	change in y [mm]	change in z [mm]	resultant [mm]
1	0.071	0.093	0.178	0.213
2	0.141	0.075	0.185	0.244
3	0.053	0.047	0.035	0.079
4	0.022	0.029	0.043	0.056

4.3 Influence of muscle forces on migration of femoral components

This section compares the behaviour of the Lubinus SPII femoral components tested under muscle loading with those tested under the hip joint reaction force only. The hypothesis to be tested is that different migrations will be found with muscle loading. If this hypothesis is confirmed then muscle loading will be required for comparative experimental tests of prosthesis designs. The argument follows that reported in Britton et al. (2003).

4.3.1 Migration of the femoral components

In three of the degrees of freedom the Lubinus SPII femoral components migrated in the same direction, i.e. medially, distally (i.e. subsided), and rotated into a varus position, see Figure 4.3. In the other three degrees of freedom, the migration directions were different in some cases. The heads of three femoral components tested under muscle loading migrated anteriorly, whereas the heads of three femoral components tested without muscle loading migrated posteriorly. One femoral component tested under muscle loading underwent negligible rotation about the medial-lateral axis (x axis) or about its longitudinal axis (z axis), the other femoral components did experience rotation about both these axes, but not in a manner that allows differentiation between the loading with and without muscle loading. Considerable variation in migration was observed between tests. Although the time series behaviour of all measured migrations was highly non-linear, the majority of the femoral components experienced rapid early migration to approximately 500,000 cycles and, thereafter migrated at steadier rates.

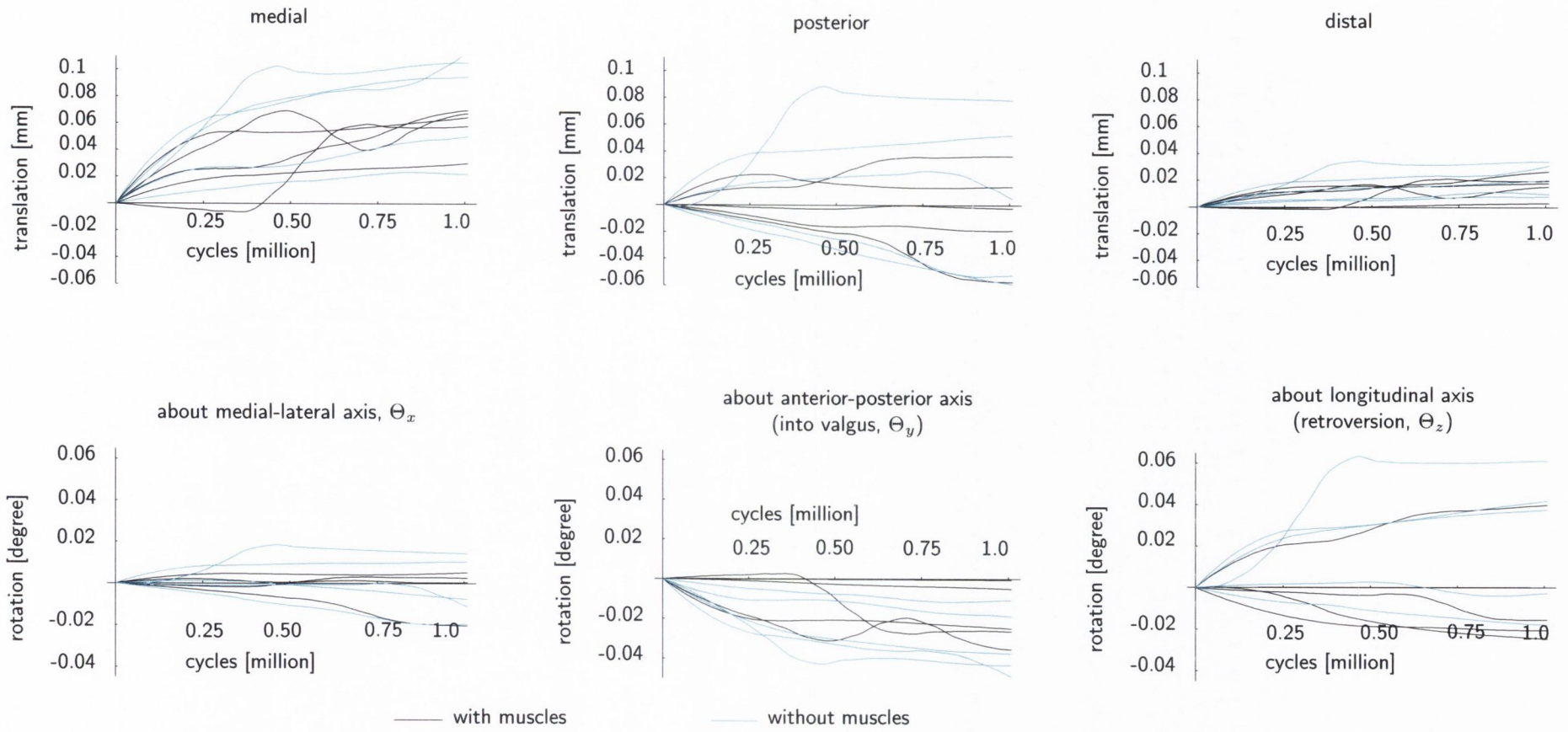

Figure 4.3: Time series curves of Lubinus SPII femoral components tested with, and without, simulated muscle loading

Less scatter and lower absolute migration was observed with muscle loading compared to without muscle loading, as shown in Figure 4.4. However, P values for mean difference tests failed to reject the null hypothesis of no difference in population means. Negligible differences between early and steady-state migration rates were detected for simulated muscle loading versus hip joint loading only, see Table 4.3 and Table 4.4. However, there is a definite trend of generally lower migration rates under simulated muscle loading, particularly in the early stage of loading.

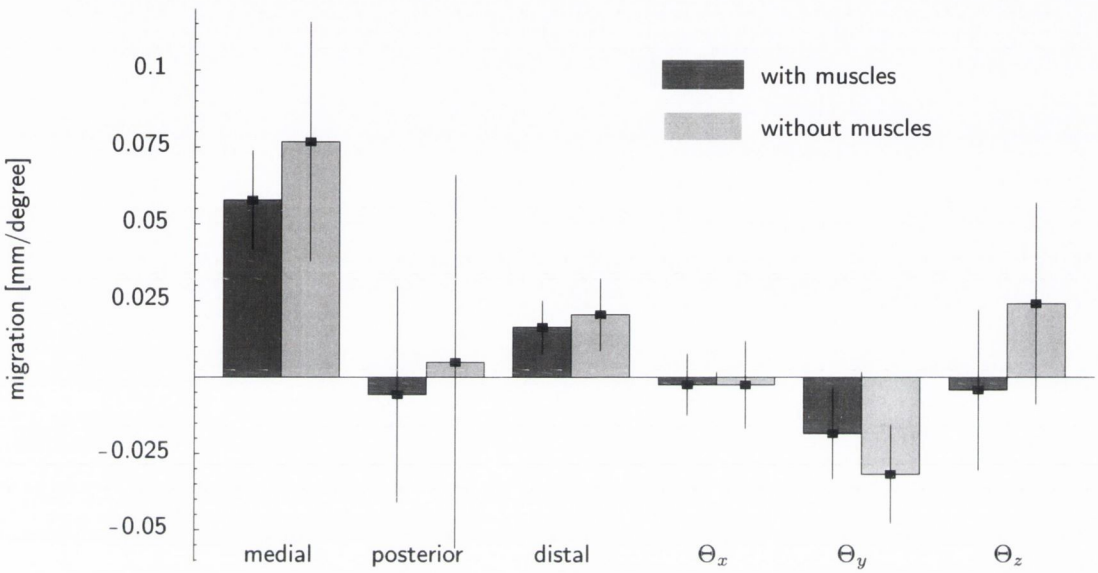

Figure 4.4: The mean migration values of the Lubinus femoral components with, and without, simulated muscle loading after one million cycles. The error bars give the 90% confidence intervals

Table 4.3: The average and 90% confidence interval *early* migration rates of the Lubinus femoral components, with and without simulated muscle loading.

	Lubinus with muscle loading	Lubinus without muscle loading	One-sided P value for mean difference test
medial [nm/cycle]	0.07±0.05	0.12±0.08	0.13
posterior [nm/cycle]	-0.01±0.03	0.05±0.11	0.20
distal [nm/cycle]	0.02±0.01	0.03±0.03	0.18
Θ_x [n°/cycle]	-2±8	-8±25	0.23
Θ_y [n°/cycle]	-23±25	-50±33	0.10
Θ_z [n°/cycle]	-7±33	51±66	0.07

Table 4.4: The average and 90% confidence interval *steady state* migration rates of the Lubinus femoral components, with and without simulated muscle loading.

	Lubinus with muscle loading	Lubinus without muscle loading	One-sided P value for mean difference test
medial [nm/cycle]	0.03±0.03	0.03±0.02	0.50
posterior [nm/cycle]	-0.02±0.04	-0.03±0.03	0.36
distal [nm/cycle]	0.01±0.01	0.01±0.01	0.46
Θ_x [n°/cycle]	-6±14	-11±9	0.27
Θ_y [n°/cycle]	-11±8	-14±14	0.25
Θ_z [n°/cycle]	-6±18	2±16	0.23

4.3.2 Inducible displacement of the femoral components

Inducible displacement is the reversible micromotion experienced by a femoral component during a single loading cycle (it can be due to several mechanisms, including cement elasticity or sliding at the prosthesis/cement interface). Most of the inducible translations underwent rapid early increases as expected, and then tended to stabilise, see Figure 4.5. In particular most of the femoral components tested under simulated muscle loading had lower inducible posterior translations than the femoral components tested without muscle loading. The inducible rotations displayed more varied behaviour with sudden random increases and decreases (Figure 4.5). Reasons for this will be presented in the discussion.

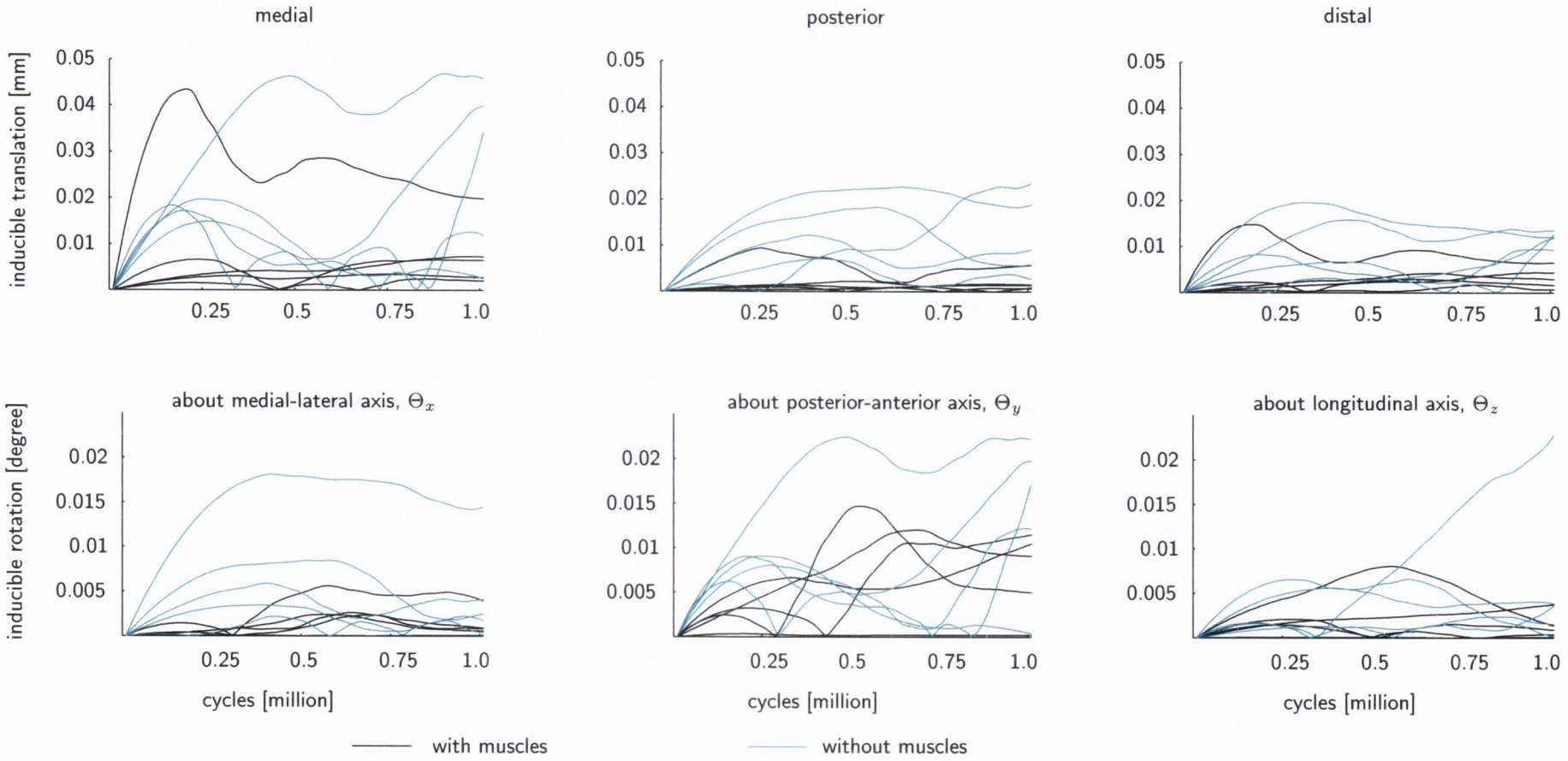

Figure 4.5: Time series curves showing the development of inducible displacements of the Lubinus SPII femoral components tested with, and without, simulated muscle loading

Muscle loading caused a reduction in inducible displacement, see Figure 4.6. No significant differences were found, see Table 4.5.

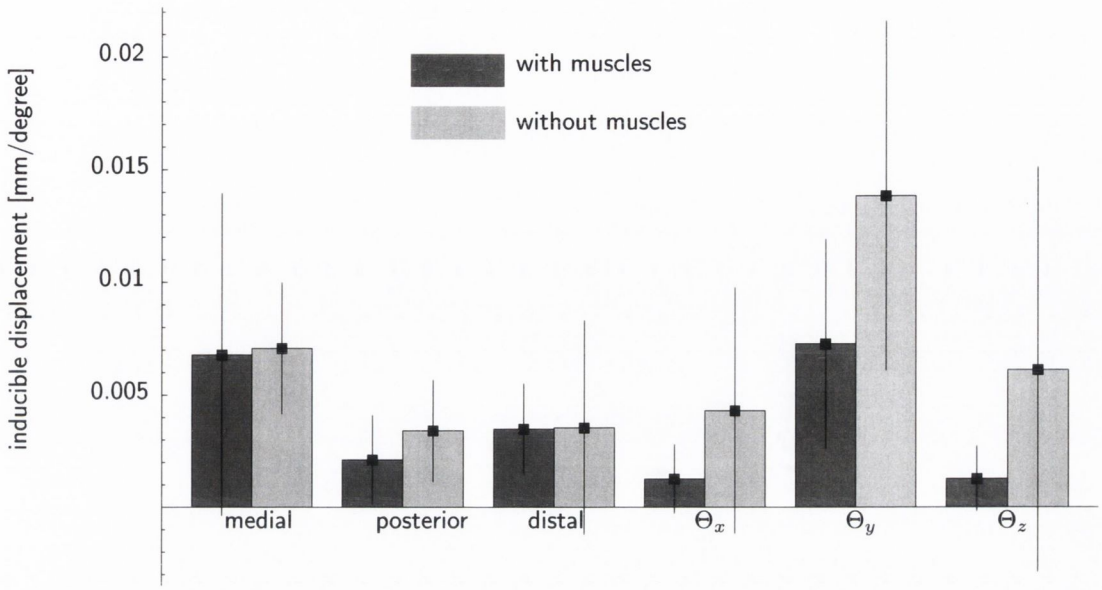

Figure 4.6: The mean inducible displacement values of the Lubinus femoral components, with and without muscle loading, at one million cycles. The error bars give the respective 90% confidence intervals

Table 4.5: One-sided P values for mean inducible displacements difference test between the Lubinus femoral components tested, with and without muscle loading, after one million loading cycles

medial	posterior	distal	Θ_x	Θ_y	Θ_z
0.47	0.19	0.49	0.15	0.08	0.14

4.3.3 Rate of change of inducible displacement

The early inducible rotation about the medial-lateral axis (Θ_x) is significantly greater for the prostheses tested without muscle loading, see Table 4.6. However the other inducible displacements are similar for both loadprofiles, though the mean values of the inducible rotations are lower for the prostheses tested under muscle loading.

Table 4.6: The average and 90% confidence interval *early* inducible displacement rates of the Lubinus femoral components, with and without simulated muscle loading per cycle

	Lubinus with muscle loading	Lubinus without muscle loading	One-sided P value for mean difference test
medial [nm]	0.00±0.01	0.00±0.01	0.47
posterior [nm]	0.00±0.00	0.00±0.00	0.48
distal [nm]	0.00±0.00	0.01±0.01	0.20
Θ_x [n^o]	3±3	14±12	0.05
Θ_y [n^o]	11±11	12±19	0.44
Θ_z [n^o]	4±6	5±4	0.34

The steady state inducible translation rates are similar for both load profiles, see Table 4.7. However while the inducible rotation rates decrease for the prostheses tested under muscle loading, both the inducible rotation rate about the posterior-anterior axis and the inducible rotation rate about the longitudinal axis have an increasing tendency for the femoral components tested without simulated muscle loading. This is significantly different in the case of the inducible rotation rate about the posterior-anterior axis (Θ_y), Table 4.7.

Table 4.7: The average and 90% confidence interval *steady state* inducible displacement rates of the Lubinus femoral components, with and without simulated muscle loading per cycle

	Lubinus with muscle loading	Lubinus without muscle loading	One-sided P value for mean difference test
medial [nm]	0.00±0.01	0.01±0.00	0.14
posterior [nm]	0.00±0.00	0.00±0.01	0.29
distal [nm]	0.00±0.00	0.00±0.00	0.38
Θ_x [n^o]	-2±2	-4±8	0.25
Θ_y [n^o]	-8±14	14±15	0.03
Θ_z [n^o]	-6±8	5±17	0.14

4.3.4 Are the rates of change of inducible displacement increasing or decreasing?

It is arguable that the most important feature of inducible displacement is whether or not it is increasing or decreasing with time. Increasing inducible displacement

indicates continuing loosening while decreasing inducible displacement is a sign of stability, or that the prosthesis is "settling-in". This was investigated by calculating the slope of the straight line fitted by linear least-squares to the inducible displacement data during the steady state period (i.e. the last 0.5 million cycles). If the inducible displacement changed by less than a micron or 0.001° during this period it was regarded as stable, i.e. exhibiting neither increasing nor decreasing tendencies. The number of degrees of freedom where inducible displacement tended to decrease was greatest with muscle loading, see Table 4.8. Therefore, we could infer that muscle loading tended to stabilise the prosthesis in the medullary canal.

Table 4.8: The number of decreasing (↓), stable (-), and increasing (↑) inducible displacements tendencies of the Lubinus femoral components tested with, and without, muscle loading, during the steady-state phase

loading	medial			posterior			distal			Θ_x			Θ_y			Θ_z			total		
	↓	–	↑	↓	–	↑	↓	–	↑	↓	–	↑	↓	–	↑	↓	–	↑	↓	–	↑
muscle loading	1	0	3	0	2	3	3	1	1	3	2	0	2	1	2	1	3	1	10	10	10
without muscle loading	0	0	5	1	2	2	1	2	2	3	1	1	1	0	4	1	1	3	7	6	17

4.4 Finite element modelling of muscle loading

This section presents the results obtained from the finite element analyses performed. Initially the gross deflection of the finite element mesh is examined, followed by the contact status of the femoral component, the stress state of the cement mantle, the strain state of the cement mantle, the probability of failure of the cement mantle, and finally, the migration of the femoral component.

4.4.1 Gross deflection of the finite element mesh

Muscle loading induced greater deflection of the finite element mesh in the medial and distal directions, as shown in Figure 4.7. However, hip joint loading only resulted in greater posterior displacement of the mesh. Through comparison of the original and deflected positions of the superior surface of the femoral component mesh, it is apparent that muscle loading produced greater overall deflection. This deflection was primarily in the medial direction.

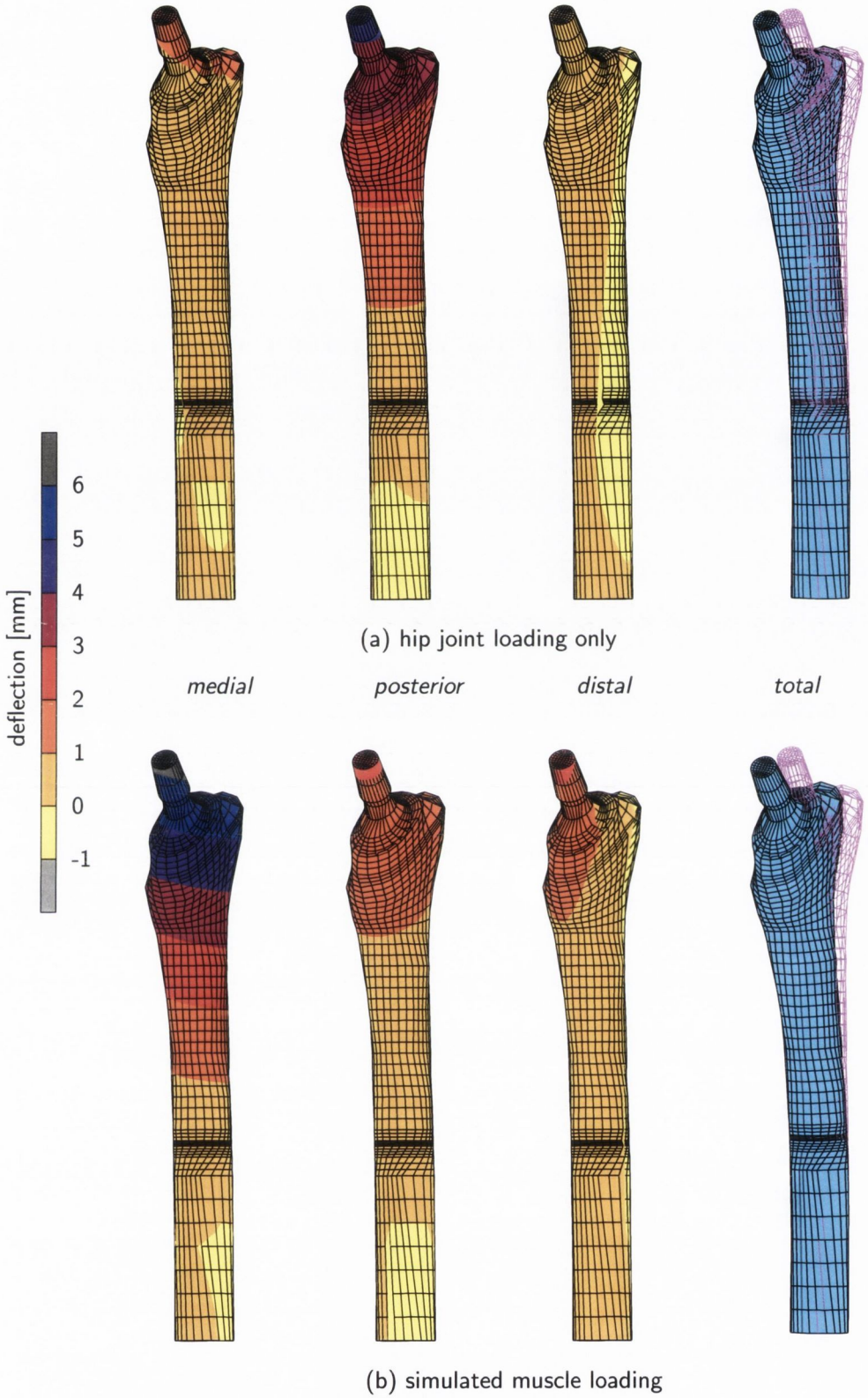

Figure 4.7: Contour plots showing medial, posterior, distal, and comparative total gross deflections of the finite element mesh when (a) loaded with the hip joint force and (b) hip joint and muscle forces. The unloaded position of the finite element mesh is represented by the wireframe outline in the total deflection plots (the deflection is scaled 2.5 times).

4.4.2 Contact status of the femoral components

As described in Section 3.3.2, the femoral component/cement interface was modelled as being initially fully bonded but was free to debond as loading was applied. After one million loading cycles both muscle loaded and non-muscle loaded prostheses had debonded in similar locations; however, the femoral component loaded with the hip joint force retained a larger bonded area, see Figure 4.8.

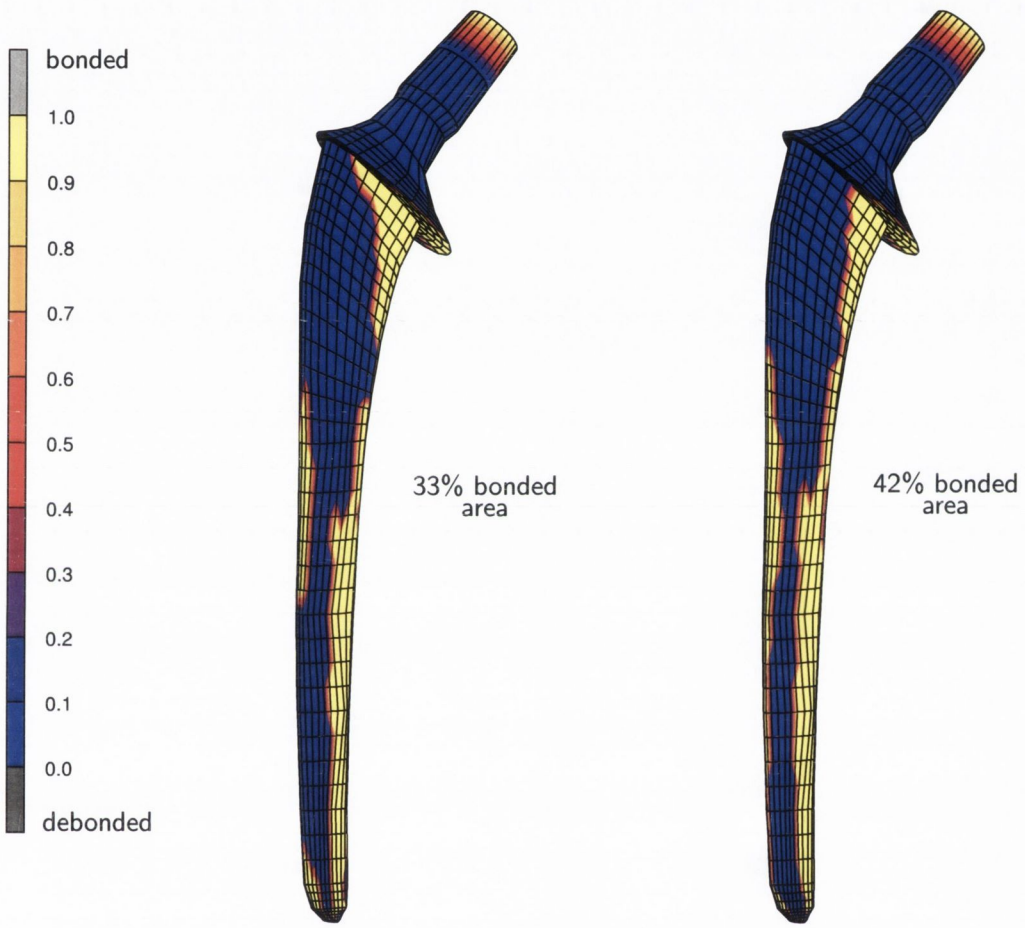

(a) simulated muscle loading (b) hip joint force only

Figure 4.8: Contour plot of contact status of the femoral components after one million loading cycles for (a) simulated muscle loading, and (b) hip joint force only. A contact status = 1.0 implies the femoral component/cement interface is fully bonded. (The superior surface of the neck of the femoral component appears bonded due to application of loading at that point)

4.4.3 Stresses in the cement mantle

4.4.3.1 Stress contours

As bone cement (PMMA) has lower tensile strength than compressive strength, it is usual to examine the tensile stresses only. The tensile stress state can be summarised by calculating the maximum principal stresses. The highest principal stresses are located distally for the cement mantle in both muscle loaded and hip joint loaded cases, see Figure 4.9. The simulated muscle loading appears to create a more highly stressed cement mantle (Figure 4.9). While the majority of both cement mantles have maximum principal stresses in the 0-2 MPa range, there is a higher stressed region proximally on the medial side of both cement mantles. The muscle loaded cement mantle has higher stresses mid-way along its lateral side than the cement mantle with hip joint loading only. This is confirmed by plotting the percentage by volume of the cement mantle which lies within a particular stress range, as shown in Figure 4.10. It is apparent that muscle loading shifts cement volumes up the stress range, as the FE model with muscle loading had higher volumes of cement in each of the stress ranges from 1-2 MPa upwards. However the percentage increase in cement volume in the higher stress volumes is very small. If the minimum principal stresses are considered, it is apparent that simulating muscle loading produces larger compressive stresses in more of the cement volume than the case with hip joint loading only, see Figure 4.11.

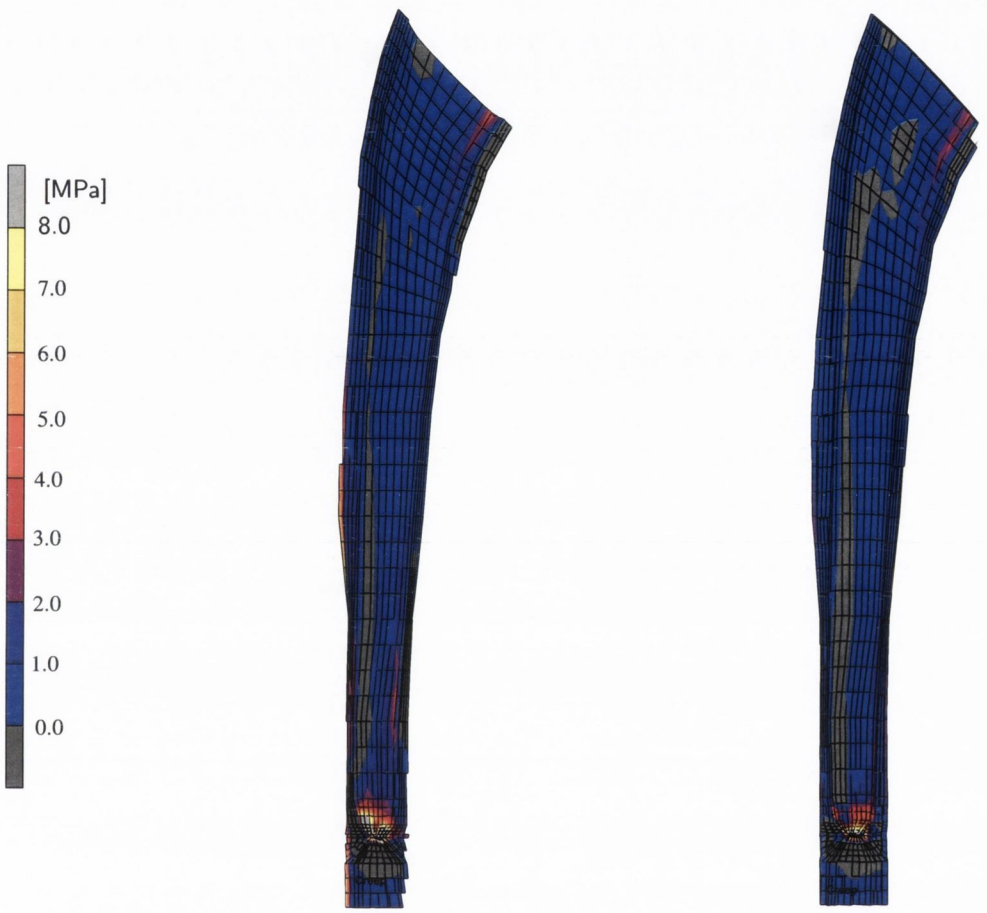

(a) simulated muscle loading (b) hip joint force only

Figure 4.9: Contour plot of maximum principal stresses after one million loading cycles for (a) simulated muscle loading, and (b) hip joint force only

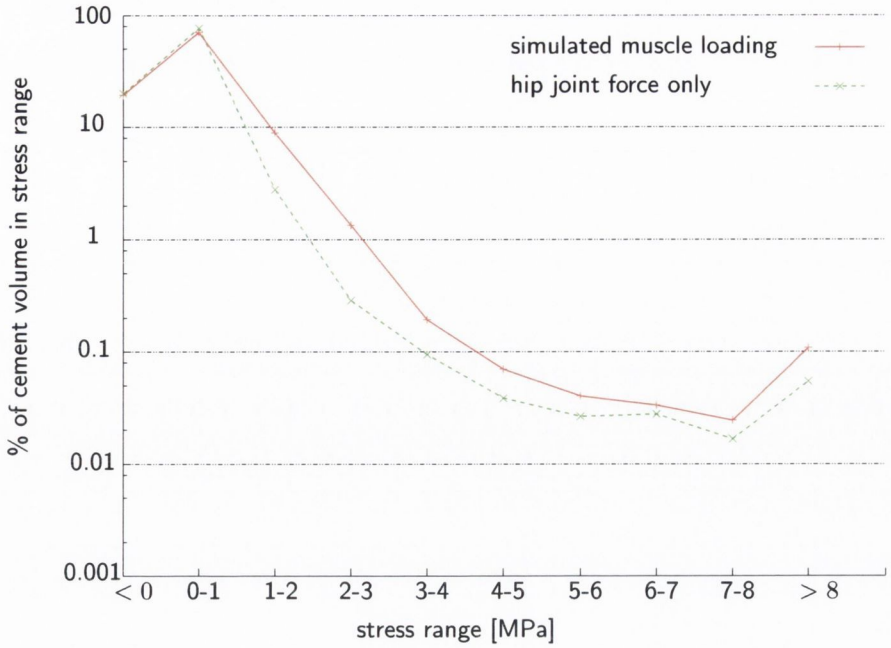

Figure 4.10: Maximum principal stress cement volumes for both FE models after one million loading cycles. *Note: log-scale used for y-axis*

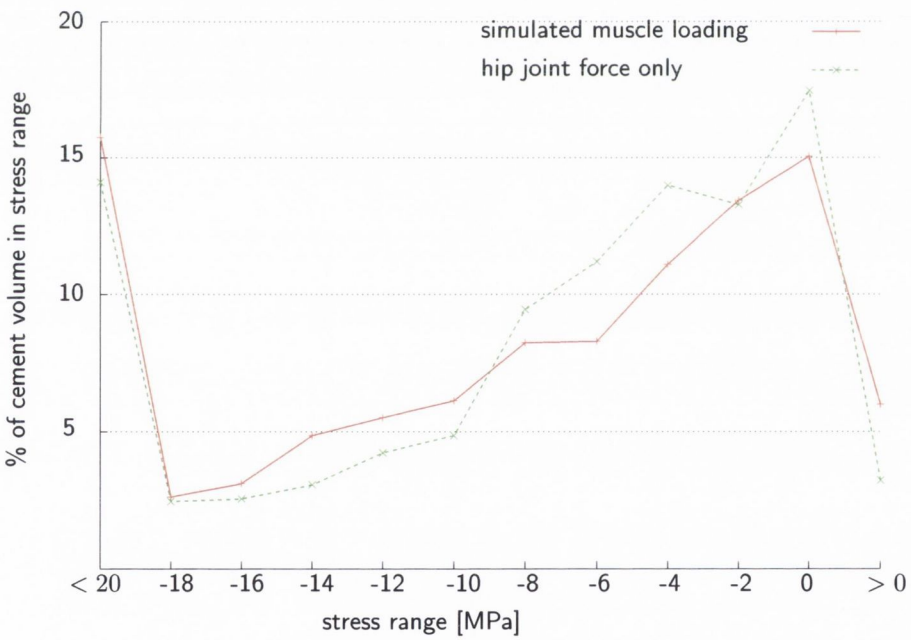

Figure 4.11: Minimum principal stress cement volumes for both FE models after one million loading cycles

4.4.3.2 Stress orientation

In the proximal and middle regions of the cement mantle, hip joint force loading only resulted in the majority of tensile stress vectors being oriented in the hoop direction (though the vectors with the largest magnitudes are aligned axially), while the stress vectors calculated when muscle loading was applied, were primarily oriented axially, as shown in Figure 4.12(a). This indicates that the cement mantle was subjected to a combination of bending and wedging, with some shearing apparent in the distal region (as some of the tensile stress vectors point in opposite directions).

The compressive stress vectors were generally aligned axially in the cement mantle for both loadcases, though a large radial component was apparent in the distal sections, see Figure 4.12(b). This confirmed that the femoral component had debonded and wedged in the cement mantle. There were more axially aligned compressive stress vectors of large magnitude in the distal cement section with hip joint loading only, particularly in the lateral-posterior region.

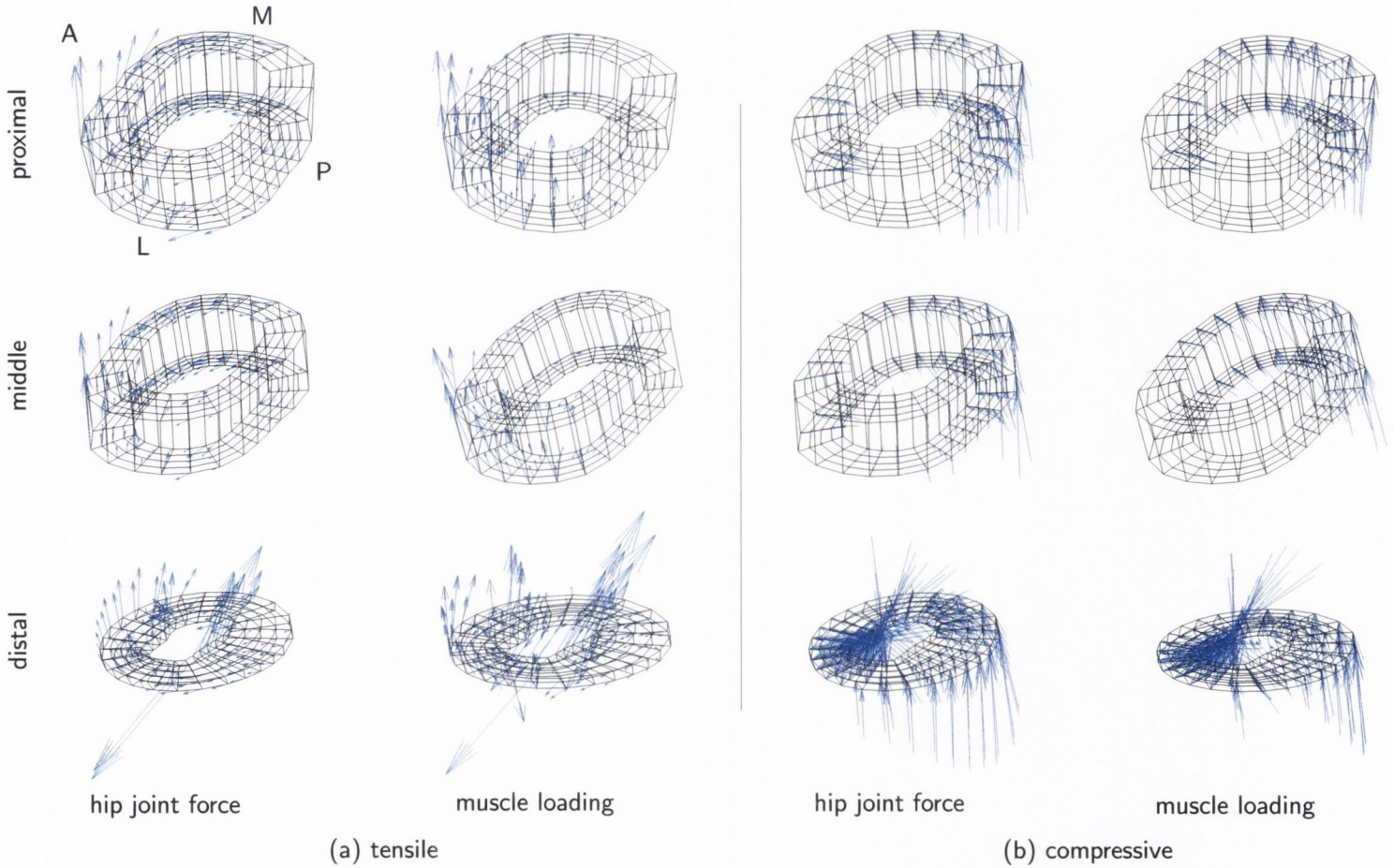

Figure 4.12: Vector plots of (a) maximum tensile principal stress vectors and (b) maximum compressive principal stress vectors in proximal, middle and distal cement mantle sections. The vector lengths indicate their relative magnitudes. Sections containing peak stresses were excluded to give a more representative view of the stress distributions. A = anterior, L = lateral, M = medial, and P = posterior. After Prendergast et al. (1989).

4.4.4 Strain in the cement mantle

Figure 4.13 shows the strain in the cement mantle, with the insets showing the strain component due to creep. Both FE models had their peak strains located distally (as expected from the stress results, section 4.4.3), with the muscle loading model displaying slightly larger areas of high strains. Creep strain constitutes a substantial portion of the total strain.

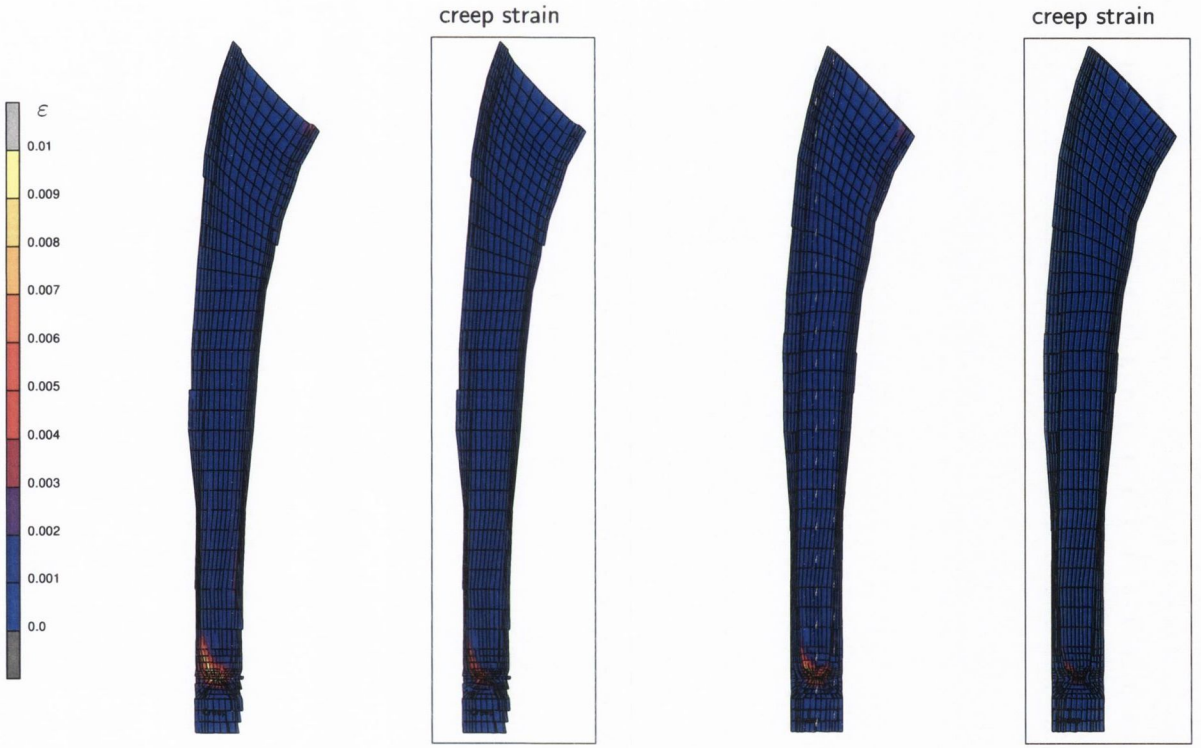

(a) simulated muscle loading

(b) hip joint force only

Figure 4.13: Contour plots of total equivalent strain after one million loading cycles for (a) simulated muscle loading, and (b) hip joint force only. The respective insets show creep strain

4.4.5 Probability of failure of cement mantle

The probability of failure of the cement mantle is highest distal to the stem tip for both loadprofiles, see Figure 4.14. The FE model which applied simulated muscle loading had higher percentages of cement volumes in each probability of failure range, though the difference in actual cement volumes is small in reality, see Figure 4.15.

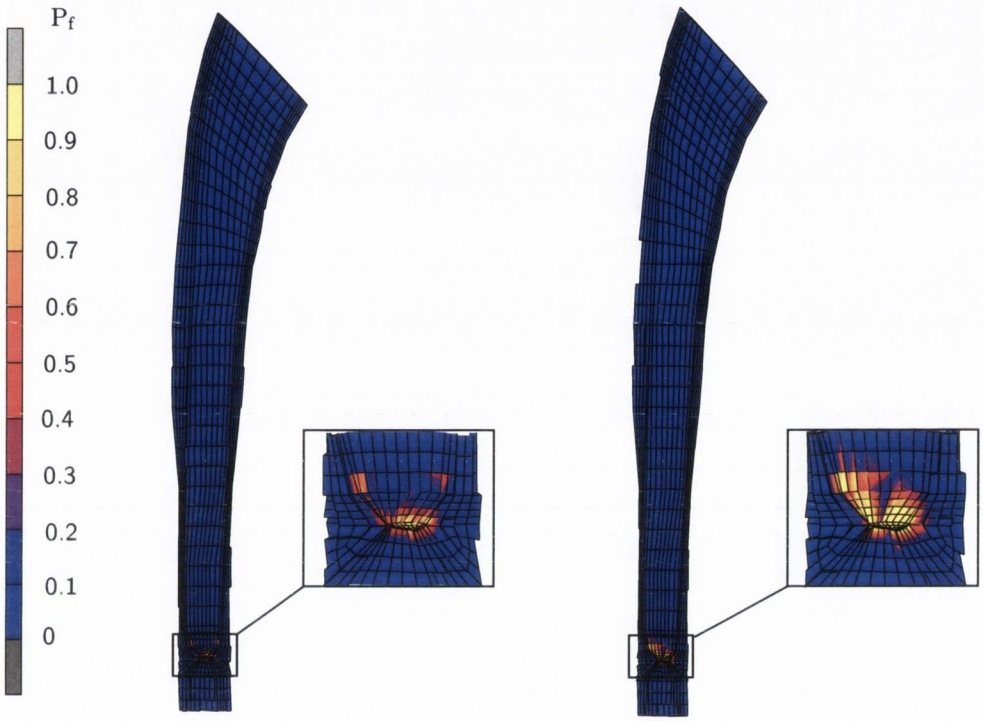

(a) hip joint force only (b) simulated muscle loading

Figure 4.14: Contour plots of the probability of failure, P_f, of the cement mantle (a) under hip joint loading only, and (b) with muscle loading. $P_f = 1$ implies failure

4.4.6 Migration of the femoral component

The migration of the femoral component in each FE model was calculated in an equivalent fashion to the experimental migrations. Nodes were selected on the femoral component at the same level as the target device was press-fitted in the experimental models. Similarly nodes on the exterior surface of the bone were selected at the same level as the points of attachment of the migration measurement

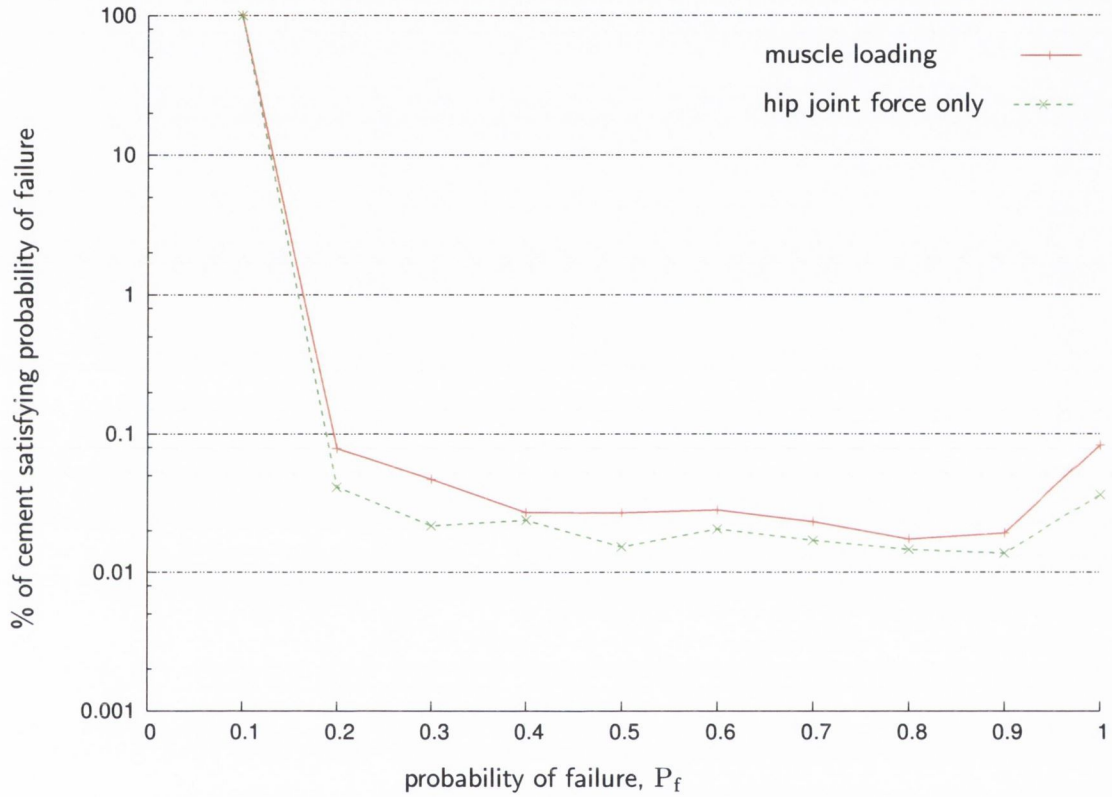

Figure 4.15: Cement volume satisfying a particular probability of failure for both FE models. $P_f = 1$ implies failure

device. Once the displacements of these points were calculated, the relative migration of the femoral component was transformed to the head centre using the same relationships as the experimental calculations. The gross deflection of the FE model during the early stages of loading (from no loading to 50% loading) was discounted. This is equivalent to the experimental tests which started at 50% of peak load (the hydraulic fatigue testing machine outputted a sinusoidal load based on the user specifying the mean value and amplitude of the wave, hence 50% loading was applied prior to the commencement of cyclic loading).

Muscle loading produced higher medial translation, higher distal translation, and larger Θ_x rotation but lower posterior translation, smaller Θ_y rotation, and smaller Θ_z rotation, see Table 4.9.

Table 4.9: Head centre migration of the femoral components in the FE models after the simulation of one million loading cycles. The experimental results are included also for comparison.

loading	medial [mm]	posterior [mm]	distal [mm]	Θ_x [degree]	Θ_y [degree]	Θ_z [degree]
simulated muscle loading	0.020	0.014	0.022	-0.014	-0.003	0.008
experimental	0.058	-0.006	0.016	-0.002	-0.018	-0.004
hip joint force only	0.014	0.029	0.020	-0.008	-0.003	-0.028
experimental	0.072	0.004	0.020	-0.002	-0.033	0.023

4.5 Experimental tests of different prosthesis designs under simulated muscle loading

In this section the behaviour of the four cemented hip replacement femoral component designs during the experimental tests described in Chapter 3 is presented.

4.5.1 Migration of the prosthesis designs

A feature of the results obtained was that considerable variation in magnitude and direction occurred, though all prostheses migrated medially and distally (subsided), see Figure 4.16. The heads of the Charnley prostheses migrated anteriorly, but the other prostheses migrated posteriorly or anteriorly somewhat randomly. One Exeter prosthesis displays unusual behaviour of quite low medial and distal migration to approximately 0.6 million cycles, but then undergoes extremely rapid medial and distal migration to 0.8 million cycles, at which stage the prosthesis reverts to more steady state behaviour. The migration results of this prosthesis were examined carefully to ascertain if it was an outlier using Grubb's test with $P = 0.05$. The conclusion was negative, which when taken with the lack of any particular experimental explanation for the prosthesis's behaviour, indicated that its results should not be discarded.

Similar considerable variation is seen in the time series curves of the prostheses' rotations, see Figure 4.17. All prostheses ultimately rotated into varus. The Charnley prostheses typically rotated such that their heads moved posteriorly and the Exeter prostheses typically rotated about their longitudinal axis into anteversion. One Lubinus femoral component experienced virtually negligible rotations.

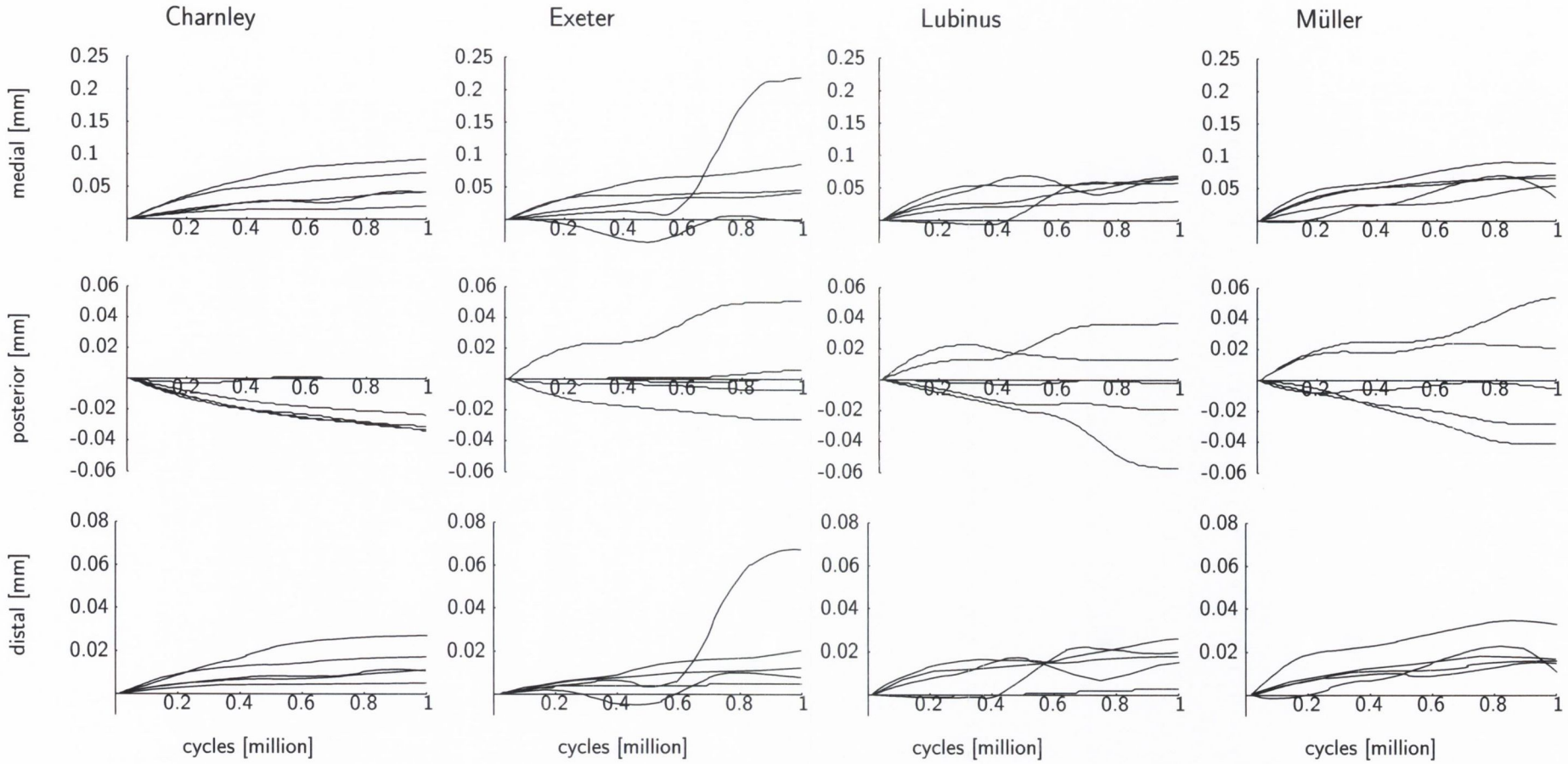

Figure 4.16: Time series curves of the prostheses translations during the course of the experimental tests

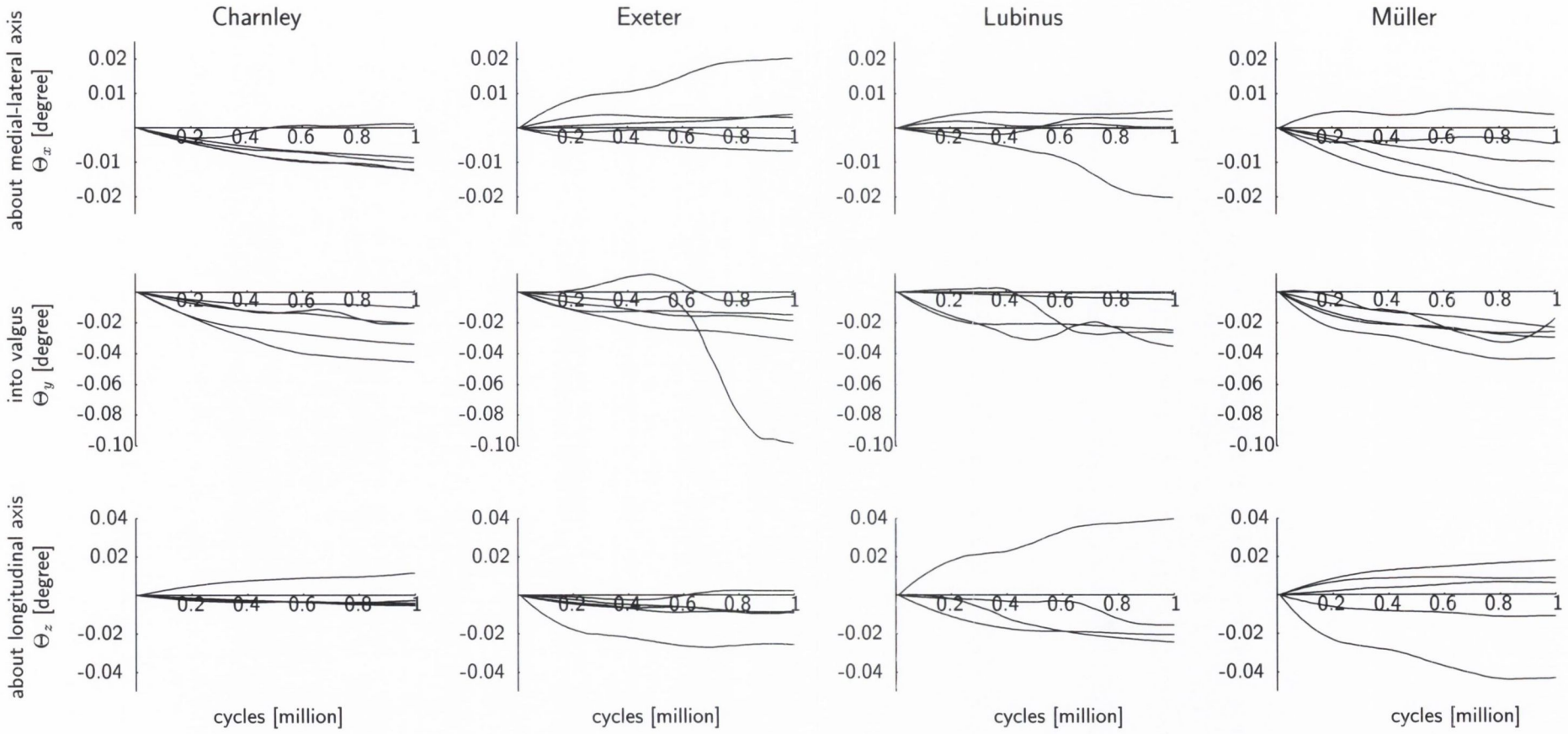

Figure 4.17: Time series curves of the prostheses' rotations during the course of the experimental tests

4.5.2 Migration after one million loading cycles

The mean migration value of each degree of freedom was calculated for the prosthesis designs, see Figure 4.18. The Exeter femoral components have the largest medial and distal translation mean values and variability. The Charnley has the largest posterior mean value, but the lowest medial and distal mean values. The Lubinus has lower mean translation values than the Müller. Medial translation is the dominant feature. The Exeter also has the largest Θ_y and Θ_z mean values. The Müller has the largest Θ_x mean value. The Lubinus has the lowest Θ_x and Θ_y mean values, while the Charnley has the lowest Θ_z mean value. It is clear that the overall trend is for the Exeter and Müller to migrate more than the Charnley and Lubinus, though these trends are not statistically significant ($\alpha = 0.05$), see Table 4.10.

Table 4.10: P values calculated using an one-way ANOVA to test for significant differences between the mean migration values of the Charnley, Exeter, Lubinus, and Müller prostheses after one million loading cycles

medial	posterior	distal	Θ_x	Θ_y	Θ_z
0.85	0.36	0.83	0.13	0.76	0.90

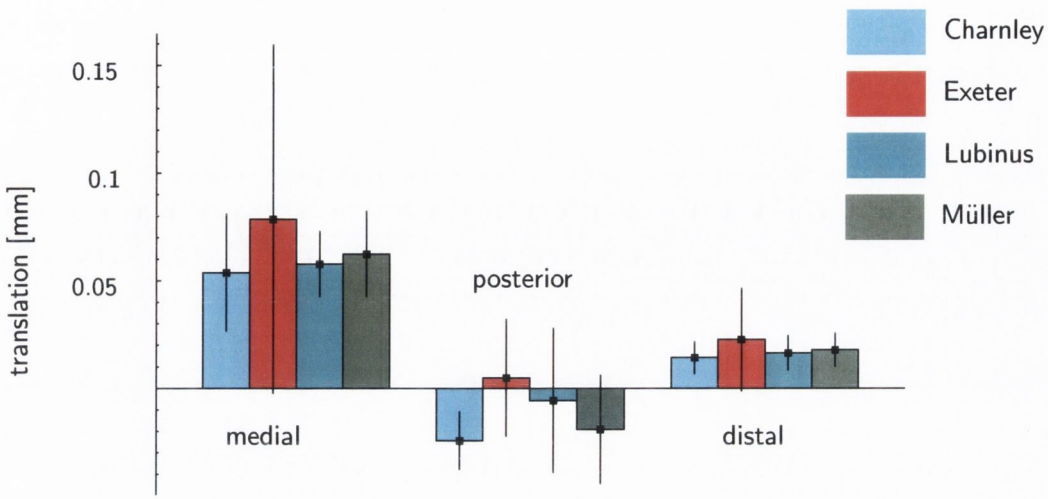

(a) translation

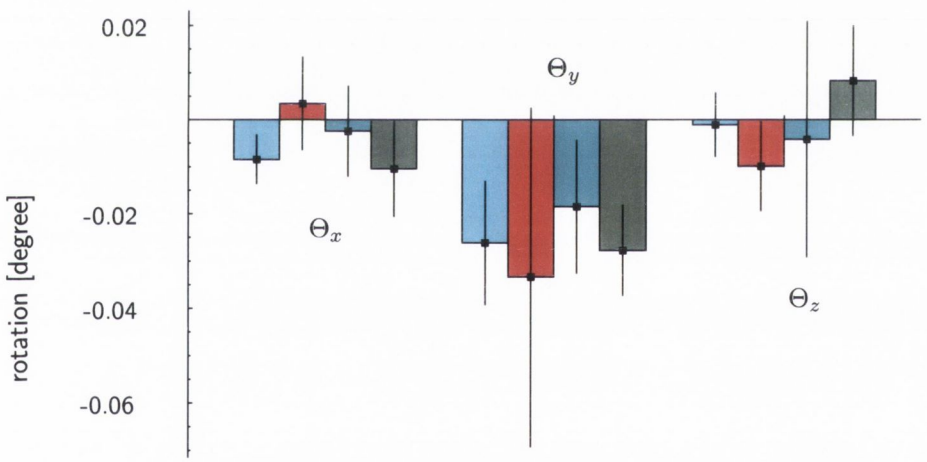

(b) rotation

Figure 4.18: Barcharts showing mean values of (a) translation, and (b) rotation after one million loading cycles for the four prosthesis designs (n=5 for each design). The error bars give 90% confidence intervals

4.5.3 Migration rates of the prosthesis designs

The early migration rates of the four prosthesis designs are similar, apart from the Θ_x rotation rate which appears to be different, see Table 4.11. Considerable variability in the migration rates is obvious from the large confidence intervals.

The steady state translation rates are quite similar for the four prosthesis designs apart from the medial translation rate of the Exeter, see Table 4.12. This is due to the unusual behaviour of one Exeter femoral component mentioned earlier in subsection 4.5.1. The generally decreasing steady-state rotation rates (Table 4.12) appear to be an artifact of individual femoral components rotating in the opposite sense (e.g. into valgus rather than into varus) to the majority of femoral components of that design (Figure 4.17). Therefore, it is difficult to discern any apparent differences or trends in the steady state rotation rates.

Table 4.11: *Early* migration rates with 90% confidence intervals for the Charnley, Exeter, Lubinus, and Müller prostheses. One-way ANOVA used to test for significant differences

	Charnley (n = 5)	Exeter (n = 5)	Lubinus (n = 5)	Müller (n = 5)	P
medial [nm/cycle]	0.08±0.04	0.04±0.08	0.07±0.05	0.09±0.03	0.41
posterior [nm/cycle]	-0.03±0.02	0.00±0.03	-0.01±0.03	-0.03±0.03	0.30
distal [nm/cycle]	0.02±0.01	0.01±0.01	0.01±0.01	0.03±0.01	0.19
Θ_x [n°/cycle]	-12±8	4±11	-2±8	-13±13	0.06
Θ_y [n°/cycle]	-39±21	-15±27	-23±25	-41±13	0.26
Θ_z [n°/cycle]	-2±10	-18±13	-7±33	14±18	0.18

Table 4.12: *Steady state* migration rates with 90% confidence intervals for the Charnley, Exeter, Lubinus, and Müller prostheses. One-way ANOVA used to test for significant differences

	Charnley (n = 5)	Exeter (n = 5)	Lubinus (n = 5)	Müller (n = 5)	P
medial [nm/cycle]	0.03±0.01	0.14±0.22	0.03±0.03	0.04±0.02	0.43
posterior [nm/cycle]	-0.02±0.01	0.01±0.02	0.02±0.04	-0.02±0.02	0.35
distal [nm/cycle]	0.01±0.00	0.04±0.06	0.01±0.01	0.01±0.00	0.38
Θ_x [n°/cycle]	-4±3	2±8	-6±14	-10±7	0.28
Θ_y [n°/cycle]	-16±6	-59±97	-11±8	-18±8	0.44
Θ_z [n°/cycle]	0±4	-1±6	-6±14	-3±11	0.84

4.5.4 Inducible displacement - time series curves

All the inducible translations display rapid early increase as expected, see Figure 4.19. Later, more stable behaviour tends to develop, though highly non-linear behaviour is apparent for several femoral components. The inducible translations of the Charnley femoral components are typically lower than those of the other prosthesis designs, particularly the inducible translations in the distal direction.

Similarly, the inducible rotations also undergo rapid early increase, see Figure 4.20, before slowing to a stable state in most instances. Again non-linear behaviour is apparent for several of the femoral components.

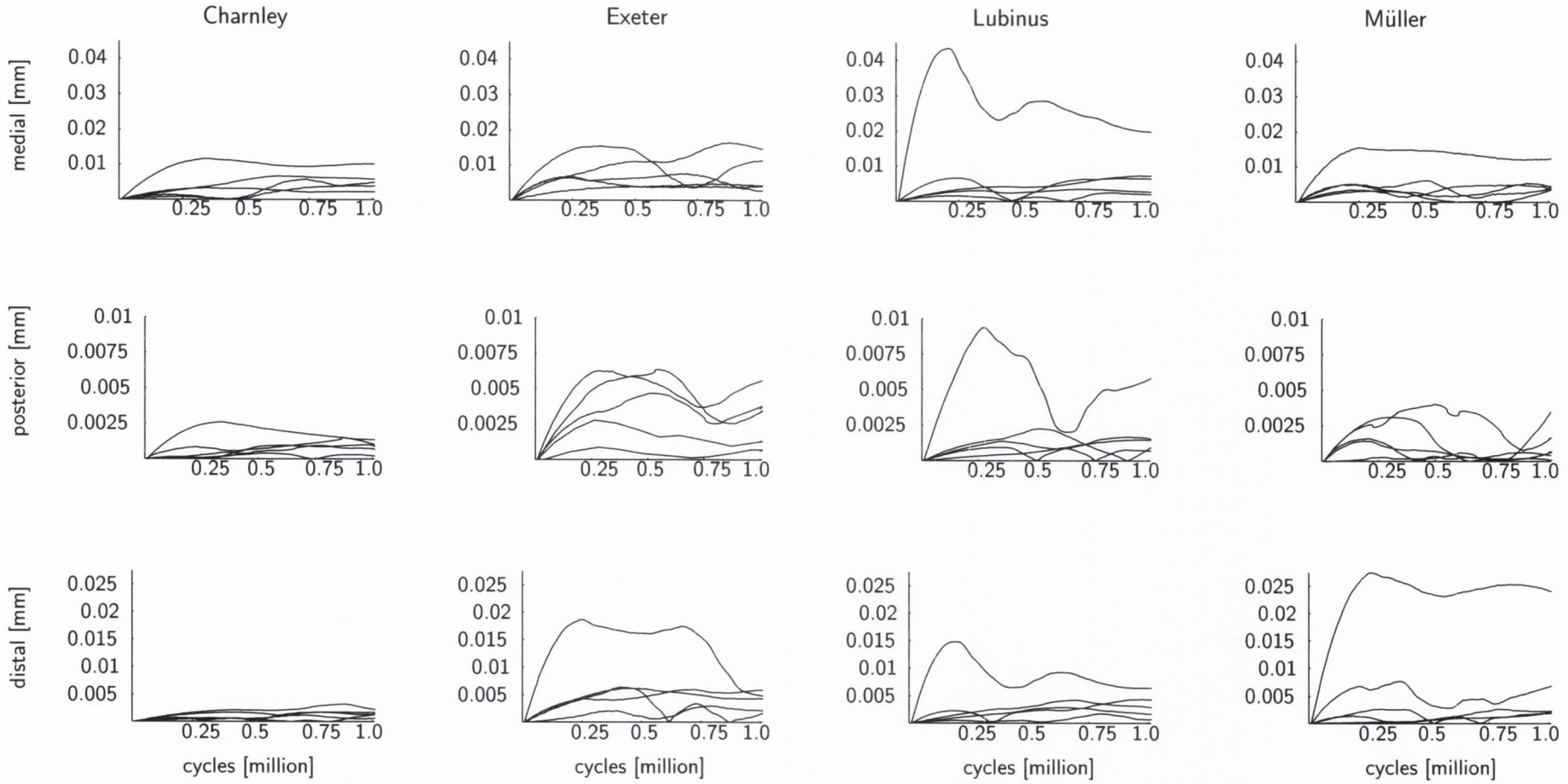

Figure 4.19: Time series curves showing the development of inducible translations of the femoral components tested under simulated muscle loading

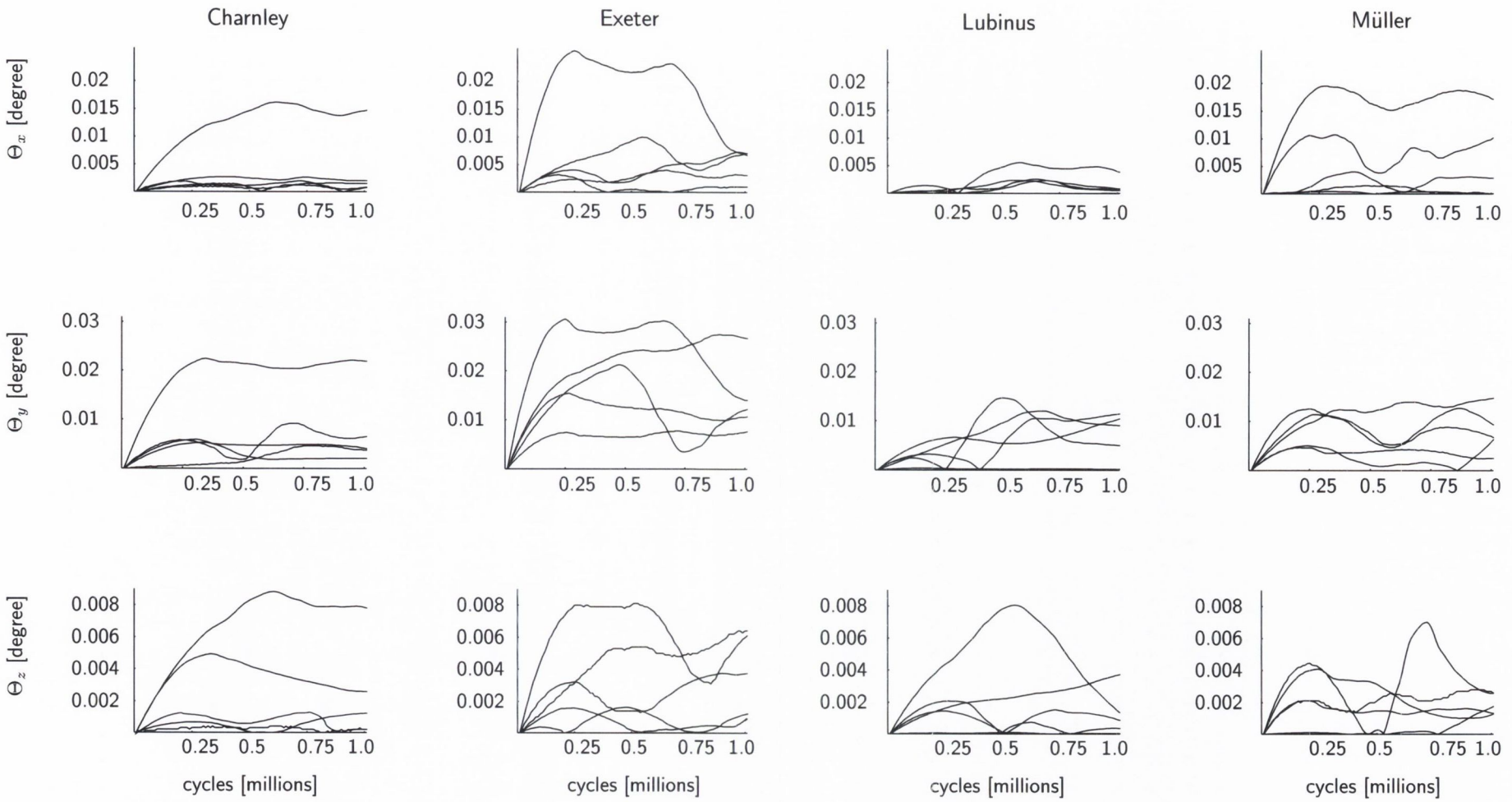

Figure 4.20: Time series curves showing the development of inducible rotations of the femoral components tested under simulated muscle loading

4.5.5 Inducible displacement values after one million loading cycles

Figure 4.21 shows mean inducible displacements after one million loading million cycles. Similarly to the mean migration results, the Charnley and Lubinus tend to have lower mean inducible displacements than the Exeter and Müller, with the Exeter having the largest medial, posterior, Θ_y, and Θ_z mean values. The Müller has the largest distal and Θ_x mean values. No significant differences in the mean inducible displacements were found, see Table 4.13.

Table 4.13: P values calculated using an one-way ANOVA to test for significant differences between the mean inducible displacement values for the Charnley, Exeter, Lubinus, and Müller prostheses after one million loading cycles

medial	posterior	distal	Θ_x	Θ_y	Θ_z
0.92	0.08	0.32	0.50	0.29	0.40

4.5.6 Inducible displacement rates for the four prosthesis designs

All the early inducible displacement rates increased as expected, see Table 4.14. No statistically significant differences in the rates were found. All the four prosthesis designs have stable steady-state inducible translation rates, i.e. neither increasing nor decreasing, apart from the distal inducible translation rate of the Exeter which is slightly decreasing (Table 4.15). The inducible Θ_x and Θ_y rates are decreasing for the Charnley, Exeter, and Lubinus femoral components while increasing for the Müller femoral components, though considerable variation is clear from the 90% confidence intervals. Inducible Θ_z rates are stable with only the Exeter femoral components showing a very slight increase. Significant differences in inducible displacement rates are not apparent, Table 4.15.

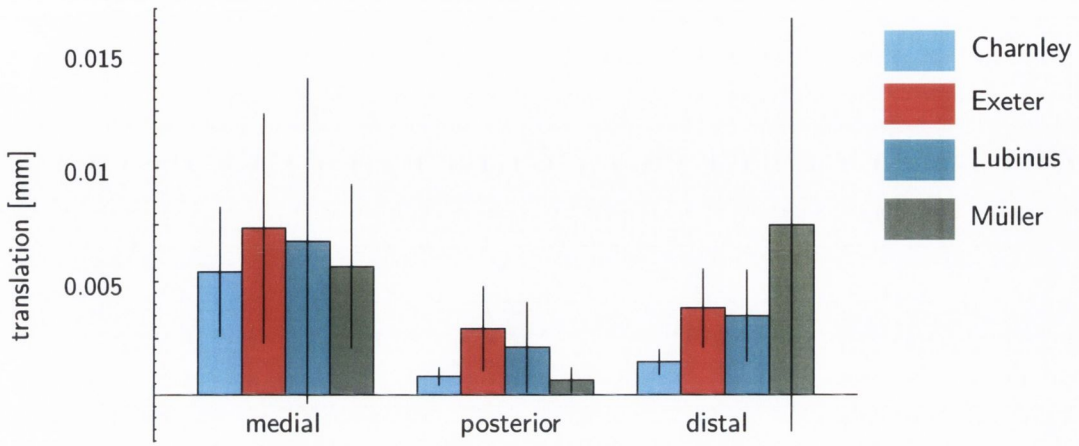

(a) inducible translation

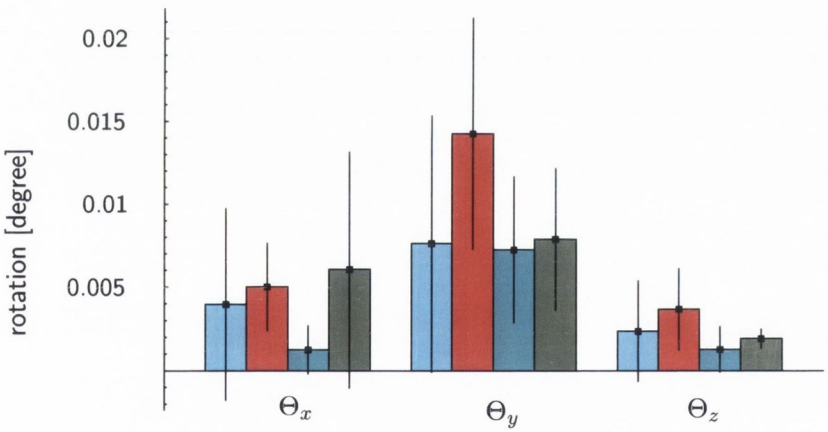

(b) inducible rotation

Figure 4.21: Barcharts showing mean values of (a) inducible translation, and (b) inducible rotation after one million loading cycles for the different prosthesis designs (n = 5 for each design). The error bars give 90% confidence intervals

Table 4.14: *Early* inducible displacement rates with 90% confidence intervals for the Charnley, Exeter, Lubinus, and Müller prostheses. One-way ANOVA used to test for significant differences

	Charnley (n = 5)	Exeter (n = 5)	Lubinus (n = 5)	Müller (n = 5)	P
medial [nm/cycle]	0.01±0.01	0.01±0.01	0.00±0.01	0.01±0.01	0.25
posterior [nm/cycle]	0.00±0.00	0.01±0.00	0.00±0.00	0.00±0.00	0.10
distal [nm/cycle]	0.00±0.00	0.01±0.01	0.00±0.00	0.01±0.02	0.21
Θ_x [n°/cycle]	7±12	9±13	3±3	8±10	0.79
Θ_y [n°/cycle]	11±15	29±15	11±11	9±9	0.09
Θ_z [n°/cycle]	5±7	6±6	4±6	0±3	0.52

Table 4.15: *Steady state* inducible displacement rates with 90% confidence intervals for the Charnley, Exeter, Lubinus, and Müller prostheses. One-way ANOVA used to test for significant differences

	Charnley (n = 5)	Exeter (n = 5)	Lubinus (n = 5)	Müller (n = 5)	P
medial [nm/cycle]	0.00±0.01	0.00±0.04	0.00±0.00	0.00±0.01	0.99
posterior [nm/cycle]	0.00±0.01	0.00±0.01	0.00±0.03	0.00±0.02	0.33
distal [nm/cycle]	0.00±0.00	-0.01±0.01	0.00±0.00	0.00±0.00	0.15
Θ_x [n°/cycle]	-1±5	-7±8	-1±10	4±13	0.38
Θ_y [n°/cycle]	-1±13	-9±81	-2±15	5±19	0.25
Θ_z [n°/cycle]	0±3	0±6	1±15	0±8	0.80

4.5.7 Rates of change of inducible displacement of the four prosthesis designs

The Exeter had the greatest number of degrees of freedom with *decreasing* inducible displacements, while the Müller had the greatest number of degrees of freedom with *increasing* inducible displacements, see Table 4.16. The Exeter also had the least number of increasing inducible displacements. Although the Charnley had the least number of decreasing inducible displacements, it also had the greatest number of stable inducible displacements (the Müller having the least).

Table 4.16: The decreasing (↓), stable (-), and increasing (↑) inducible displacements tendencies of the femoral components tested with, and without, muscle loading, during the *steady state* phase

prosthesis	medial			posterior			distal			Θ_x			Θ_y			Θ_z			total		
	↓	-	↑	↓	-	↑	↓	-	↑	↓	-	↑	↓	-	↑	↓	-	↑	↓	-	↑
Charnley	0	3	2	0	5	0	1	3	1	1	3	1	0	3	2	3	1	1	5	18	7
Exeter	1	3	1	2	3	0	3	1	1	2	2	1	3	1	1	1	2	2	12	12	6
Lubinus	1	1	3	0	2	3	3	1	1	3	2	0	2	1	2	1	3	1	10	10	10
Müller	2	0	3	1	4	0	0	1	4	1	1	3	1	0	4	1	2	2	6	8	16

Note: A ranking by number of increasing inducible displacement degrees of freedom would be, from best to worst: Exeter, Charnley, Lubinus, Müller

4.6 Summary of results

This section summarises the main results obtained from the experimental tests and numerical simulations which are pertinent to the hypotheses of this thesis.

4.6.1 Migration

- Muscle loading produced lower mean migration after one million loading cycles, typically with reduced experimental scatter, compared to hip joint loading. However, the differences do not appear to be significant.
- Muscle loading produced lower migration rates, both early and steady state. Again this difference does not appear to be significant.
- No discernible differences in measured migration values of comparative tests after one million loading cycles. Medial translation and Θ_y rotation largest.
- Muscle loading produced higher medial and distal translations, and higher Θ_x rotation in the FE calculations, and this is the opposite to the experimental results.

4.6.2 Inducible displacement

- The mean inducible displacement values, particularly the inducible rotation values, were lower under muscle loading at one million loading cycles.
- Muscle loading produced more degrees of freedom of inducible displacement having a decreasing tendency, and less degrees of freedom of inducible displacements having an increasing tendency.
- No significant differences in the mean inducible displacement values at one million cycles in the comparative tests.
- If a ranking is done, based on degrees of freedom of inducible displacement with increasing tendencies, the Exeter performs the best and the Müller has the worst performance. However, this must be considered in the context that inducible displacement magnitudes depend on the location of the target device.

Chapter 5

DISCUSSION

Contents

5.1 Introduction

As described in Chapter 1, the author's thesis is that an experimental test can be devised which can differentiate the performances of four cemented hip replacement femoral components. An ancillary hypothesis is that such an experimental test requires the simulation of muscle loading.

To defend this thesis, a mechanism capable of applying the hip joint reaction force and muscle forces simultaneously to the proximal femur to mimic physiological loading over several million cycles of loading was designed and fabricated. It was used to load proximal composite femurs implanted with cemented hip replacement femoral components; in doing so the pre-clinical tests developed previously by Maher (2000) were advanced by the simulation of muscle forces.

5.2 Limitations of study

A full understanding of the limitations inherent in this study is necessary before discussion of the obtained results. Gait was the only loading activity simulated and, even for gait, simplifications were made; for example, it was assumed that all the muscle forces were in phase with the joint reaction force, and the forces were applied as sinusoidal waves rather than the typical double-peak loadprofile. These simplifications must be kept in mind because there is strong evidence to suggest that torsion of the femoral components experienced during stair climbing can significantly exceed experimentally determined torsion resistance limits of the femoral component (Bergmann et al., 2001; McCormack et al., 1999), with the torsion value being 23% greater during stair climbing than walking. Simulation of activities such as fast walking, jogging or even stumbling would require the application of considerably higher loads (Bergmann, 2001).

The experimental tests were run continuously at 5 Hz, allowing no relaxation periods. Verdonschot et al. (2002) found that including relaxation periods increased

the subsidence rate by a factor of four. The tests were conducted at room temperature in air; higher migrations might have been measured if the tests were carried out in physiological environmental conditions (as the material properties of bone cement have been found to decrease with temperature (Lee et al., 1977)). An additional consequence of conducting the experiments at room temperature was that the sensitivity of the migration measurement device fluctuated with room temperature, see Section 4.2.1. This caused a systematic error of up to five microns in measurements of translation; however, this error is contained within the observed variation in the experimental tests. The design calculations for the experimental device were carried out in the frontal plane, neglecting the out-of-plane forces as these were generally small. This limitation was modelled in a FE analysis; reduced posterior gross deflection was calculated. However, stress levels and locations in the cement mantle were very similar, e.g. the peak tensile stress was only reduced by 2.5% (from 21.6 MPa to 21.0 MPa). Finally, it was not possible to control the magnitude or location of porosity in the cement mantles.

Biological processes, such as bone remodelling or soft tissue formation, were not simulated. Furthermore, operative factors, such as variation in stem placement, bone necrosis due to trauma, and blood entrapment at the interfaces are not included in the experimental model. The measured inducible displacement values depended on the location of the migration measurement device (Section 4.2.2). To minimise the influence of this, the migration measurement device was located at the same distance (within six millimetres) from the resected surface of the composite femur for each femoral component type, corresponding to a mid-stem location for the Charnley, Exeter, and Lubinus prostheses, and a more distal location for the Müller prostheses.

Porosity, residual curing stresses, and damage accumulation, were not simulated for the cement in the finite element models. Murphy and Prendergast (1999, 2001) conducted fatigue tests of bone cement specimens and found that all cracks, hence damage accumulation, originated from pore boundaries. Similarly, Dunne and Orr (2001) found that the lower the cement porosity, the better the cement's flexural

and compressive properties. Lennon and Prendergast (2002), in an experimental and numerical study, found that residual stresses in the cement mantle caused by shrinkage during curing, were large enough to generate pre-load cracks. This finding was confirmed by Orr et al. (2003) using three-dimensional bone cement specimens. Additionally, the creep law used was derived for hand mixed cement, not vacuum mixed as used in the experimental tests (vacuum mixed cement contains less pores, but the pores which do exist tend to be larger in size, at least for the vacuum mixing system used in this study, (Murphy and Prendergast, 2000)).

5.3 Influence of simulating muscle loading in experimental tests

It was found that inclusion of muscle loading slowed the rate of prosthesis migration, and also resulted in lower inducible displacement at one million cycles.

5.3.1 Migration differences

Although there is a definite trend for reduced migration when muscle loading is applied in the experimental tests, a statistically significant result was not found. The steady state migration rates measured for both loadprofiles are similar. Therefore the differences in migration mainly result from the different rates of the early, more rapid period of migration measured in our tests. The measured migration time series curves resemble the primary and secondary stages of the dynamic creep curves of polymethylmethacrylate (bone cement) determined by Verdonschot and Huiskes (1994), see Figure 5.1. This curve was obtained from cyclic uniaxial tensile tests of hand mixed bone cement specimens conducted in saline solution at 38° Celsius; hence, the results obtained included the effects of damage accumulation in the cement. There is an initial phase of rapid increase followed by gentler, more steady state behaviour, implying it is possible that the migration curves are caused by dynamic creep. The extended duration of the migration curves probably occurred because: (i) the experimental tests were conducted in air at room temperature, (ii)

the compressive stresses partially counter-acted the tensile stresses (compression reducing the propensity of microcracks to grow), and (iii) the reduced porosity of the vacuum mixed cement.

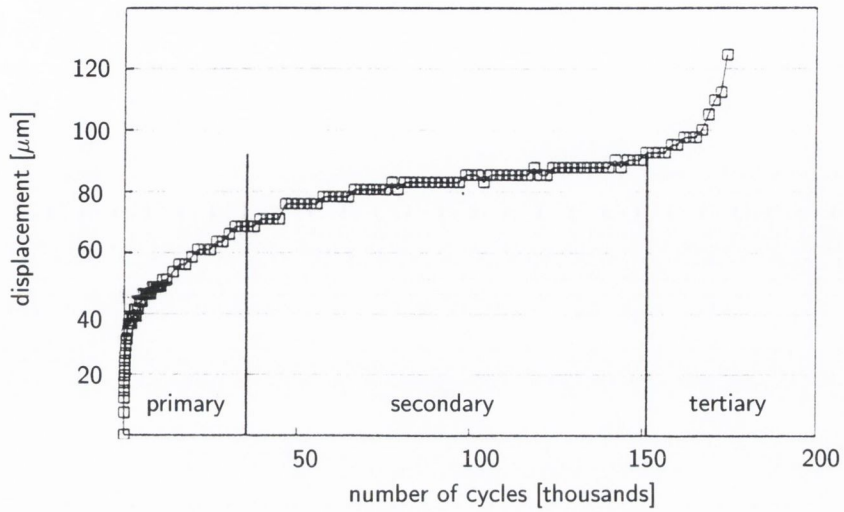

Figure 5.1: A typical dynamic creep curve of hand-mixed Simplex P bone cement tested in saline solution at 38° C. Adapted from Verdonschot and Huiskes (1994)

In the experimental tests it was found that muscle loading resulted in lower medial, higher posterior, and lower distal translation whereas the opposite was found with the finite element simulations. However, both the experimental and numerical tests found lower *resultant* translation when muscle loading was applied. The reason for reduced migration when muscle loading was simulated in the experimental tests was previously hypothesised as being due to the stabilising influence of the muscles in reducing bending moments across the implanted femur, and hence, reducing stresses in the cement mantle (Pauwels, 1965; Britton et al., 2003). This is apparently contradicted by the results of the finite element simulations which found higher peak tensile stresses with muscle loading. But the overall stress states in the cement mantles of both FE models are broadly similar, with any increase in greater volumes of cement in higher tensile stress ranges with muscle loading, compensated for with greater volumes of cement in the higher compressive stress ranges. The similar stress states are also in agreement with the lack of significant differences in the observed experimental migrations.

5.3.2 Inducible displacement differences

Muscle loading produced lower mean inducible displacements. While the differences are not statistically different, it is noteworthy that the confidence intervals for those femoral components tested under muscle loading are smaller than the corresponding confidence intervals for the femoral components tested with hip joint reaction force only, except for medial inducible displacement. This is another indicator that including muscle loading resulted in less variability in the experimental tests. It appears that including muscle loading produced lower recoverable displacements of the femoral components. A possible explanation for the random direction changes in the inducible rotations (Figure 4.5) is that, as the prosthesis migrates, the point of collar-calcar contact may vary and change the centre of rotation of the femoral component.

Whilst the early and steady state mean inducible translation rates are similar with and without muscle loading, the early and steady state mean inducible rotation rates are lower for the femoral components tested under muscle loading. This trend appears to be significantly different for the early inducible Θ_x rotation, and for the steady state inducible Θ_y rotation. However, the most obvious difference between the two modes of loading is that a greater number of degrees of freedom of the inducible displacements of the femoral components tested without muscle loading tended to increase. This may be indicative of instability and continued loosening, and is discussed further in Section 5.4.4.

5.3.3 Comparison of results with clinical studies of Lubinus SPII prostheses

In the clinical study of Kärrholm et al. (2000), the subsidence (i.e. distal migration) of 20 Lubinus SPII femoral components relative to the femur was, after a period of two years, approximately 0.050 mm, see Figure 5.2. This is of similar magnitude to the distal migration measured in the experimental tests investigating the influence of muscle loading, even more so when the number of gait cycles per year of a typical person is considered, a figure which ranges from approximately one million cycles per

annum (Zahiri et al., 1998) to in excess of three million cycles per annum (Morlock et al., 2001). Indeed, if the measured mean distal migration was extrapolated to six million cycles, using the steady state rate of migration value from Table 4.4, it was found that the extrapolated value was 0.066 mm for the femoral components tested under muscle loading, and 0.070 mm for the femoral components tested under hip joint loading only.

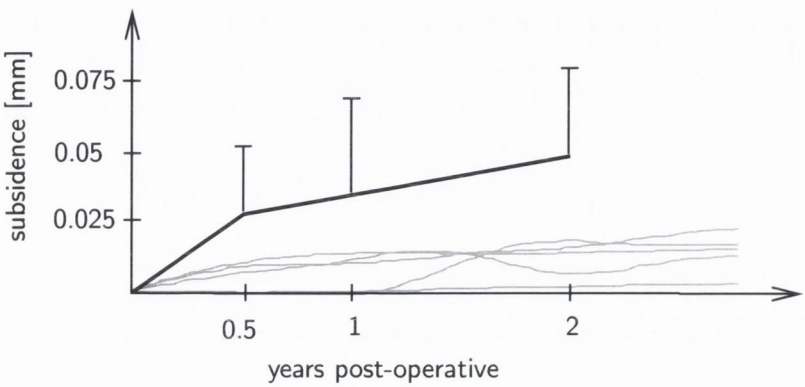

Figure 5.2: *In vivo* subsidence (distal migration) of Lubinus SPII femoral components. The error bars give one standard deviation. (The grey curves represent the distal migration of the Lubinus femoral components tested with muscle loading for one million cycles in the present study.) Adapted from Kärrholm et al. (2000).

Kärrholm et al. (2000) also observed rotations of the femoral components of median ranges 0.1° to 0.5° posterior (corresponds to Θ_x), 0.2° to 0.7° valgus (corresponds to Θ_y), and 0.0° to 0.2° retroversion (corresponds to Θ_z). These clinically observed rotations are an order of magnitude greater than the rotations measured in this study. A possible reason for this may be due to the exclusion of loads due to activities other than normal gait in the experimental tests, as mentioned in Section 5.2.

However, considerable variability is apparent in the results of Kärrholm et al. (2000), as represented by the error bars in Figure 5.2. If the percentage ratio of one standard deviation to the mean value is computed (analogous to the statistical measure known as the coefficient of variability) for the subsidence observed by Kärrholm and compared to that found in this study for the muscle loaded Lubinus

prostheses (60% vs. 30%), it seems that the scatter observed in the *in vitro* experimental tests reported in this thesis is considerably less than the scatter observed *in vivo*. A probable reason for the wider *in vivo* scatter is the different body weights and activity levels of the patients in the study of Kärrholm et al. (2000). Surgical variability may also play a role as, although the patients were all operated on in the same hospital, it is not clear whether the same surgeon performed the procedures.

5.3.4 Other measures from the numerical analyses

Dynamic creep, as modelled in the finite element simulations, appears to explain the migration of the femoral component. The migration values obtained from the finite element models lie within the ranges obtained from the experimental tests, apart from medial translation. Even if the medial translation obtained from the FE simulations is of the same order of magnitude as that measured in the experimental tests, it is significantly lower (0.020 mm vs. 0.060 mm). A possible explanation for this is that, in operation, the experimental rig may have applied greater force laterally than intended by design. When the finite element resultant translations were calculated for the two loadprofiles, the muscle loading value was less than that with hip joint loading only (0.033 mm vs. 0.038 mm). Although muscle loading produced greater deflection in the FE model, this probably was as a result of restraining the finite element mesh at the mid-diaphysis of the femur (as only the proximal part of the femur was modelled). The opposite was found by Polgar et al. (2003), who reported the head centre displacements of a finite element model of an intact femur, which was restrained at the mid-diaphysis region. The displacements they calculated were also several millimetres when the hip joint load only was applied; however, they calculated lower head centre displacements when muscle loading was included in their model. Unfortunately, Polgar et al. (2003) do not report the directions of the muscle vectors nor the magnitude or direction of the hip joint force used. Hence, it is probable that the differences between their study and that reported in this thesis result from different applied loads.

As expected from the stress results obtained from the FE models, the probabil-

ities of failure of the cement mantles were similar, with muscle loading slightly increasing the percentage of cement volume in the higher probability of failure ranges. The slight differences in orientation of the tensile stress vectors resulted from more of the lateral aspect of the femoral component remaining bonded when hip joint loading only was applied. Both loadprofiles had a small percentage of cement with a probability of failure equal to one, located distal to the tip of the femoral component. As this probability of failure calculation is based on ten million loading cycles, it suggests that the cement mantles of the Lubinus femoral components are mostly intact after one million cycles of experimental loading. The contact status of the femoral component in the FE models shows that the stem debonded similarly for both loadprofiles. When the debonding process was examined with respect to time, the femoral component started to debond at the midpoint of the ramp loading in both analyses, continued to debond until the ramp loading had peaked, and remained partially debond for the duration of the quasi-static loading. Partial debonding of the femoral component/cement interface is consistent with clinical retrieval studies (Fornasier and Cameron, 1976; Gruen et al., 1979; Jasty et al., 1991), and other finite element analyses of implanted cemented hip femoral components (Lu et al., 1996).

5.3.5 Should muscle loading be included in comparative experimental tests?

When the evidence is considered in its totality, the conclusion drawn was that muscle loading should be included in the comparative experimental tests because (i) muscle loading reduced variation in experimental results, providing increased confidence in the results obtained, (ii) muscle loading considerably reduced the number of increasing steady state inducible displacement rates, and (iii) muscle loading produced subsidence amounts more similar to clinical observations than non-muscle loading for the Lubinus prostheses.

5.4 Comparative tests of prosthesis designs

The primary hypothesis of this thesis is that the application of a physiological load-case to an implanted proximal femur should enable a long-term in vitro test to distinguish between four different cemented hip femoral component designs. To test this hypothesis, a total of 20 implanted proximal composite femurs (four prosthesis designs with five tests each) were tested under a cyclic load intended to mimic normal gait by simulating muscle loading. Differences in the mean migration at one million cycles (Figure 4.18), and both early and steady state migration rates (Table 4.11 and Table 4.12) were found. However when the results were tested using an one-way ANOVA, no statistically significant differences were found.

Due to time constraints (each test took one week between specimen preparation and test set-up) it was possible to test only five of each femoral component design for one million cycles each. However, based on the results obtained, the sample sizes required to distinguish between the femoral component designs for a particular level of statistical significance can be determined. According to Zar (1999), the sample size can be calculated as:

$$\mathrm{n} = \frac{2\mathrm{k}(\mathrm{s}^2)(\phi^2)}{\delta^2} \qquad (\text{for } \alpha = 0.05) \tag{5.1}$$

k is the number of treatments (i.e. different prosthesis designs), s is the within-group standard deviation of the individual measurements, ϕ is related to the non-centrality parameter (taken from tables, describes a normally distributed variable with a non-zero mean), and δ is the minimum detectable difference (i.e. expected difference between means). For instance, if Θ_x rotation at one million cycles is the measure under consideration, then when Equation 5.1 is evaluated, it gives n = 39. Similarly, if distal translation (subsidence) after one million loading cycles is considered, then n = 248. Therefore, with the level of variation observed in this study, the number of tests required for statistically different measurements of migration seems prohibitive. It is worth noting that Malchau et al. (1993) estimated that 48,370 patients would have to be recruited in a study comparing the survival of Exeter polished and Lubinus SP prostheses over five years to achieve a power of 80% (the

power of a statistical test is the probability of rejecting the null hypothesis correctly (Zar, 1999)).

It is interesting to consider the potential sources of the variation in the experimental results. The implantation of the prosthesis in the composite femur can result in a slightly different placement on each occasion as the dimensions of the composite femurs used can vary by 1.5 mm between specimens (Maher, 2000). This difference in positioning could cause variations in the migration and inducible displacements measured directly, and also indirectly through differences in the amount of pre-load microcracks induced by thermal stresses during cement polymerisation. In a series of experimental tests and a theoretical study, Lennon and Prendergast (2002) found that shrinkage of the cement mantle during curing caused residual stresses high enough to initiate cracks in the presence of stress raisers such as pores (the differences between different prosthesis designs may result, in part, from their different mass and thermal characteristics). As previously mentioned, Murphy and Prendergast (2000) found considerable variability in the fatigue strength of vacuum-mixed bone cement in unaxial fatigue tests. This variability is, in part, due to the random distribution of pores in the cement, which in turn, influences the damage accumulation distribution in the cement mantle (Lennon, 2002). Dunne et al. (2003) conducted fatigue tests of bone cement specimens prepared using different mixing systems, and noted that the Optivac™ (Scandimed A.B., Sweden) system produced particularly high variation in the measured fatigue life of the specimens. This mixing system was used in the present study. Murphy and Prendergast (2003) carried out multi-axial fatigue tests of tubular bone cement specimens. They found that multi-axial loading greatly increased the variability in fatigue life of the specimens, and concluded that this may partly account for variability in loosening rates of orthopaedic implants.

5.4.1 Comparison of results with other experimental studies

The results from the experimental tests of Huiskes et al. (1998), Maher and Prendergast (2002), Liu et al. (2003), and Cristofolini et al. (2003), together with the results

obtained in this study are listed in Table 5.1. It is apparent that the experimental results presented in this thesis are lower than those measured by other researchers. Only the mean distal migration of the Lubinus SPII femoral components is similar to the mean distal migrations measured by Maher and Prendergast (2002) and Cristofolini et al. (2003). The fundamental difference between the testing methodology presented herein and the methodologies of the other researchers listed in Table 5.1 is that muscle loading was included in this study. Other differences include the application of a higher peak load (Maher and Prendergast, 2002; Liu et al., 2003), the use of elevated testing temperatures (Huiskes et al., 1998), testing in fluids (Huiskes et al., 1998; Liu et al., 2003), and the direct application of moments to the femoral component head (Cristofolini et al., 2003).

Table 5.1: Summary of migration results obtained by other researchers during *in vitro* experimental fatigue tests of femoral components. All results are after one million loading cycles, except for those of Maher and Prendergast (2002) which are for two million loading cycles. The grey rows indicate the migration values measured in this study. *Note: Standard deviations, where quoted by authors, have been converted to 90% confidence intervals.*

Prosthesis Researcher	medial [mm]	posterior [mm]	distal [mm]	about medial-lateral axis [degree]	into valgus [degree]	about longitudinal axis [degree]
Charnley						
Liu et al. (2003)			0.101	-0.045	0.18	0.09
This study	0.054 ± 0.027	-0.024 ± 0.014	0.014 ± 0.008	-0.008 ± 0.005	-0.026 ± 0.013	-0.001 ± 0.007
Exeter						
Huiskes et al. (1998)			0.050 ± 0.041			
This study	0.079 ± 0.081	0.005 ± 0.027	0.023 ± 0.024	0.003 ± 0.010	-0.033 ± 0.036	-0.010 ± 0.010
Lubinus						
Maher and Prendergast (2002)	0.138 ± 0.115	0.222 ± 0.500	0.043 ± 0.081	0.071 ± 0.158	-0.056 ± 0.041	0.098 ± 0.194
This study	0.058 ± 0.015	-0.006 ± 0.034	0.016 ± 0.008	-0.002 ± 0.010	-0.018 ± 0.014	-0.004 ± 0.025
Cristofolini et al. (2003)			0.034 ± 0.026			
Müller						
Maher and Prendergast (2002)	0.296 ± 0.298	0.547 ± 0.543	0.113 ± 0.115	0.127 ± 0.125	-0.142 ± 0.140	0.419 ± 0.421
This study	0.063 ± 0.020	-0.019 ± 0.025	0.018 ± 0.008	-0.010 ± 0.010	-0.028 ± 0.010	-0.004 ± 0.023
Cristofolini et al. (2003)			0.097 ± 0.110			

5.4.2 Comparison of results with clinical findings

Kärrholm et al. (2000), Alfaro-Adrian et al. (2001), Kiss et al. (1996), Sutherland et al. (1982) made measurements of *in vivo* prosthesis migration, as listed in Table 5.2. Sutherland et al. (1982) reported 13 of 47 Müller components as radiographically loose after ten years in a study which had a minimum detectable migration amount of five mm in measuring the medial and distal translations of the femoral component. Therefore it seems reasonable to surmise that average translation rates of at least 0.5 mm/year must have occurred for those components. *In vivo* the Exeter subsides the most, and has the largest Θ_z rotation, while the Lubinus undergoes the least subsidence and rotations, see Table 5.2. The Charnley and Müller have similar subsidence rates, and the Charnley has the highest Θ_y rotation rate.

Table 5.2: Summary of observed *in vivo* (i.e. clinical) migration rates for the Charnley, Exeter, Lubinus, and Müller femoral components. The migration values measured in this study are included to aid comparison. The Charnley, Exeter, and Lubinus rates are for the first post-operative year. The Müller rates are averaged over ten years, hence considerably higher migration rates may have occurred in the first year.

Prosthesis Researcher	medial [mm/yr]	posterior [mm/yr]	distal [mm/yr]	about medial-lateral axis [degree/yr]	into valgus [degree/yr]	about longitudinal axis [degree/yr]
Charnley						
Kiss et al. (1996)			0.54 ± 0.16	0.1 ± 0.14	1.17 ± 0.69	0.32 ± 0.12
This study	0.054 ± 0.027	-0.024 ± 0.014	0.014 ± 0.008	-0.008 ± 0.005	-0.026 ± 0.013	-0.001 ± 0.007
Exeter						
Alfaro-Adrian et al. (2001)	-0.16	0.36	0.77	0.08	0.13	0.75
This study	0.079 ± 0.081	0.005 ± 0.027	0.023 ± 0.024	0.003 ± 0.010	-0.033 ± 0.036	-0.010 ± 0.010
Lubinus						
Kärrholm et al. (2000)			0.03 ± 0.03	0.1 - 0.5	0.2 - 0.7	0.0 -0.4
This study	0.058 ± 0.015	-0.006 ± 0.034	0.016 ± 0.008	-0.002 ± 0.010	-0.018 ± 0.014	-0.004 ± 0.025
Müller						
Sutherland et al. (1982)	0.5		0.5			
This study	0.063 ± 0.020	-0.019 ± 0.025	0.018 ± 0.008	-0.010 ± 0.010	-0.028 ± 0.010	-0.004 ± 0.023

The large majority of the experimentally measured migrations are much smaller than the migrations reported in the clinical studies. A possible reason for such a large difference is that, the experimental test ignores loads other than those due to normal gait. Furthermore operative factors, such as variation in stem placement, bone necrosis due to trauma, and blood entrapment at the interfaces are not included in the experimental model. It is noteworthy that the previously mentioned experimental study of Liu et al. (2003) which included lubrication, hip joint reaction forces of up to 800% bodyweight, and extension and flexion of the test specimen, also produced lower migration amounts than the *in vivo* clinical results listed in Table 5.2, even after testing durations of up to three million cycles.

5.4.3 Influence of different femoral component geometry

Several studies have examined the influence of femoral component geometry on the performance of the femoral component when implanted. Markolf et al. (1980) investigated the influence of collar-calcar contact on migration of implanted femoral components, and found that contact reduced the subsidence of the femoral component. The mechanism for this reduction is two-fold; a reduction in peak strains in the cement mantle (Harrington et al., 2002), and an increase in longitudinal compressive stress in the cement mantle (Crowninshield et al., 1980a). However some authorities have suggested that using a collar is "unnecessary and detrimental" in clinical practice (Ling, 1992), as the collar-calcar contact can result in unphysiological loading of the calcar region which leads to bone resorption in this area. In this study only the Exeter femoral components are collarless, see Figure 5.3.

The relationship between the cross-sectional geometry of the femoral component and stresses in the cement mantle was investigated by Crowninshield et al. (1980b) and Chang et al. (1998) using finite element models. Their findings are similar; a cross-sectional geometry with flat broad surfaces which are gently rounded or tapered produces lower tensile stresses (e.g. Charnley, Exeter, or Lubinus) than a cross-sectional geometry which has sharp changes in geometry, such as the Müller Curved, as shown in Figure 5.3. Experimental support for the above findings is

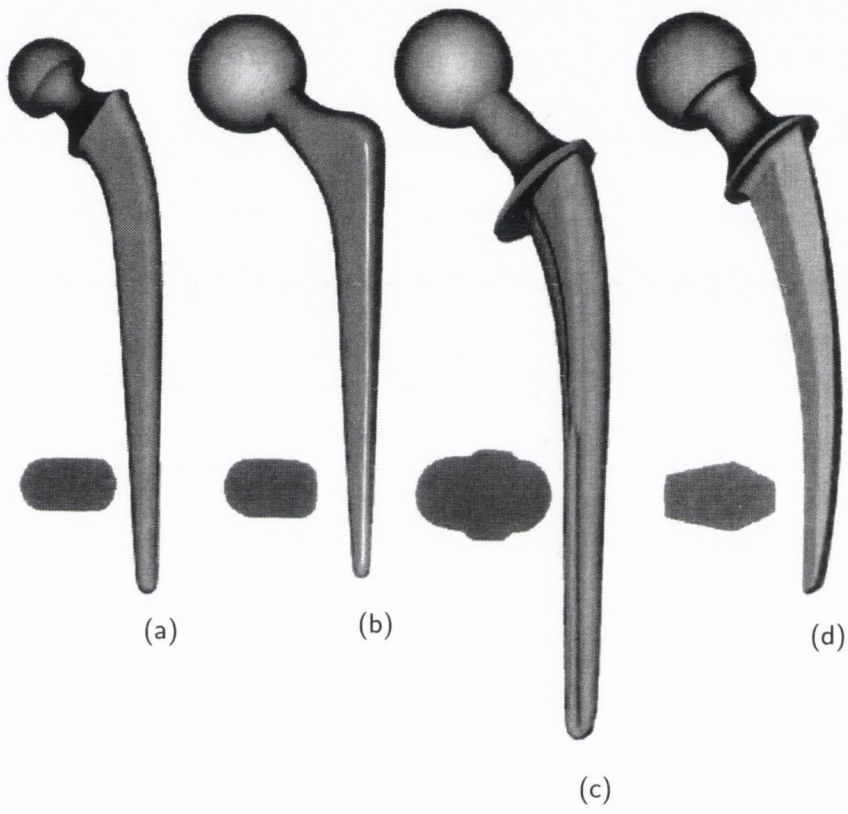

Figure 5.3: View of the femoral component shape and cross-sectional geometry of (a) the Charnley, (b) the Exeter, (c) the Lubinus, and (d) the Müller. Adapted from Stolk (2002).

provided by Orr et al. (1986) who used the theory of photoelasticity to measure stress levels around various cross-sectional profiles. They also reported that stress concentrations produced at sharp corners were higher than those observed with more rounded cross-sectional profiles.

Figure 5.4 shows the relative positions of the implanted head centre locations of the four prosthesis designs tested in this thesis in the x-z plane. Different positions in the z direction have no effect on the applied loading as the design of the experimental rig compensates. However, different x displacements do alter the applied loading. From the perspective of the experimental rig, the relative lever lengths are fixed regardless of the femoral component head centre location (which is the fulcrum), but the angles of application of the muscle forces will change slightly. The most extreme example of this is the Lubinus femoral component. When the loads applied by the experimental rig were re-calculated to account for the change in muscle loading angles (two degrees) due to the head centre location of a Lubinus femoral component, the resulting changes were a decrease in the magnitude of the resolved muscle force of 28 N and an increase in the vastus lateralis muscle force of 32 N. These changes do not alter the applied muscle forces significantly. It is improbable that the altered force magnitudes could explain the measured differences in migration, as the prosthesis designs with the most varied head centre locations, i.e. the Charnley and Lubinus, have similar results, while the Exeter and Lubinus femoral components have similar head centre locations but considerably different migration results.

5.4.4 Potential of test for use as a pre-clinical test

The clinical performance of the different designs can be gauged from their respective revision rates. Malchau et al. (2002) provides survival rates (i.e. the percentage not revised) for various femoral component designs contained in the Swedish Hip Register. After seven years, the survival rates for the Charnley, Exeter, and Lubinus SPII are, respectively, 94.7%, 97.8%, and 98.4% (note: survival rates for several different types of acetabular components used with a polished femoral component are reported for the Exeter, these were averaged to provide the survival rate quoted

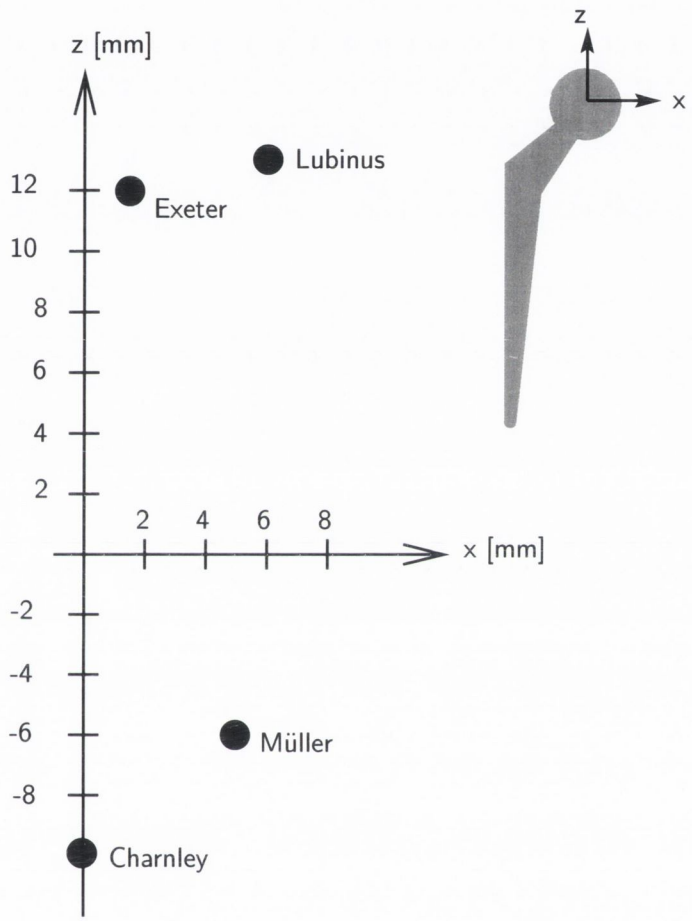

Figure 5.4: Schematic showing the difference in head centre locations of the four prosthesis designs when implanted. The origin is located at the head centre of an intact composite femur.

in this section). With respect to the Müller Curved femoral component, Sutherland et al. (1982) report that surgical use of this design was discontinued in the late 1970s in their institution due to high numbers of revision operations necessitated by aseptic loosening relative to other prostheses. Malchau et al. (1993) provides a ten year survival rate of 81.7% taken from the Swedish Hip Register between 1979 and 1990. A clinical performance ranking is therefore, from best to worst: (1) Lubinus SPII, (2) Exeter, (3) Charnley, and (4) Müller Curved.

The suitability of any test for use as a normative test or standard pre-clinical test can be determined by applying the criterion of Paul (1999) that "the standard test should fail those components which are found to fail in service and should not produce failure in those which are found to be satisfactory in normal service". If it is assumed that low migration of the femoral component is preferable then, based on the experimental results, a performance ranking would conclude that the Charnley and Lubinus femoral components are better than the Exeter and Müller components, see Figure 4.18.

Clearly, such a ranking for the Exeter is incorrect, and indicates that migration measurements *per se* are not sufficient to rank prosthesis performance. A reason for this is that, the Exeter has a different design rationale than the other designs tested in this study because of its polished surface (Lee, 1994; Alfaro-Adrian et al., 2001). The Charnley, Lubinus, and Müller femoral components have a collar, some degree of anatomical curvature and matte surface finishes (shape-closed designs intended to provide immediate stability through geometric matching of shapes as described by Huiskes et al. (1998)), whereas the Exeter has no collar, a doubly tapered stem, and a highly polished surface finish (a force-closed design which is intended to migrate until equilibrium of forces is obtained, Huiskes et al. (1998)). Therefore, the Exeter femoral components should be expected to undergo greater migration. If the design differences of the prostheses are taken into account then, the experimental performance ranking is similar to the clinical performance ranking.

Stolk (Stolk, 2002; Stolk et al., 2003) used the finite element method as a pre-clinical test for cemented femoral components, and compared the same four designs

of component as tested in this study. He simulated creep and damage accumulation in the cement mantle, applying a hip joint reaction force of 2.3 kN for up to 25 million loading cycles. Migration amounts comparable to those reported in this study were found, and, similarly to this study, the Exeter femoral component had the greatest migration. He concluded that it was not meaningful to rank the performance of the designs based on migration. Instead it was found that a ranking based on damage in the cement mantle predicted by the finite element simulations agreed with the above listed clinical performance ranking. In an experimental study, Lennon et al. (2003) found that polished femoral components did not induce significantly greater amounts of damage in the cement mantle than matte femoral components. It is also noteworthy that Race et al. (2003) determined that cement damage did not correlate with prosthesis migration, based on a set of experiments in which loading intended to replicate stair climbing was applied to cadaveric femurs implanted with Charnley femoral components for 300,000 cycles, and the implanted femurs then sectioned for microscopic examination. This finding is supported by Colombi (2002) who also found, using a quasi-three-dimensional numerical analysis (the "third" dimension was represented by connecting side plates), that cement damage modelled using a non-linear damage accumulation algorithm did not explain *in vivo* femoral component distal migration magnitudes. Therefore, migration and damage accumulation do not seem to be correlated and, since damage leads to failure of cemented femoral components, this seems to preclude the use of migration as a measure of cemented femoral component performance.

However, measurement of rate of change of inducible displacement does rank the Exeter highest as it has a decreasing tendency for its inducible displacement. It is possible for two femoral components to have migrated similar amounts but for one to have increasing inducible displacement and the other to have decreasing inducible displacement, as is illustrated in Figure 5.5.

Increasing inducible displacement is indicative of continued loosening and growing instability. The underlying reason for increasing inducible displacement is probably that microcracks continue to be initiated, grow, and in some cases, coalesce

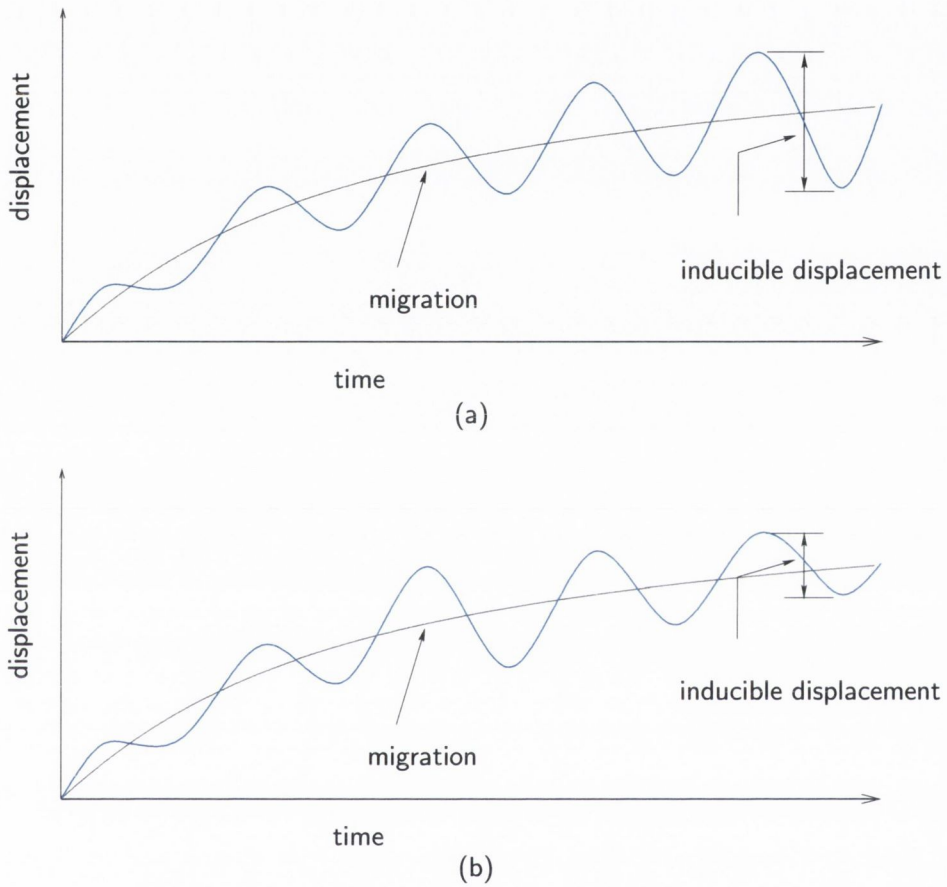

Figure 5.5: Graphs showing (a) increasing inducible displacement with respect to time, and (b) decreasing inducible displacement with respect to time. Note that both graphs have the same migration curve.

into macrocracks, thereby reducing the mechanical integrity of the cement mantle (the *damage accumulation* failure scenario (Huiskes, 1993)).

5.5 Experimental testing vs. numerical analysis

Both experimental and numerical methods were employed in this thesis to provide evidence by which the author's hypotheses could be tested. Hence, there was an opportunity to compare the relative merits of each approach.

Experimental models are time consuming to construct and to utilise. Compromise is often necessary during the design stage. Defects may occur randomly between test setups, introducing uncontrolled variability, which usually is not desirable. However, experimental tests are essential to provide fundamental information regarding the physical properties of the test subject. It is the author's opinion that, in general, experimental models are regarded as more authoritative than numerical models. This subjective view may result from a number of factors, such as the fact that numerical models are a relatively recent development, and that experimental models are considered to more closely represent physical reality.

Much greater control of important variables is possible with numerical models. While the initial creation of the numerical model may be time consuming, any desired alteration of a parameter can be quickly implemented. The capacity to utilise more complex models increases in line with Moore's Law (computer processing power doubles every 18 months, Dr. Gordon Moore, Intel Inc., USA), though our ability to do so does not necessarily follow suit. Modelling highly complex biological systems that behave in a non-linear fashion can require some simplification.

Perhaps the optimal approach is to combine both techniques, as in this thesis and by other researchers, e.g. Viceconti et al. (2001). Computational algorithms can be validated through comparison with experimentally obtained results (Stolk et al., 2004). Stochastic variation of parameters in numerical models is possible to incorporate random variation about a statistical distribution (Lennon and Prendergast, 2003). Once a computational model of sufficient complexity to capture all the salient aspects of the system under investigation, as determined by corroborating

its results with experimental or clinical studies, has been created it should prove possible to customise the model to account for the unique differences between individuals. Then, the immediate and long-term effects of implanting a medical device can be calculated for that individual.

5.6 Summary and some perspectives

The motivation for this thesis was to develop an experimental test which could discriminate the performances of four cemented hip replacement prostheses. The primary benefit of such a test is the ability to examine new cemented hip replacement prosthesis designs during pre-clinical trials, and by doing so reduce the likelihood of a design which may perform poorly being released onto the market. Initially it was proposed that this experimental test be based on migration measurements, and that physiological loading should be mimicked.

In a series of *in vitro* fatigue tests, it was found that applying simplified muscle loading did alter the migration measured during the tests, reduced experimental scatter, and stabilised the femoral component within the medullary canal. Based on these findings, further *in vitro* fatigue tests comparing the performances of four cement hip replacement designs were carried out.

No significant migration differences between prosthesis designs were found in the comparative tests. In general, the measured migration magnitudes considerably underestimated *in vivo* migration. A performance ranking based on *in vitro* migration did not agree with the clinical survival rates of the prosthesis designs tested. Hence, it must be concluded that migration is not a suitable measure on which to compare prosthesis designs. This statement is in agreement with finite element based comparisons. However, evidence obtained during the *in vitro* tests strongly suggests that measurement of inducible displacement and calculation of its rate of change does generate a performance ranking which bears comparison with clinical survival rates.

Chapter 6

CONCLUSIONS

Contents

6.1 Main conclusions

(a) It is possible to devise an experimental test which can distinguish the performance of four cemented hip replacement femoral component designs. However the number of tests required for statistical significance is prohibitive.

(b) The inclusion of muscle loading in the experimental tests stabilised the femoral component within the medullary canal.

6.1.1 Conclusions on the influence of muscle loading in experimental tests

(a) Muscle loading stabilises the femoral component within the medullary canal, reducing the magnitude of migration and inducible displacement.

(b) Muscle loading which only mimics normal gait is not sufficient to obtain clinically observed *in vivo* migration.

(c) Muscle loading does reduce the observed variation in experimental results, but significant scatter remains.

6.1.2 Conclusions regarding comparative tests of cemented hip femoral components

(a) Migration is not a suitable performance measure for experimental pre-clinical tests of femoral components with different design rationales.

(b) The experimental test presented herein may prove useful for the analysis of design changes within a cemented femoral component system.

(c) Inducible displacement measurements, in particular of whether the inducible displacements are increasing or decreasing with respect to time, could provide the basis of an experimental test for the performance ranking of different prosthesis designs by indicating the growth or otherwise of damage within the cement mantle.

6.2 Future Work

Activities which induce high and abnormal loads in the proximal femur could be simulated. These include stair climbing, fast walking, and stumbling. Activities which result in low or no load, e.g. sleeping, should also be simulated as rest periods may affect the behaviour of bone cement. Malpositioning of the femoral component could

be introduced to mimic surgical variability, and investigate whether particular prosthesis designs are more sensitive to this factor than others. Further investigation into the relationship between inducible displacement and cement mantle damage is possible. This investigation would preferably be numerically based to allow greater control of important variables, such as, porosity within the cement mantle. Given the continuing exponential increases in computational power, it seems feasible that a numerical model which integrates the mechanical and biological behaviours of an implanted femur could be developed. Once such a model has been developed, a logical progression is to model the unique attributes of individual patients, such as their anatomy, pathology, and lifestyle. More generally with regard to pre-clinical testing of THA systems, future work should consider the possibility of examining the performance of the acetabular component and the femoral component simultaneously, as the failure mechanisms of both components interact *in vivo*.

Bibliography

AAOS, 2000. Arthroplasty and total joint replacement procedures: United States 1990 to 1997. Web publication, AAOS. www.aaos.org/wordhtml/press/arthropl.htm.

Alfaro-Adrian, J., Gill, H. S., and Murray, D. W., 2001. Should total hip arthroplasty femoral components be designed to subside? A radiostereometric analysis study of Charnley Elite and Exeter stems. *Journal of Arthroplasty*, **16**(5):598–606.

An, K.-N., Chao, E. Y. S., and Kaufman, K. F., 1997. Analysis of muscle and joint loads. In V. C. Mow and W. C. Hayes, eds., *Basic Orthopaedic Biomechanics*, chapter 1, pages 1–35. Lippincott Raven, Philadelphia, second edition.

Asperberg, P. and der Vis, H. V., 1998a. Fluid pressure may cause periprosthetic osteolysis. *Acta Orthopaedica Scandinavia*, **69**(1):1–4.

Asperberg, P. and der Vis, H. V., 1998b. Migration, particles, and fluid pressure: A discussion of causes of prosthetic loosening. *Clinical Orthopaedics and Related Research*, **325**:75–80.

Bachus, K. N., Bloebaum, R. D., and Jones, R. E., 1999. Comparative micromotion of fully and proximally cemented femoral stems. *Clinical Orthopaedics and Related Research*, **366**:248–257.

Baleani, M., Cristofolini, L., and Toni, A., 2000. Initial stability of a new hybrid fixation hip stem: experimental measurement of implant-bone micromotion under torsional load in comparison with cemented and cementless stems. *Journal of Biomedical Materials Research*, **50**(4):605–615.

Bauer, T. W. and Schils, J., 1999. The pathology of total arthroplasty: mechanisms of implant failure. *Skeletal Radiology*, **28**(9):483–497.

Bergmann, G., ed., 2001. *Hip98, Loading of the hip joint*. Published as a cd-rom attachment to the Journal of Biomechanics. ISBN 3-9807848-0-0.

Bergmann, G., Deuretzbacher, G., Heller, M., Graichen, F., Rohlmann, A., Strauss, J., and Duda, G. N., 2001. Hip contact forces and gait patterns from routine activities. *Journal of Biomechanics*, **34**(7):859–871.

Bergmann, G., Graichen, F., and Rohlmann, A., 1993. Hip joint loading during walking and running measured in two patients. *Journal of Biomechanics*, **26**(8):969–990.

Bergmann, G., Graichen, F., and Rohlmann, A., 1995. Is staircase walking a risk for the fixation of hip implants? *Journal of Biomechanics*, **28**(5):535–553.

Berry, D. J., Harmsen, W. S., and Ilstrup, D. M., 1998. The natural history of debonding of the femoral component from the cement and its effect on long-term survival of Charnley total hip replacements. *Journal of Bone and Joint Surgery*, **80A**(5):715–721.

Berzins, A., Sumner, D. R., Andriacchi, T. P., and Galante, J. O., 1993. Stem curvature and load angle influence the initial relative bone-implant motion of cementless femoral stems. *Journal of Orthopaedic Research*, **11**(5):785–769.

Borelli, G. A., 1680. *De motu animalium*. Translated by P. Maquet as "On the Movement of Animals", Springer-Verlag, Berlin, 1989.

Boss, J. H., Shajrawi, I., and Mendes, D. G., 1994. The nature of the bone-implant interface. *Medical Progress through Technology*, **20**(3-4):119–142.

Brand, R. A., Pedersen, D. R., and Yoder, S. A., 1986. How definition of 'Loosening' affects the incidence of loose total hip reconstructions. *Clinical Orthopaedics and Related Research*, **210**:185–191.

Britton, J. R. and Prendergast, P. J., 2004. Migration measurement as a basis for a pre-clinical test of cemented hip implants: an investigation of four prostheses under simulated muscle loading. *Proceedings of the Institution of Mechanical Engineers. Part H: Journal of Engineering in Medicine*. Submitted for publication.

Britton, J. R., Walsh, L. A., and Prendergast, P. J., 2003. Mechanical simulation of muscle loading on the proximal femur: Analysis of cemented femoral component migration with and without muscle loading. *Clinical Biomechanics*, **18**(7):637–646.

Buhler, D. W., Berlemann, U., Lippuner, K., Jaeger, P., and Nolte, L. P., 1997a. Three-dimensional primary stability of cementless femoral stems. *Clinical Biomechanics*, **12**(2):75–86.

Buhler, D. W., Oxland, T. R., and Nolte, L. P., 1997b. Design and evaluation of a device for measuring three-dimensional micromotions of press-fit femoral stems prostheses. *Medical Engineering and Physics*, **19**(2):187–199.

Burke, D. W., O'Connor, D., Zalenski, E. B., Jasty, M., and Harris, W. H., 1991. Micromotion of cemented and uncemented femoral components. *Journal of Bone and Joint Surgery*, **73B**(1):33–37.

Callaghan, J., Fulghum, C. S., Glisson, R. R., and Stranne, S. K., 1992. The effect of femoral stem geometry on interface motion in uncemented porous-coated total hip prostheses. *Journal of Bone and Joint Surgery*, **74A**(6):839–847.

Chafetz, N., Baumrind, S., Murray, W. R., Genant, H. K., and Korn, E. L., 1985. Subsidence of the femoral prosthesis: A stereophotogrammetric evaluation. *Clinical Orthopaedics and Related Research*, **201**:60–67.

Chang, P. B., Mann, K. A., and Bartel, D. L., 1998. Cemented femoral stem performance: Effects of proximal bonding, geometry, and neck length. *Clinical Orthopaedics and Related Research*, **355**:57–69.

Charnley, J., 1961. Arthroplasty of the hip. *The Lancet*, pages 1129–1132.

Charnley, J. and Kettlewell, J., 1965. The elimination of slip between prosthesis and femur. *Journal of Bone and Joint Surgery*, **47B**(1):56–60.

Claes, L., Fiedler, S., Ohnmacht, M., and Duda, G. N., 2000. Initial stability of fully and partially cemented femoral stems. *Clinical Biomechanics*, **15**(10):750–755.

Cleveland, W. S. and Devlin, S. J., 1988. Locally weighted regression: an appoach to regression analysis by local fitting. *Journal of the American Statistical Association*, **83**(403):596–610.

Colombi, P., 2002. Fatigue analysis of cemented hip prosthesis: damage accumulation scenario and sensitivity analysis. *International Journal of Fatigue*, **24**(7):739–746.

Cristofolini, L., 1997. A critical analysis of stress shielding evaluation of hip prostheses. *Critical Reviews in Biomedical Engineering*, **25**(4-5):409–483.

Cristofolini, L., McNamara, B. P., Freddi, A., and Viceconti, M., 1997. In vitro measured strains in the loaded femur: quantification of experimental error. *Journal of Strain Analysis*, **32**(3):193–200.

Cristofolini, L., Teutonico, A. . S., Monti, L., Cappello, A., and Toni, A., 2003. Comparative in vitro study on the long term performance of cemented hip stems: validation of a protocol to discriminate between "good" and "bad" designs. *Journal of Biomechanics*, **36**(11):1603–1615.

Cristofolini, L., Viceconti, M., Cappello, A., and Toni, A., 1996. Mechanical validation of whole bone composite femur models. *Journal of Biomechanics*, **29**(4):525–535.

Cristofolini, L., Viceconti, M., Toni, A., and Giunti, A., 1995. Influence of thigh muscles on the axial strains in a proximal femur during early stance in gait. *Journal of Biomechanics*, **28**(5):617–624.

Crowninshield, R. D., Brand, R. A., Johnston, R. C., and Milroy, J. C., 1980a. An analysis of femoral component stem design in total hip arthroplasty. *Journal of Bone and Joint Surgery*, **52A**(1):68–78.

Crowninshield, R. D., Brand, R. A., Johnston, R. C., and Milroy, J. C., 1980b. The effect of femoral stem cross-sectional geometry on cement stresses in total hip reconstruction. *Clinical Orthpaedics and Related Research*, **146**:71–77.

Darwin, C., 1859. *The Origin of Species*. John Murray & Sons, London.

Davy, D. T., Kotzar, G. M., Brown, R. H., Heiple, K. G., Goldberg, V. M., Jr., K. G. H., Berilla, J., and Burstein, A. H., 1988. Telemetric force measurement across the hip after total arthroplasty. *Journal of Bone and Joint Surgery*, **70A**(1):45–50.

Doehring, T. C., Rubash, H. E., and Dore, D. E., 1999. Micromotion measurements with hip center and modular neck length alterations. *Clinical Orthopaedics and Related Research*, **362**:230–239.

Duda, G. N., Heller, M., Albinger, J., Schulz, O., Schneider, E., and Claes, L., 1998. Influence of muscle forces on femoral strain distribution. *Journal of Biomechanics*, **31**(9):841–846.

Duda, G. N., Schneider, E., and Chao, E. Y. S., 1997. Internal forces and moments in the femur during walking. *Journal of Biomechanics*, **30**(9):933–941.

Dunne, N. J. and Orr, J. F., 2001. Influence of mixing techniques on the physical properties of acrylic bone cement. *Biomaterials*, **22**(13):1819–1826.

Dunne, N. J., Orr, J. F., Mushipe, M. T., and Eveleigh, R., 2003. The relationship between porosity and fatigue characteristics of bone cements. *Biomaterials*, **24**(2):239–245.

Engh, C. A., O'Connor, D., Jasty, M., McGovern, T. F., Bobyn, J. D., and Harris, W. H., 1992. Quantification of implant micromotion, stress shield-

ing, and bone resorption with porous-coated anatomic medullary locking femoral prostheses. *Clinical Orthopaedics and Related Research*, **285**:13–29.

English, T. A. and Kilvington, M., 1979. In vivo records of hip forces using a femoral implant with telemeteric output. *Journal of Biomedical Engineering*, **1**(2):111–115.

Espehaug, B., Havelin, L. I., Engesaeter, L. B., Vollset, S. E., and Langeland, N., 1995. Early revision among 12,719 hip prostheses. *Acta Orthopaedica Scandinavia*, **66**(6):487–493.

Faro, L. M. C. and Husikes, R., 1992. Quality assurance of joint replacement: Legal regulation and medical judgement. *Acta Orthopaedica Scandinavia*, **63**(250). Suppl. 250.

Faulkner, A., Kennedy, L. G., Baxter, K., Donovan, J., Wilkinson, M., and Bevan, G., 1998. Effectiveness of hip prostheses in primary total hip replacement: a critical review of evidence and an economic model. *Health Technology Assessment*, **2**(6):1–129.

Fielding, J. W. and Stillwell, W. T., 1987. *The Art of Total Hip Arthroplasty*. Grune and Stratton, Orlando.

Fornasier, V. L. and Cameron, H. U., 1976. The femoral stem/cement interface in total hip replacement. *Clinical Orthopaedics and Related Research*, **116**:248–252.

Freeman, M. A. R. and Plante-Bordeneuve, P., 1994. Early migration and late aseptic failure of proximal femoral prostheses. *Journal of Bone and Joint Surgery*, **76B**(3):432–438.

Gardner, M. J. and Altman, D. G., 1986. Confidence intervals rather than P values: estimation rather than hypothesis testing. *British Medical Journal*, **292**:746–750.

Gilbert, J. L., Bloomfield, R. S., Lautenschlager, E. P., and Wixson, R. L., 1992. A computer-based biomechanical analysis of the three-dimensional motion of cementless hip prostheses. *Journal of Biomechanics*, **25**(4):329–340.

Gruen, T. A., McNeice, G. M., and Amstutz, H. C., 1979. "Modes of Failure" of cemented stem-type femoral components. *Clinical Orthopaedics and Related Research*, **141**:17–27.

Hardinge, K., 1983. *Hip Replacement. The Facts*. Oxford University Press.

Harman, M. K., Toni, A., Cristofolini, L., and Viceconti, M., 1995. Initial stability of uncemented hip stems: an in-vitro protocol to measure torsional interface motion. *Medical Engineering and Physics*, **17**(3):163–171.

Harrington, M. A., O'Connor, D. O., Lozynsky, A. J., Kovach, I., and Harris, W. H., 2002. Effects of femoral neck length, stem size, and body weight on strains in the proximal cement mantle. *Journal of Bone and Joint Surgery*, **84A**(4):573–579.

Harris, W. H., 1992. Is it advantageous to strengthen the cement-metal interface and use a collar for cemented femoral components of total hip replacements? *Clincial Orthopaedics and Related Research*, **285**:67–72.

Harris, W. H., 1994. Osteolysis and particle disease in hip replacement. *Acta Othop Scandinavia*, **65**(1):113–123.

Heller, M. O., Bergmann, G., Deuretzbacher, G., Dürselen, L., Pohl, M., Claes, L., Haas, N. P., and Duda, G. N., 2001. Musculo-skeletal loading conditions at the hip during walking and stair climbing. *Journal of Biomechanics*, **34**(7):883–893.

Hua, J. and Walker, P. S., 1994. Relative motion of hip stems under load. *Journal of Bone and Joint Surgery*, **76A**(1):95–103.

Hua, J. and Walker, P. S., 1995. Closeness of fit of uncemented stems improves the strain distribution in the femur. *Journal of Orthopaedic Research*, **13**(3):339–346.

Huiskes, R., 1990. The various stress patterns of press-fit, ingrown, and cemented femoral stems. *Clinical Orthopaedics and Related Research*, **261**:27–38.

Huiskes, R., 1993. Failed innovation in total hip replacement: Diagnosis and proposals for a cure. *Acta Orthopaedica Scandinavia*, **64**(6):699–716.

Huiskes, R. and Verdonschot, N., 1997. Biomechanics of artificial joints: the hip. In V. C. Mow and W. C. Hayes, eds., *Basic Orthopaedic Biomechanics*, chapter 11. Lippincott-Raven, Philadelphia, second edition.

Huiskes, R., Verdonschot, N., and Nivbrant, B., 1998. Migration, stem shape, and surface finish in cemented total hip arthroplasty. *Clinical Orthopaedics and Related Research*, **355**:103–112.

Humphreys, P. K., Orr, J. F., and Bahrani, A. S., 1989. An investigation into the effect of cyclic loading and frequency on the temperature of PMMA bone cement in hip prostheses. *Proceedings of the Institution of Mechanical Engineers. Part H: Journal of Engineering in Medicine*, **203**(3):167–170.

Humphreys, P. K., Orr, J. F., and Bahrani, A. S., 1991. An investigation into the fixation of hip replacements. *Proceedings of the Institution of Mechanical Engineers. Part H: Journal of Engineering in Medicine*, **205**(3):145–153.

Jasty, M., Maloney, W. J., Bragdon, C. R., O'Connor, D., Haire, T., and Harris, W. H., 1991. The initiation of failure in cemented femoral components of hip arthoplasties. *Journal of Bone and Joint Surgery*, **73B**(4):551–8.

Kärrholm, J., Borssen, B., Lowenhielm, G., and Snorrason, F., 1994. Does early micromotion of femoral stem prostheses matter? *Journal of Bone and Joint Surgery*, **76B**(6):912–917.

Kärrholm, J., Herberts, P., Hultmark, P., Malchau, H., Nivbrant, B., and Thanner, J., 1997. Radiostereometry of hip prostheses. *Clinical Orthopaedics and Related Research*, **344**:94–110.

Kärrholm, J., Nivbrant, B., Thanner, J., Anderberg, C., Borlin, N., Herberts, P., and Malchau, H., 2000. Radiostereometric evaluation of hip implant design and surface finish. Technical report, Departments of Orthopaedics and Computing Science at Göteborg University and Umeå University, Sweden. Scientific exhibition presented at the 67th annual meeting of the American Academy of Orthopaedic Surgeons, Orlando, Florida.

Kassi, J.-P., Heller, M. O. W., Stoeckle, U., Perka, C., and Duda, G. N., 2002. Muscle activity is essential for a realistic pre-clinical evaluation of primary stability in THA. In R. Bedzinski, C. Pezowicz, and K. Scigala, eds., *Acta of Bioengineering and Biomechanics: Proceedings of the 13th conference of European Society of Biomechanics*, page 47. European Society of Biomechanics, 2002.

Kiss, J., Murray, D. W., Turner-Smith, A. R., Bithell, J., and Bulstrode, C. J., 1996. Migration of cemented femoral components after THR - roentgen sterophotogrammetric analysis. *Journal of Bone and Joint Surgery*, **78B**(5):796–801.

Kiss, J., Murray, D. W., Turner-Smith, A. R., and Bulstrode, C. J., 1995. Roentgen stereophotogrammetric analysis for assessing migration of total hip replacement femoral components. *Proceedings of the Institution of Mechanical Engineers. Part H: Journal of Engineering in Medicine*, **209**(3):169–175.

Kobayashi, S. and Terayama, K., 1992. Factors influencing survivorship of the femoral component after primary low-friction hip arthroplasty. *Journal of Arthroplasty*, **7**:327–338.

Kreyszig, E., 1999. *Advanced Engineering Mathematics*. John Wiley & Sons, New York, 8th edition.

Lee, A. J. C., 1994. Implants for cement fixation with and without a collar. In G. H. Buchhorn and H. G. Willert, eds., *Technical Principles, Design and Safety of Joint Implants*. Hogrefe and Huber, Seattle.

Lee, A. J. C., Ling, R. S. M., and Vangala, S. S., 1977. The mechanical properties of bone cements. *Journal of Medical Engineering and Technology*, **1**(3):137–140.

Lennon, A. B., 2002. *A Stochastic Model of Damage Accumulation in Arcylic Bone Cement*. Ph.D. thesis, University of Dublin.

Lennon, A. B., McCormack, B. A. O., and Prendergast, P. J., 2003. The relationship between cement fatigue damage and implant surface finish in proximal femoral prostheses. *Medical Engineering and Physics*, **25**(10):833–841.

Lennon, A. B. and Prendergast, P. J., 2001. Evaluation of cement stresses in finite element analyses of cemented orthopaedic implants. *Journal of Biomechanical Engineering*, **123**(6):623–628.

Lennon, A. B. and Prendergast, P. J., 2002. Residual stress due to curing can initiate damage in porous bone cement: experimental and theoretical evidence. *Journal of Biomechanics*, **35**(3):311–321.

Lennon, A. B. and Prendergast, P. J., 2003. Modelling damage in elastic materials with random defect distributions. *Proceedings of the Royal Irish Academy*. Accepted for publication.

Lieberman, J. R., Thomas, B. J., Finerman, G. A. M., and Dorey, F., 2003. Patients' reasons for undergoing total hip arthroplasty can change over time. *Journal of Arthroplasty*, **18**(1):63–68.

Ling, R. S. M., 1992. The use of a collar and precoating on cemented femoral stems is unnecessary and detrimental. *Clinical Orthopaedics and Related Research*, **285**:73–83.

Liu, C., Green, S. M., Watkins, N. D., Gregg, P. J., and McCaskie, A. W., 2003. A preliminary hip joint simulator study of the migration of a cemented femoral stem. *Proceedings of the Institution of Mechanical Engineers. Part H: Journal of Engineering in Medicine*, **217**(2):127–135.

Lu, T.-W., Taylor, S. T. G., O'Connor, J. J., and Walker, P. S., 1997. Influence of muscle activity on the forces in the femur: an in vivo study. *Journal of Biomechanics*, **30**(11-12):1101–1106.

Lu, Z., Ebramzadeh, E., McKellop, H., and Sarmiento, A., 1996. Stable partial debonding of the cement interfaces indicated by a finite element model of a total hip prosthesis. *Journal of Orthopaedic Research*, **14**(2):238–244.

Lucht, U., 2000. The Danish Hip Arthroplasty Register. *Acta Orthopaedica Scandinavia*, **71**(5):433–439.

Maher, S. A., 2000. *Design and Development of a Pre-Clinical Test for Cemented Femoral Hip Replacements*. Ph.D. thesis, University of Dublin.

Maher, S. A. and Prendergast, P. J., 2002. Discriminating the loosening behaviour of cemented hip prostheses using measurements of migration and inducible displacement. *Journal of Biomechanics*, **35**(2):257–265.

Maher, S. A., Prendergast, P. J., and Lyons, C. G., 2001. Measurement of the migration of a cemented hip prosthesis in an in vitro test. *Clinical Biomechanics*, **16**(4):307–314.

Maher, S. A., Prendergast, P. J., Reid, A. J., Waide, D. V., and Toni, A., 2000. Design and validation of a machine for reproducible precision insertion of femoral hip prostheses for preclinical testing. *Journal of Biomechanical Engineering*, **122**(2):203–207.

Malchau, H., Herberts, P., Ahnfelt, L., and Johnell, O., 1993. Prognosis of total hip replacements: Results from the national register of revised failures 1979-1990 in Sweden - A ten year follow-up of 92,675 THR. Technical report,

Department of Orthopaedics, University of Göteborg, Sweden. Scientific exhibiton presented at the 61st Annual Meeting of the American Academy of Orthopaedic Surgeons, San Francisco, USA.

Malchau, H., Herberts, P., Garellick, G., Söderman, P., and Eisler, T., 2002. Prognosis of total hip replacement: Update of results and risk-ratio analysis for revision and re-revision from the Swedish National Hip Arthroplasty Register 1979-2000. Technical report, Department of Orthopaedics, Göteborg University, Sweden. Scientific exhibiton presented at the 69th Annual Meeting of the American Academy of Orthopaedic Surgeons, Dallas, USA.

Malchau, H., Herberts, P., Söderman, P., and Odén, A., 2000. Prognosis of Total Hip Replacement: Update and validation of results from the Swedish National Hip Arthroplasty Registry 1979-1998. Technical report, Department of Orthopaedics, Göteborg University, Sweden. Scientific exhibition presented at the 67th annual meeting of the American Academy of Orthopaedic Surgeons, Orlando, USA.

Malchau, H., Karrholm, J., Wang, Y. X., and Herberts, P., 1995. Accuracy of migration analysis in hip arthroplasty. *Acta Orthopaedica Scandinavia*, **66**(5):418–424.

Maloney, W., Jasty, M., Burke, D., O'Connor, D., Zalenski, E., Bragdon, C., and Harris, W., 1989. Biomechanical and histologic investigation of cemented total hip arthroplasties. *Clinical Orthopaedics and Related Research*, **249**:129–140.

Manley, M., Stern, L. S., Kotzar, G., and Stulberg, B. N., 1987. Femoral component loosening in hip arthroplasty. *Acta Orthopaedica Scandinavia*, **58**(5):485–490.

Markolf, K. L., Amstutz, H. A., and Hirschowitz, D. L., 1980. The effect of calcar contact on femoral component micromotion. *Journal of Bone and Joint Surgery*, **62A**(8):1315–1323.

Massoud, S. A., Hunter, J. B., Holdsworth, B. J., Wallace, W. A., and Juliusson, R., 1997. Early femoral component loosening in one design of cemented hip replacement. *Journal of Bone and Joint Surgery*, **79B**(4):603–608.

McCormack, B. A. O., Prendergast, P. J., and O'Dwyer, B., 1999. Fatigue of cemented hip replacements under torsional loads. *Fatigue & Fracture of Engineering Materials & Structures*, **22**(1):33–40.

McGrath, L. R., Shardlow, D. L., Ingham, E., Andrews, M., Ivory, J., Stone, M. H., and Fisher, J., 2001. A retrieval study of Capital hip prostheses with titanium alloy femoral stems. *Journal of Bone and Joint Surgery*, **83B**(8):1195–1201.

McKellop, H., Ebramzadeh, E., Niederer, P. G., and Sarmiento, A., 1991. Comparison of the stability of press-fit hip prosthesis femoral stems using a synthetic model femur. *Journal of Orthopaedic Research*, **9**(2):297–305.

Mjoberg, B., Selvik, G., Hansson, L. I., Rosenqvist, R., and Onnerfalt, R., 1986. Mechanical loosening of total hip prostheses. *Journal of Bone and Joint Surgery*, **68B**(5):770–773.

Monti, L., Cristofolini, L., and Viceconti, M., 1999. Methods for quantitative analysis of the primary stability in uncemented hip prostheses. *Artificial Organs*, **23**(9):851–859.

Morlock, M., Schneider, E., Bluhm, A., Vollmer, M., Bergmann, G., Müller, V., and Honl, M., 2001. Duration and frequency of every day activities in total hip replacements. *Journal of Biomechanics*, **34**(7):873–881.

Mow, V. C., Radcliffe, A., and Poole, A. R., 1992. Cartilage and diarthrodial joints as paradigms for hierarchical materials and structures. *Biomaterials*, **13**(2):67–97.

Munting, E. and Verhelpen, M., 1993. Mechanical simulator for the upper femur. *Acta Orthopaedica Belgica*, **59**(2):123–129.

Munting, E. and Verhelpen, M., 1995. Fixation and effect on bone strain pattern of a stemless hip prosthesis. *Journal of Biomechanics*, **28**(8):949–961.

Murphy, B. P. and Prendergast, P. J., 1999. Measurement of non-linear microcrack accumulation rates in polymethylmethacrylate bone cement under cyclic loading. *Journal of Materials Science: Materials in Medicine*, **10**(12):779–781.

Murphy, B. P. and Prendergast, P. J., 2000. On the magnitude and variability of the fatigue strength of acrylic bone cement. *International Journal of Fatigue*, **22**(10):855–864.

Murphy, B. P. and Prendergast, P. J., 2001. The relationship between stress, porosity, nonlinear damage accumulation in acrylic bone cement. *Journal of Biomedical Materials Research*, **59**(4):646–654.

Murphy, B. P. and Prendergast, P. J., 2003. Mulit-axial failure of orthopedic bone cement - experiments with tubular specimens. *Journal of Materials Science: Materials in Medicine*, **14**(10):857–861.

Nunn, D., Freeman, M. A. R., Tanner, K. E., and Bonfield, W., 1989. Torsional stability of the femoral component of hip arthroplasty. *Journal of Bone and Joint Surgery*, **71B**:452–455.

Orr, J. F., Dunne, N. J., and Quinn, J. C., 2003. Shrinkage stresses in bone cement. *Biomaterials*, **24**(17):2933–2940.

Orr, J. F., James, W. V., and Bahrani, A. S., 1986. The effects of hip prosthesis stem cross-sectional profile on the stresses induced in bone cement. *Proceedings of the Institution of Mechanical Engineers. Part H: Journal of Engineering in Medicine*, **15**(1):13–18.

Ostendorf, M., Johnell, O., Malchau, H., Dhert, W. J. A., Schrijvers, A. J. P., and Verbout, A. J., 2002. The epidemiology of total hip replacement in the Netherlands and Sweden. *Acta Orthopaedica Scandinavia*, **73**(3):282–286.

Paul, J. P., 1997a. Development of standards for orthopaedic implants. *Proceedings of the Institution of Mechanical Engineers. Part H: Journal of Engineering in Medicine*, **211**(11):119–126.

Paul, J. P., 1997b. Letter to the editor - re: Stress and strain distribution within the intact femur: compression or bending? by Taylor et al. *Medical Engineering and Physics*, **19**(1):p.97.

Paul, J. P., 1999. Strength requirements for internal and external prostheses. *Journal of Biomechanics*, **32**(4):381–393.

Pauwels, F., 1965. *Gesammelte Abhandlungen zur funktionellen Anatomie des Bewegungsapparates*. Springer-Verlag, Berlin, Germany. Translated by P. Maquet and R. Furlong as "Biomechanics of the Locomotor Apparatus", 1980.

Pellicci, P. M., Salvati, E. A., and Robinson, H. J., 1979. Mechanical failures in total hip replacement requiring reoperation. *Journal of Bone and Joint Surgery*, **61A**(1):28–36.

Petty, W., 1991. *Total Joint Replacement*. W. B. Saunder, Orlando.

Polgar, K., Gill, H. S., Viceconti, M., Murray, D. W., and O'Connor, J. J., 2003. Strain distribution with the human femur due to physiological and simplified loading: finite element analysis using the muscle standardized femur model. *Proceedings of the Institution of Mechanical Engineers. Part H: Journal of Engineering in Medicine*, **217**(3):173–189.

Prendergast, P. J., 2001a. *Biomechanical techniques for pre-clinical testing of prostheses and implants*. Polish Academy of Sciences, Warsaw.

Prendergast, P. J., 2001b. Bone prostheses and implants. In S. C. Cowin, ed., *Bone Mechanics*. CRC Press, Boca Raton.

Prendergast, P. J. and Maher, S. A., 2001. Issues in pre-clinical testing of implants. *Journal of Materials Processing Technology*, (118):237–342.

Prendergast, P. J., Monaghan, J., and Taylor, D., 1989. Materials selection in the artifical hip joint using finite element stress analysis. *Clinical Materials*, **4**:361–376.

Puolakka, T. J. S., Pajamäki, K. J. J., Halonen, P. J., Pulkkinen, P. O., Paavolainen, P., and Nevalainen, J. K., 2001. The Finnish arthroplasty register: Report of the hip register. *Acta Orthopaedica Scandinavia*, **72**(5):433–441.

Race, A., Miller, M. A., Ayers, D. C., and Mann, K. A., 2003. Early cement damage around a femoral stem is concentrated at the cement/bone interface. *Journal of Biomechanics*, **36**(4):489–496.

Rydell, N. W., 1966. Forces acting on the femoral head-prosthesis. *Acta Orthopaedica Scandinavia*, **37**. Supplement 88.

Schmalzried, T. and Callaghan, J., 1999. Wear in total hip and knee replacements. *Journal of Bone and Joint Surgery*, **81A**(1):115–136.

Schmalzried, T. P., Szuszczewicz, E. S., Northfield, M. R., Akizuki, K., Frankel, R. E., Belcher, G., and Amstutz, H. C., 1998. Quantitative assessment of walking activity after total hip or knee replacement. *Journal of Bone and Joint Surgery*, **80A**(1):54–58.

Schneider, E., Kinast, C., Eulenberger, J., Wyder, D., Eskilsson, G., and Perren, S. M., 1989. A comparative study of the initial stability of cementless hip prostheses. *Clinical Orthopaedics and Related Research*, **248**:200–209.

Sobotta, J., 1988. *Atlas of Human Anatomy*, volume 2. Urban and Schwarzenberg.

Speirs, A. D., Slomczykowski, M. A., Orr, T. E., Siebenrock, K., and Nolte, L.-P., 2000. Three-dimensional measurement of cemented femoral stem stability: an in vitro cadaver study. *Clinical Biomechanics*, **15**(4):248–255.

Sterne, J. A. C. and Smith, G. D., 2001. Sifting the evidence - what's wrong with significance tests? *British Medical Journal*, **322**:226–231.

Stolk, J., 2002. *A Computerized Pre-Clinical Test for Cemented Hip Prostheses Based on Ffinite Element Techniques*. Ph.D. thesis, University of Nijmegen.

Stolk, J., Maher, S. A., Verdonschot, N., Prendergast, P. J., and Huiskes, R., 2003. Can finite element models detect clinically inferior cemented hip implants? *Clinical Orthopaedics and Related Research*, **409**:138–150.

Stolk, J., Verdonschot, N., and Huiskes, R., 2001. Hip-joint and abductor muscle forces adequately represent in vivo loading of a cemented total hip reconstruction. *Journal of Biomechanics*, **34**(7):917–926.

Stolk, J., Verdonschot, N., Murphy, B. P., Prendergast, P. J., and Huiskes, R., 2004. Finite element simulation of anisotropic damage accumulation and creep in acrylic bone cement. *Engineering Fracture Mechanics*, **71**(4-6):513–528.

Strömberg, C. N., Herberts, P., Palmetrz, B., and Garelick, G., 1996. Radiographic risk signs for loosening after cemented THA. *Acta Orthopaedica Scandinavia*, **67**(1):43–48.

Sutherland, C. J., Wilde, A. H., Borden, L. S., and Marks, K. E., 1982. A ten-year follow-up of one hundred consecutive Müller Curved Stem total hip-replacement arthoplasties. *Journal of Bone and Joint Surgery*, **64A**(7):970–981.

Szivek, J. A., Benjamin, J. B., and Anderson, P. L., 2000. An experimental method for the application of lateral muscle loading and its effect on femoral strain distribution. *Medical Engineering and Physics*, **22**(2):109–116.

Szivek, J. A., Weng, M., and Karpman, R., 1990. Variability in the torsional and bending response of a commerically available composite femur. *Journal of Applied Biomaterials*, **1**:183–186.

Taylor, S. J. G., Perry, J. S., Meswania, J. M., Donaldson, N., Walker, P. S., and Cannon, S. R., 1997. Telemetry of forces from proximal femoral replacements and relevance to fixation. *Journal of Biomechanics*, **30**(3):225–234.

Verdonschot, N., Barink, M., Stolk, J., Gardeniers, J. W. M., and Schreurs, B. W., 2002. Do unloading periods affect migration characteristics of cemented femoral components? An in vitro evaluation with the Exeter stem. *Acta Orthopaedica Belgica*, **68**(4):348–355.

Verdonschot, N. and Huiskes, R., 1994. Creep behaviour of hand-mixed Simplex P bone cement under cyclic tensile loading. *Journal of Applied Biomaterials*, **5**(3):235–243.

Verdonschot, N. and Huiskes, R., 1995. Dynamic creep behaviour of acrylic bone cement. *Journal of Biomedical Materials Research*, **29**(5):575–581.

Verdonschot, N. and Huiskes, R., 1997. Cement debonding process of total hip arthroplasty stems. *Clinical Orthopaedics and Related Research*, **336**:297–307.

Verdonschot, N. and Huiskes, R., 1998. Surface roughness of debonded straight-tapered stems in cemented THA reduces subsidence but not cement damage. *Biomaterials*, **19**(19):1773–1779.

Viceconti, M., Casali, M., Massari, B., Cristofolini, L., Bassini, S., and Toni, A., 1996. Letter to the editor: The 'Standardized Femur Program' proposal for a reference geometry to be used for the creation of finite element models of the femur. *Journal of Biomechanics*, **29**(9):1241.

Viceconti, M., Cristofolini, L., Baleani, M., and Toni, A., 2001. Pre-clinical validation of a new partially cemented femoral prosthesis by synergetic use of numerical and experimental methods. *Journal of Biomechanics*, **34**(6):723–731.

Walker, P. S., Schneeweis, D., Murphy, S., and Nelson, P., 1987. Strains and micromotions of press-fit femoral stem prostheses. *Journal of Biomechanics*, **20**(9):693–702.

Whiteside, L. A. and Easley, J. C., 1989. The effect of collar and distal stem fixation on micromotion of the femoral stem in uncemented total hip arthroplasty. *Clinical Orthopaedics and Related Research*, **239**:145–152.

Whittle, M. W., 2001. *Gait Analysis: An Introduction*. Butterworth Heinemann, Oxford, 3rd edition.

Zahiri, C. A., Schmalzreid, T. P., Szuszczewicz, E. S., and Amstutz, H. C., 1998. Assessing activity in joint replacement patients. *Journal of Arthroplasty*, **13**(8):890–895.

Zar, J. H., 1999. *Biostatistical Analysis*. Prentice-Hall Inc., New Jersey, 4th edition.

Appendix A

Relevant published articles

Available online at www.sciencedirect.com
SCIENCE DIRECT®
Clinical Biomechanics 18 (2003) 637–646
CLINICAL BIOMECHANICS
www.elsevier.com/locate/clinbiomech

Mechanical simulation of muscle loading on the proximal femur: analysis of cemented femoral component migration with and without muscle loading

J.R. Britton, L.A. Walsh, P.J. Prendergast *

Centre for Bioengineering, Department of Mechanical Engineering, Trinity College, Dublin 2, Ireland

Received 6 February 2003; accepted 1 May 2003

Abstract

Objective. This study examines the effect of including muscle forces in fatigue tests of cemented total hip arthroplasty reconstructions.

Design. An experimental device capable of applying the joint reaction force, the abductor force, the vastus lateralis force, and the tensor fasciae latae force to the implanted femur is described.

Background. Current in vitro fatigue tests of cemented total hip arthroplasty reconstructions do not apply physiological muscle loads. Experimental and numerical studies report significant differences in stresses obtained in the cement mantle depending on the loads applied. The differing stresses may alter the outcome of an in vitro test.

Methods. Ten femoral components were reproducibly implanted into proximal composite femurs. Five of these femoral components were tested using a loadprofile which included muscle loading, five were tested without muscle loading. The migration of each femoral component was monitored continuously during dynamic fatigue tests.

Results. Clinically comparable migration amounts were found for both sets of femoral components, with the femoral components tested with muscle loading experiencing lower mean migration, lower mean inducible displacement, and less experimental scatter.

Conclusions. The inclusion of muscle forces seems to stabilise the femoral component during the test. In vitro fatigue tests of cemented total hip arthroplasty reconstructions should include muscle loading to provide increased confidence in the results obtained.

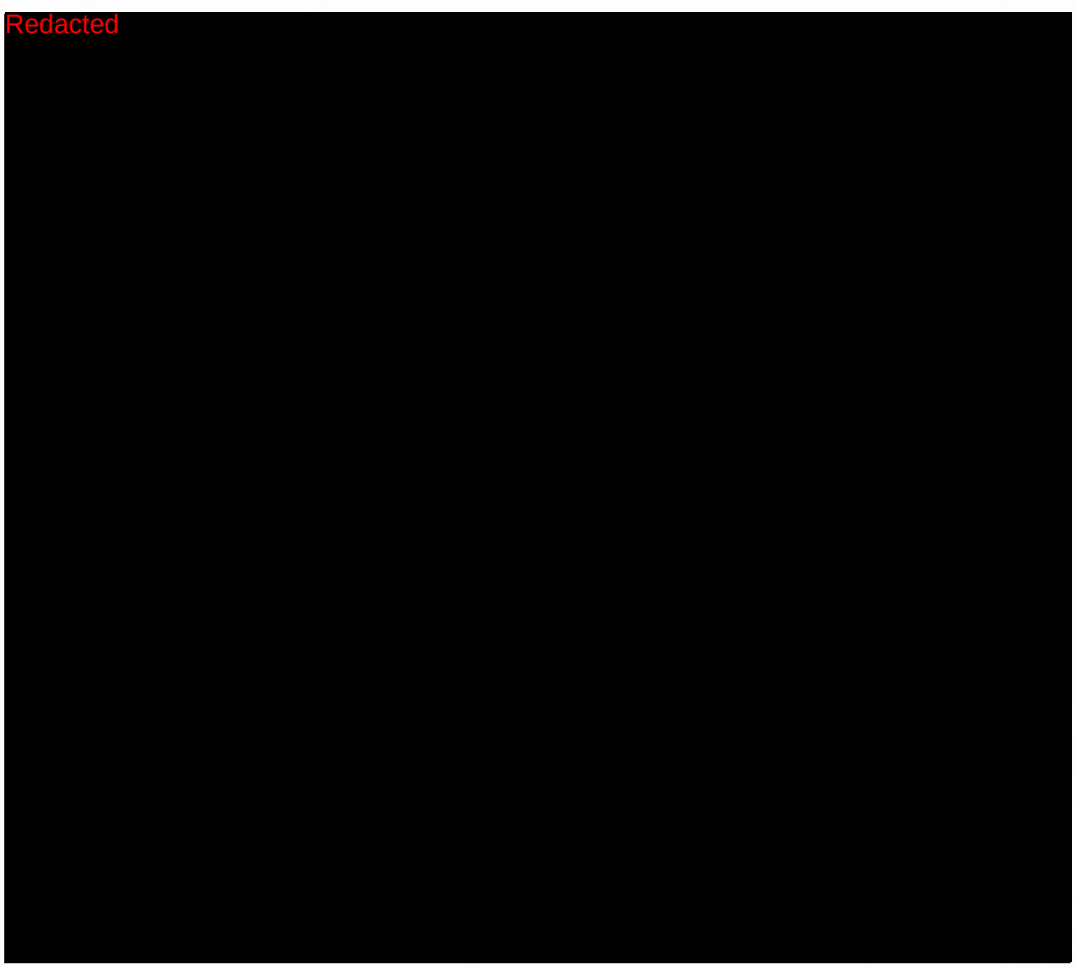

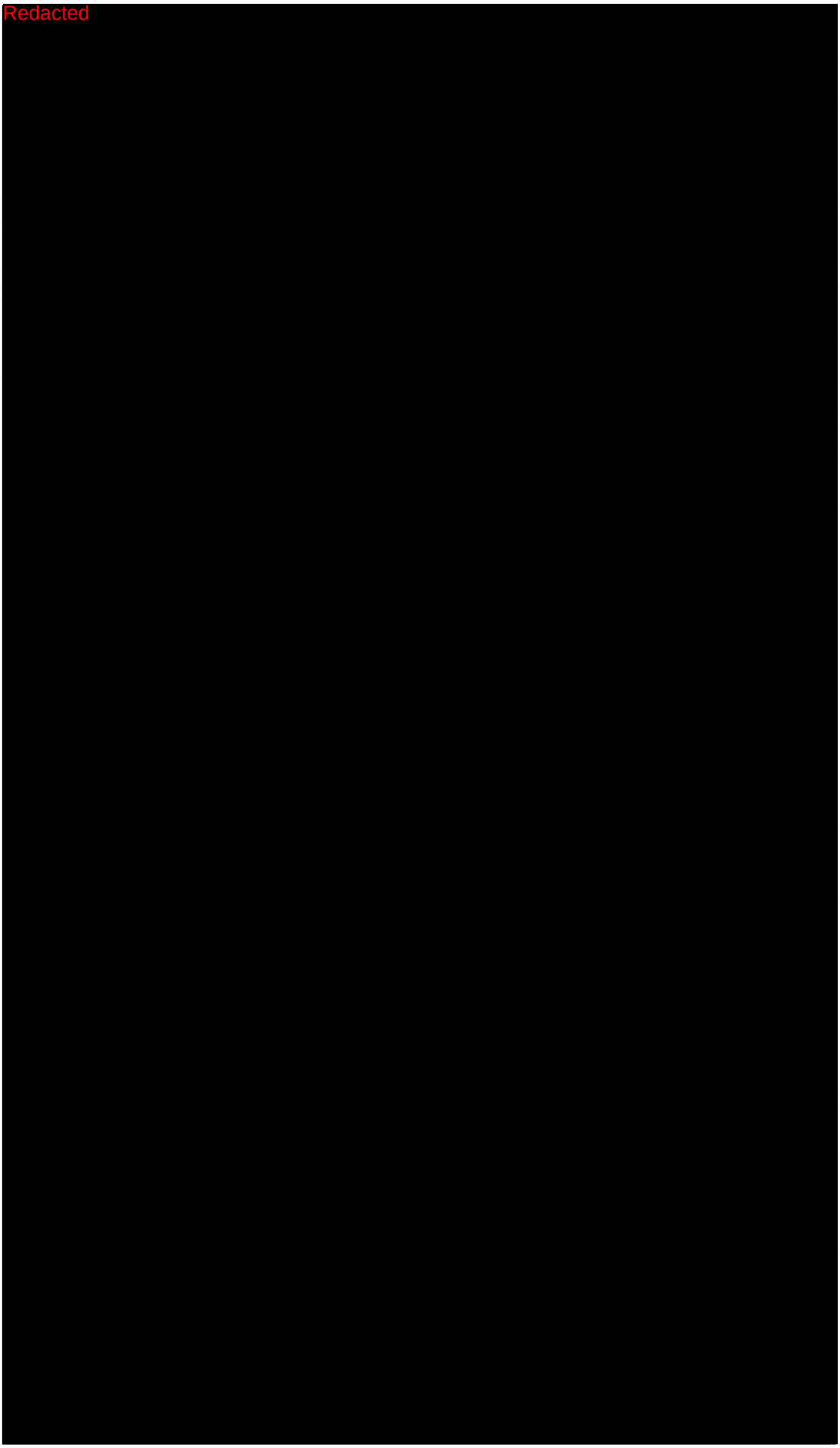
Redacted

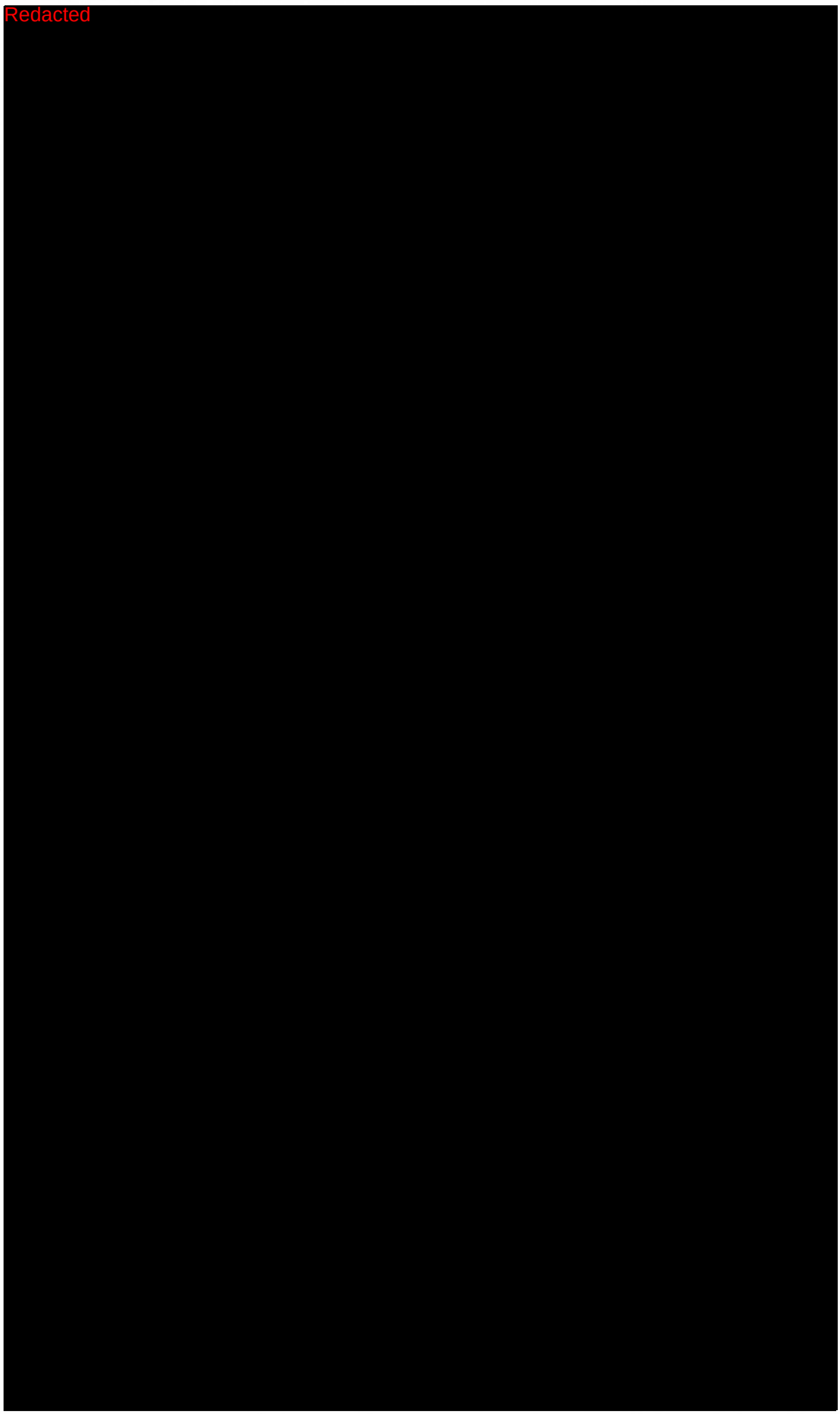
Redacted

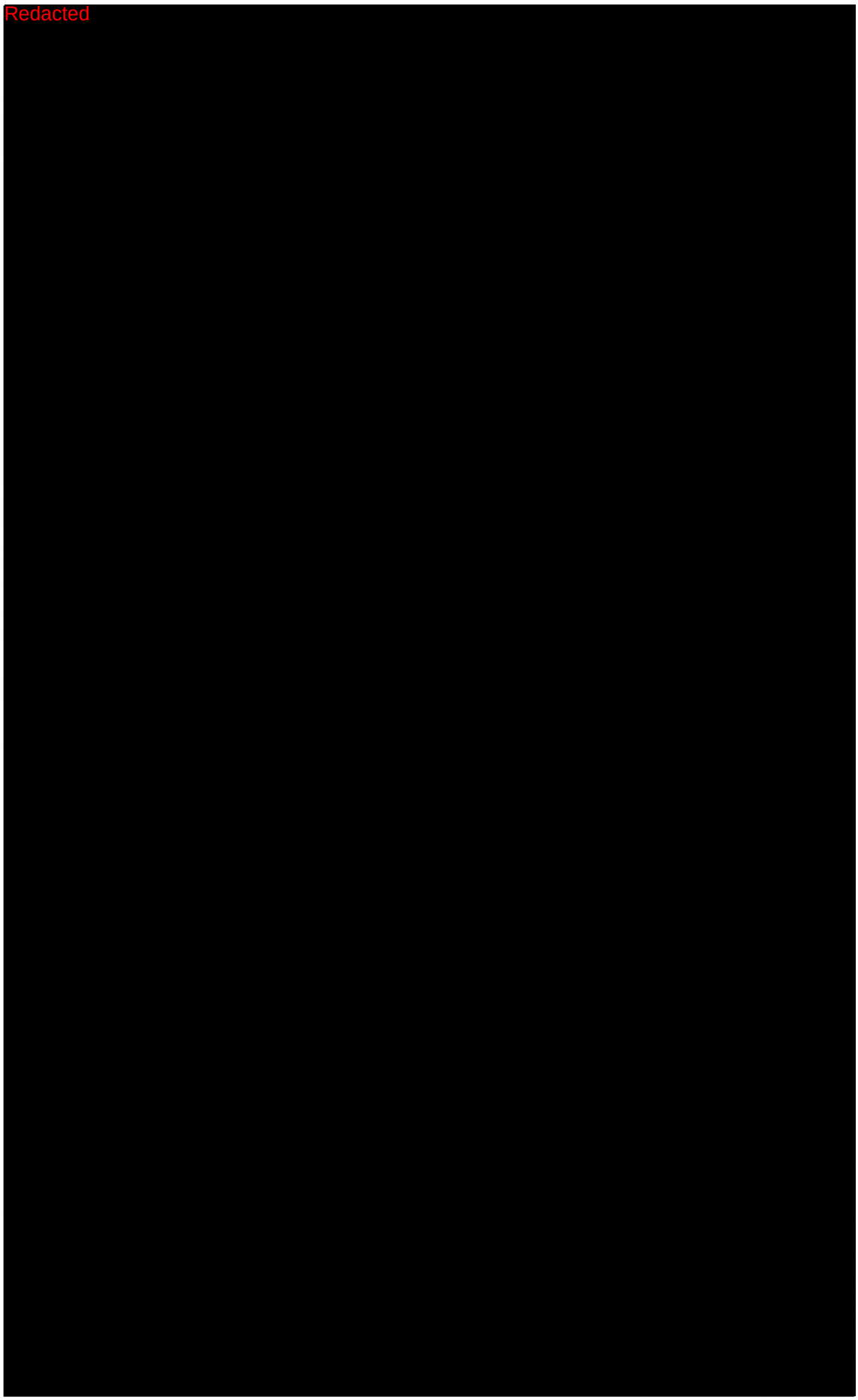
Redacted

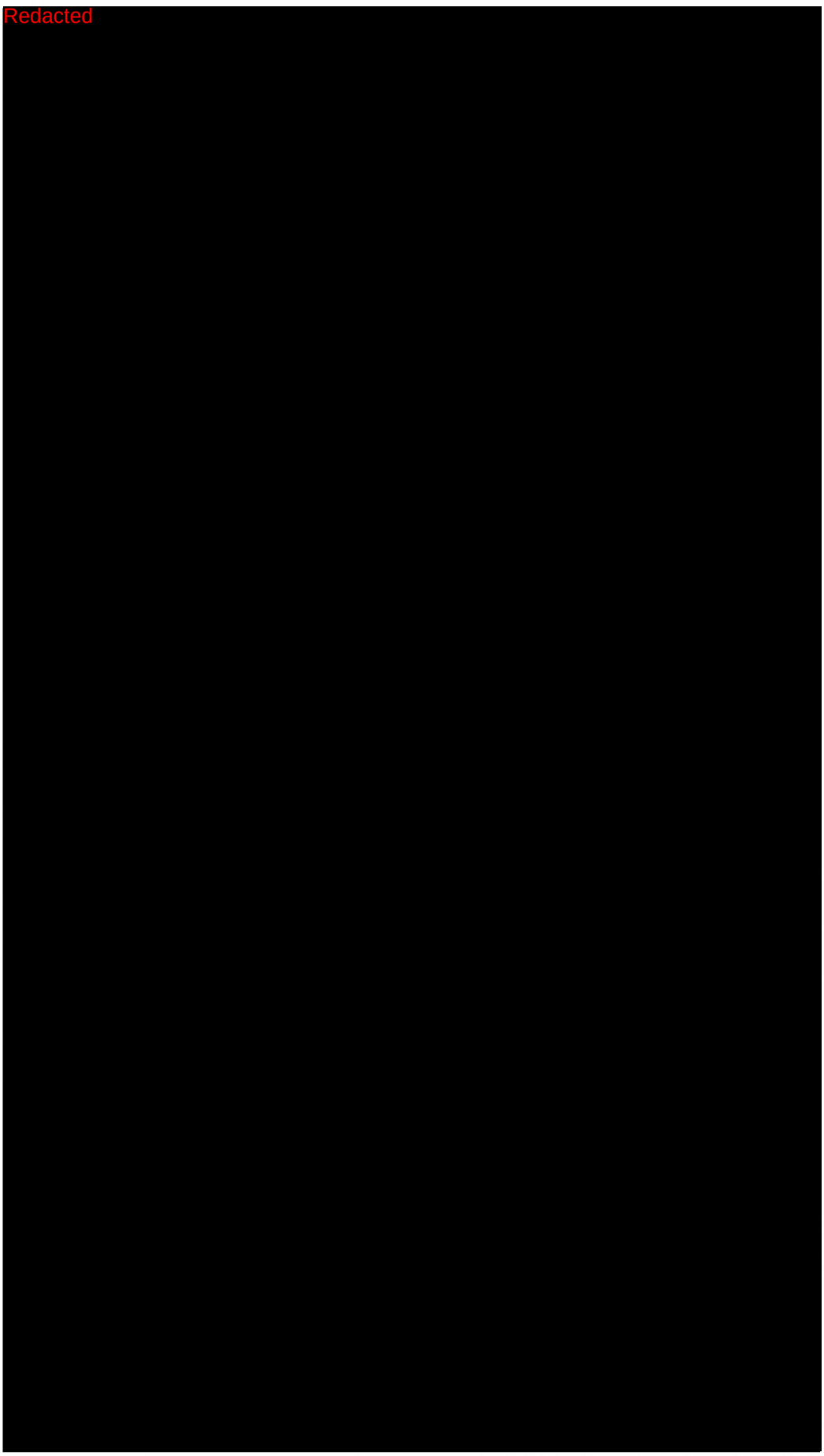
Redacted

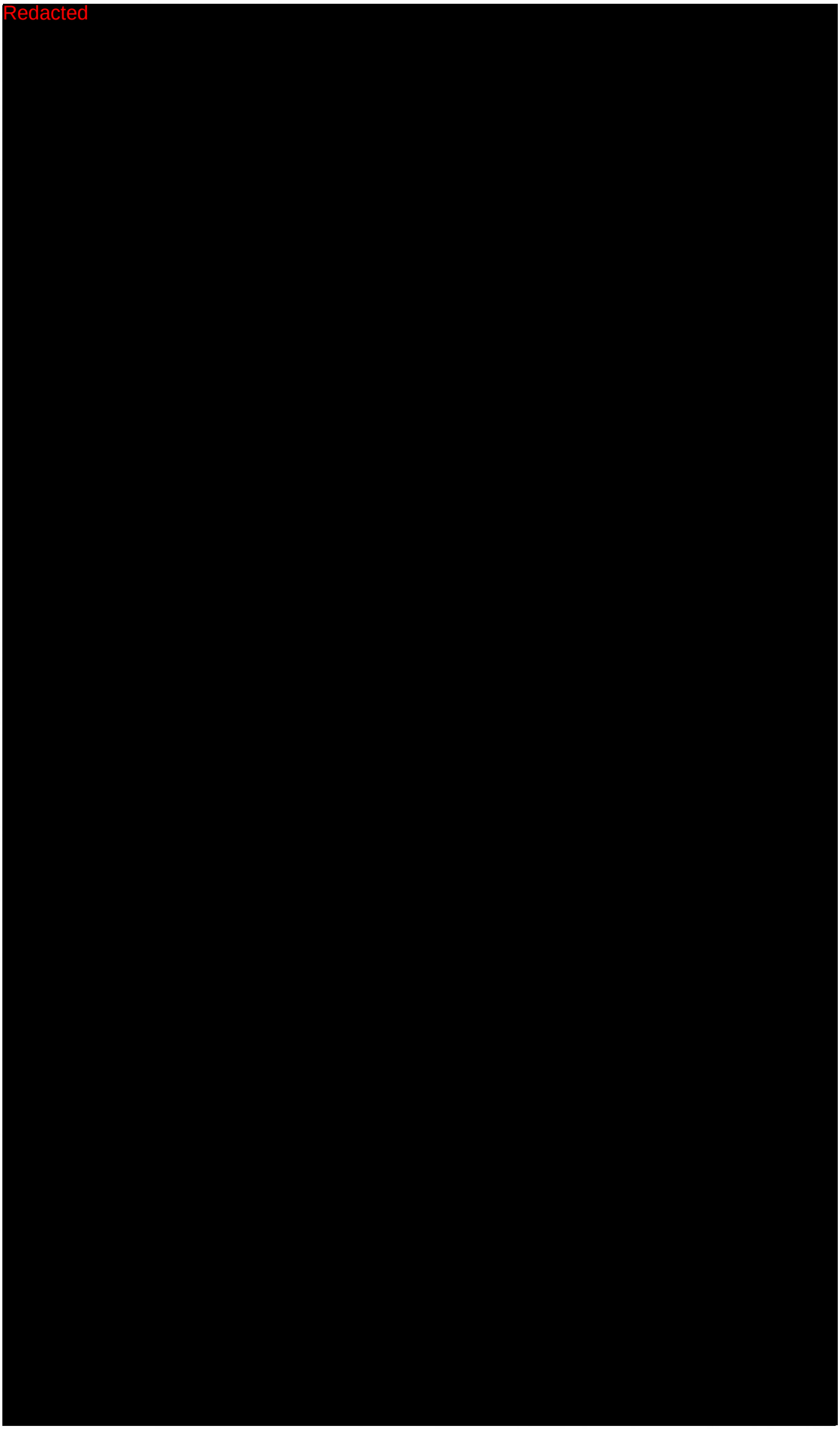
Redacted

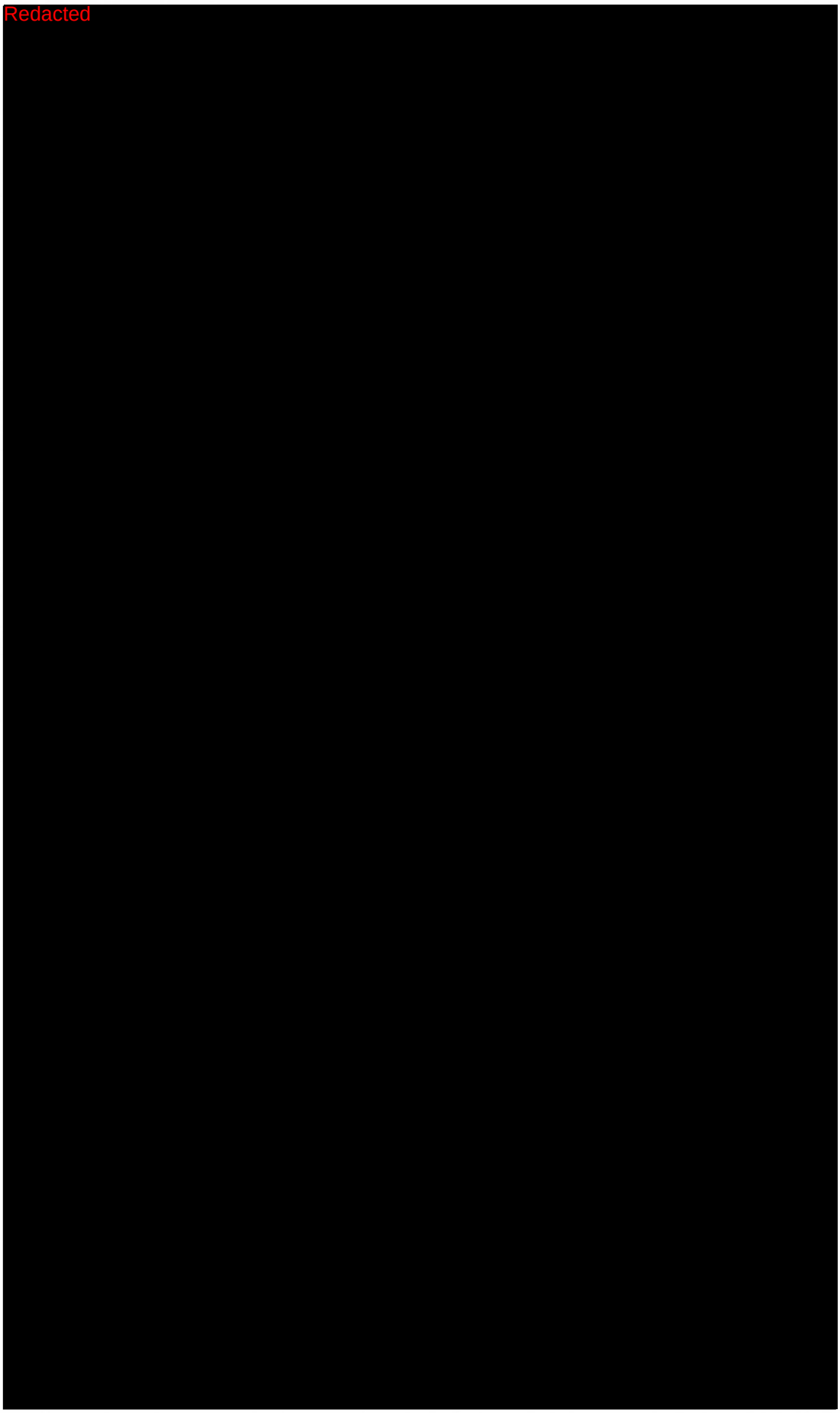
Redacted

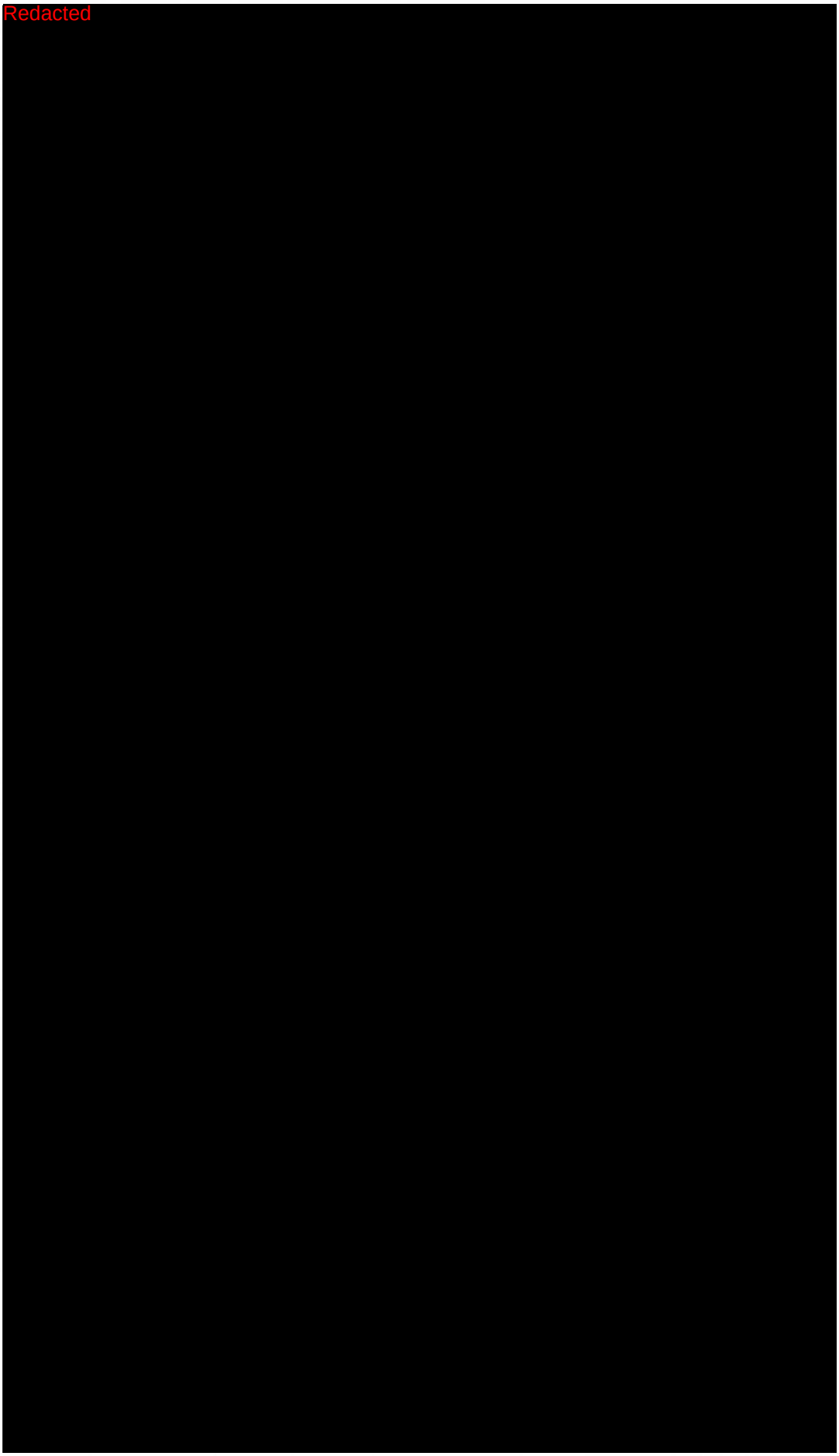
Redacted

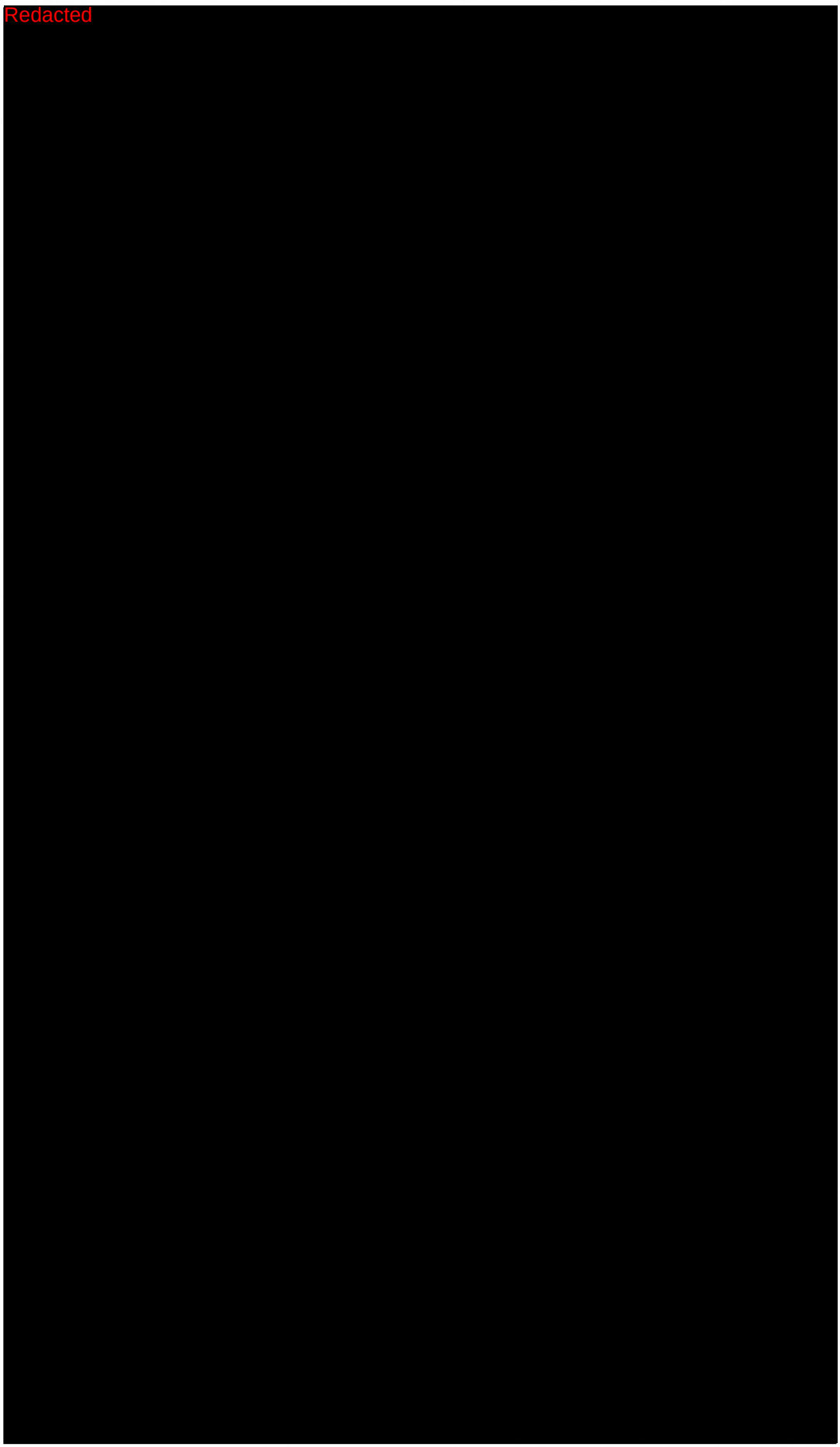
Redacted


Redacted

Appendix B

Drawings of experimental rig

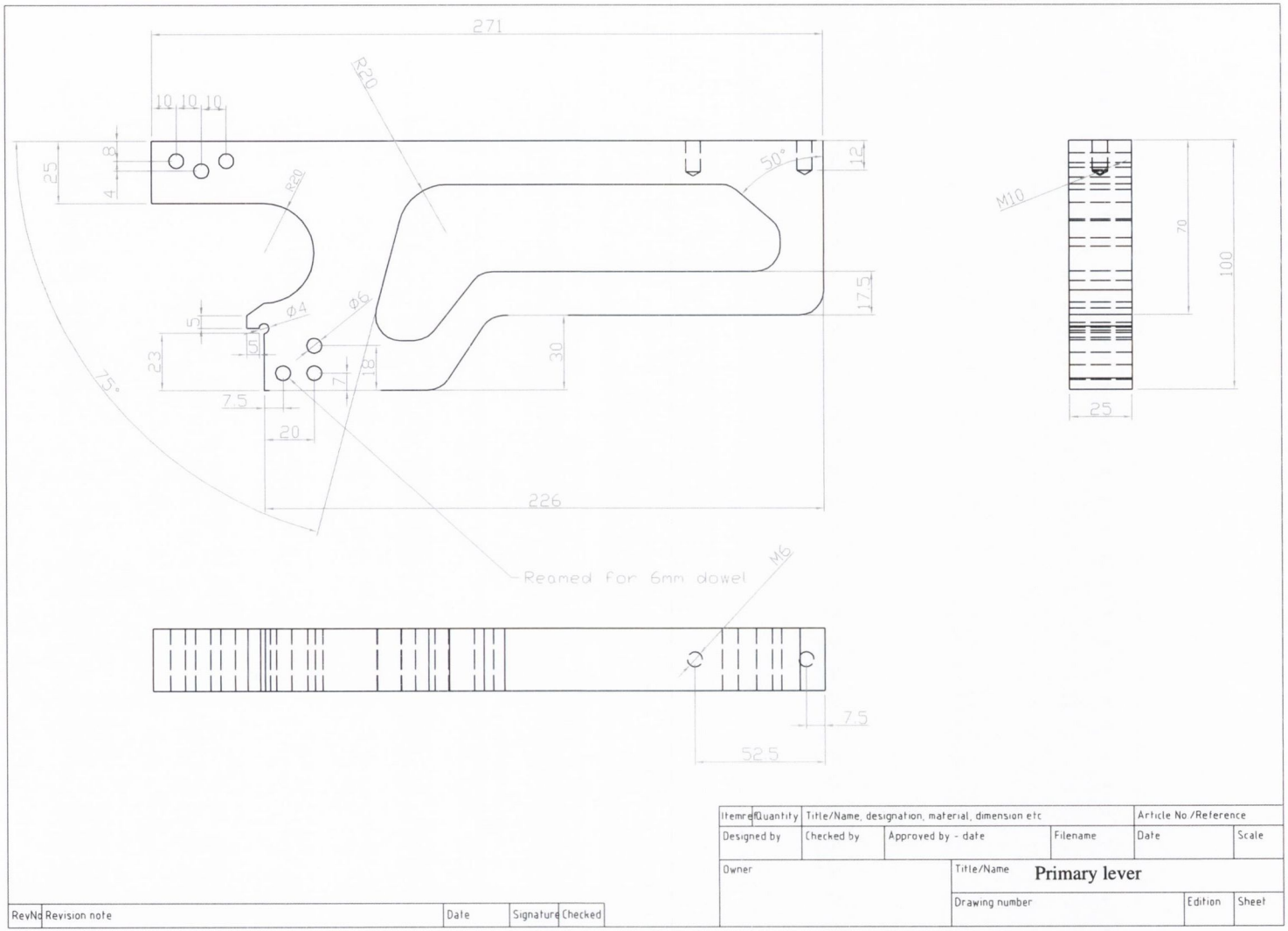

Item nr	Quantity	Title/Name, designation, material, dimension etc			Article No./Reference
Designed by	Checked by	Approved by - date	Filename	Date	Scale
Owner		Title/Name	Primary lever		
		Drawing number		Edition	Sheet

RevNo	Revision note	Date	Signature	Checked

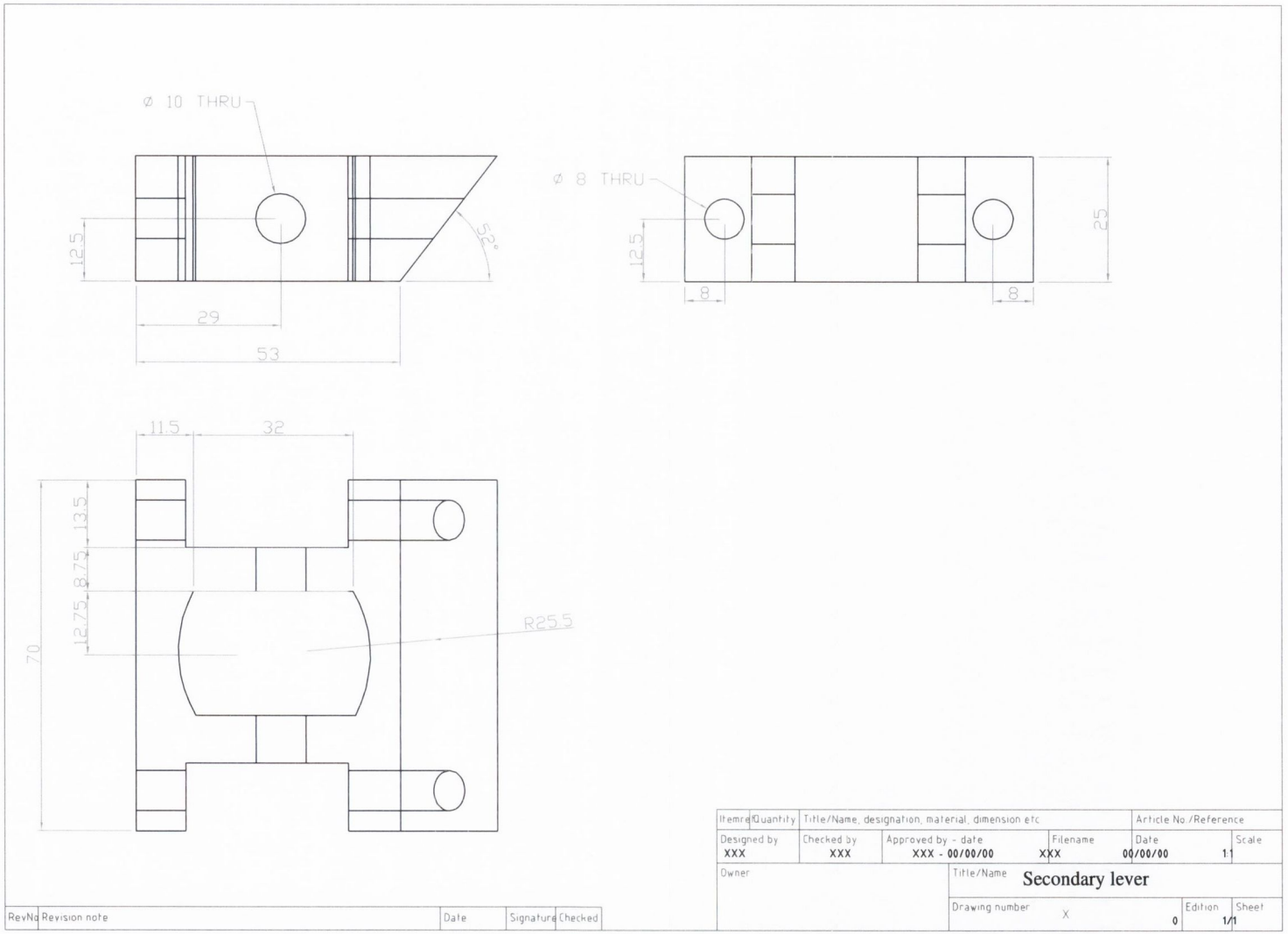
ø 10 THRU
ø 8 THRU
12.5
52°
29
53
12.5
25
8
8
11.5
32
13.5
8.75
12.75
R25.5
70
RevNo Revision note
Date
Signature
Checked
Item/ref Quantity
Title/Name, designation, material, dimension etc
Article No./Reference
Designed by
XXX
Checked by
XXX
Approved by - date
XXX - 00/00/00
Filename
XXX
Date
00/00/00
Scale
1:1
Owner
Title/Name
Secondary lever
Drawing number
X
0
Edition
Sheet
1/1

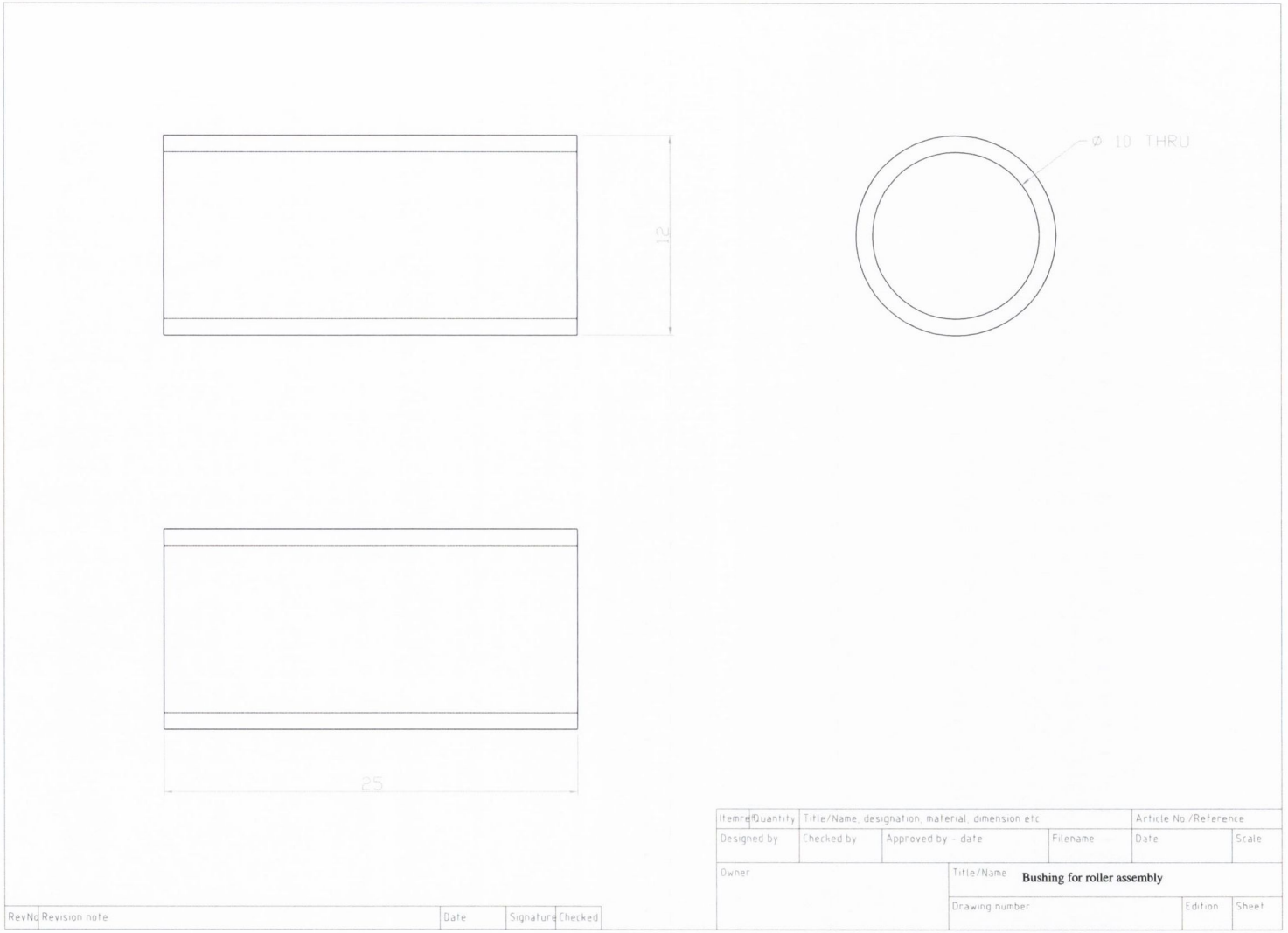
12
Ø 10 THRU
25
RevNo Revision note
Date
Signature Checked
Item nr Quantity Title/Name, designation, material, dimension etc
Article No./Reference
Designed by
Checked by
Approved by - date
Filename
Date
Scale
Owner
Title/Name
Bushing for roller assembly
Drawing number
Edition
Sheet

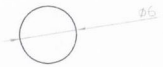

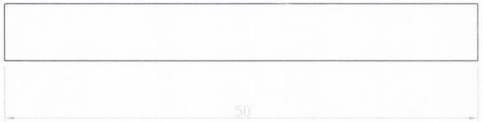

Item nr	Quantity	Title/Name, designation, material, dimension etc.			Article No./Reference	
Designed by		Checked by	Approved by - date	Filename	Date	Scale
Owner			Title/Name: **Dowel**			
			Drawing number		Edition	Sheet

Rev.No	Revision note	Date	Signature	Checked

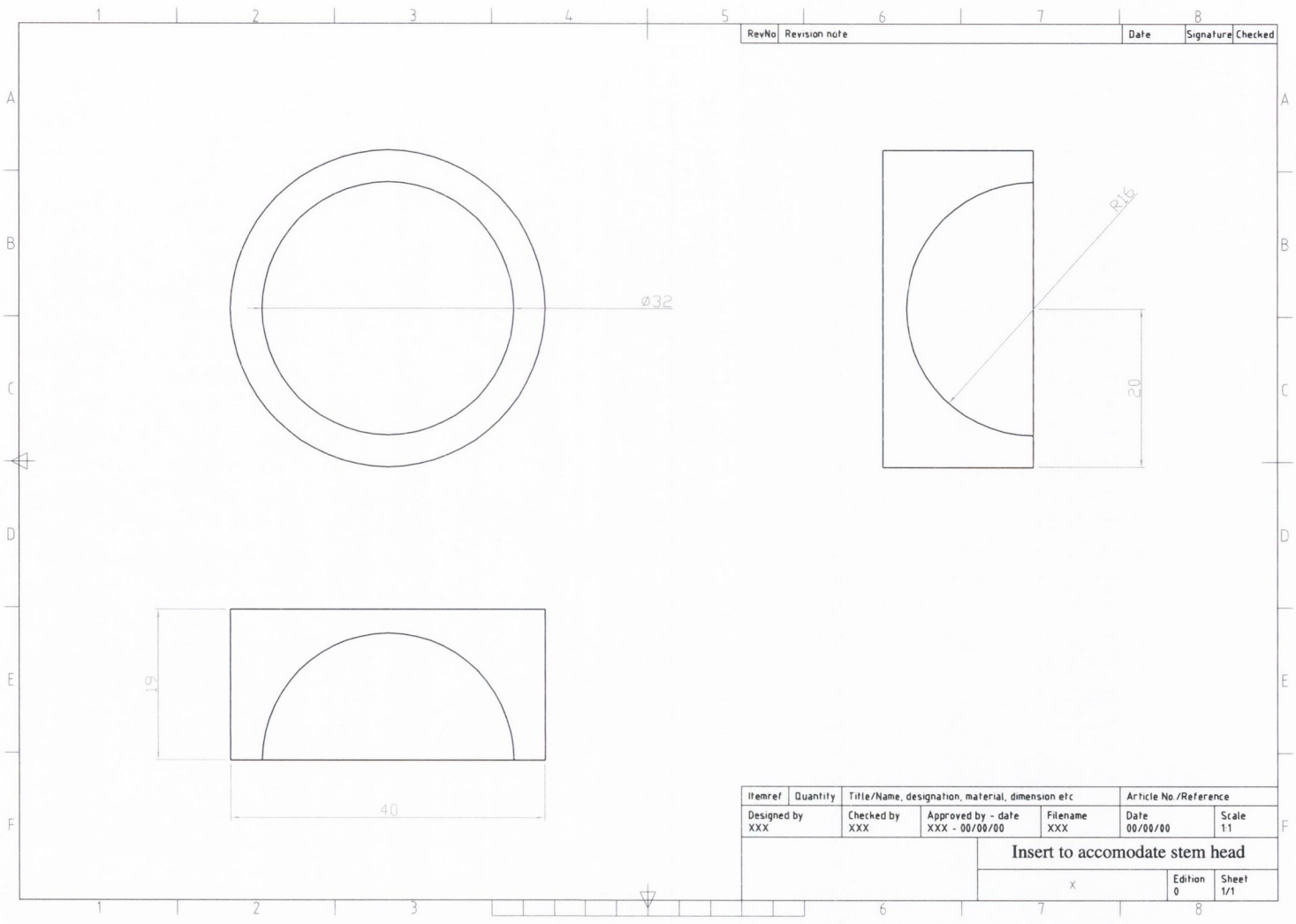
RevNo
Revision note
Date
Signature
Checked
Ø32
R16
20
19
40
Itemref
Quantity
Title/Name, designation, material, dimension etc
Article No./Reference
Designed by
XXX
Checked by
XXX
Approved by - date
XXX - 00/00/00
Filename
XXX
Date
00/00/00
Scale
1:1
Insert to accomodate stem head
x
Edition
0
Sheet
1/1

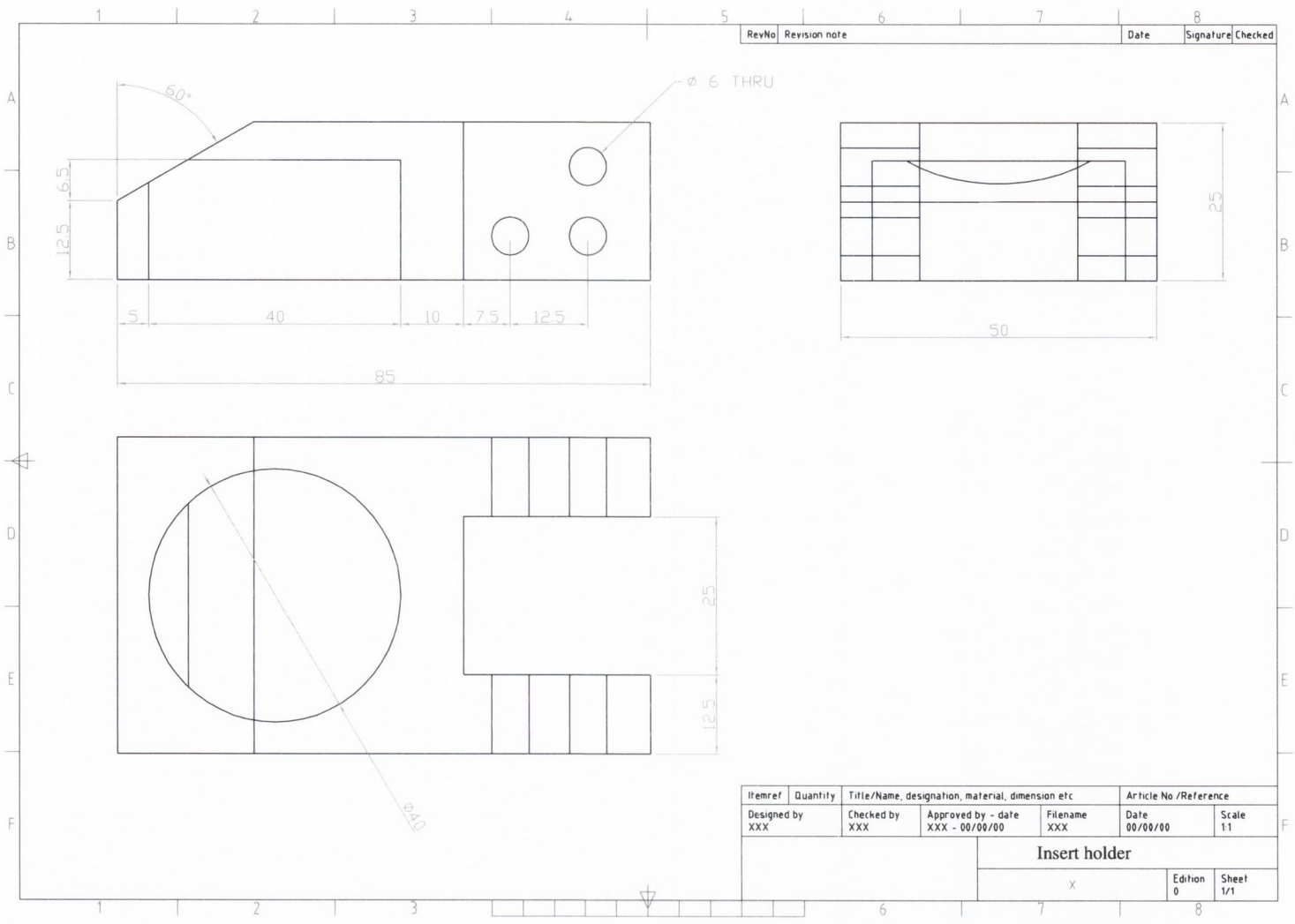
RevNo
Revision note
Date
Signature
Checked
60°
ø 6 THRU
6.5
12.5
5
40
10
7.5
12.5
85
25
50
25
12.5
ø40
Itemref
Quantity
Title/Name, designation, material, dimension etc
Article No./Reference
Designed by
XXX
Checked by
XXX
Approved by - date
XXX - 00/00/00
Filename
XXX
Date
00/00/00
Scale
1:1
Insert holder
X
Edition
0
Sheet
1/1

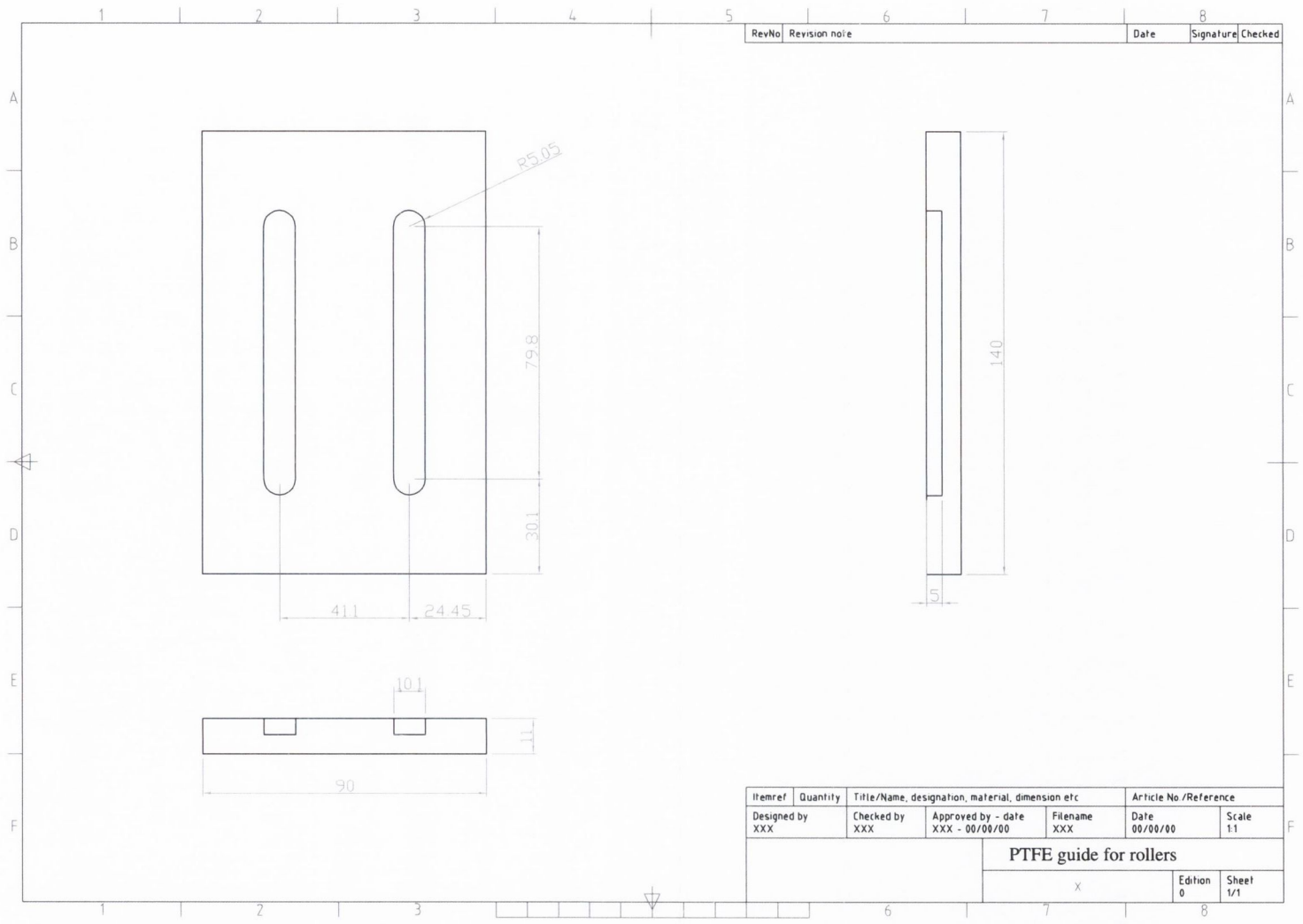
RevNo
Revision note
Date
Signature
Checked
R5.05
79.8
30.1
41.1
24.45
140
5
10.1
11
90
Itemref
Quantity
Title/Name, designation, material, dimension etc
Article No./Reference
Designed by
XXX
Checked by
XXX
Approved by - date
XXX - 00/00/00
Filename
XXX
Date
00/00/00
Scale
1:1
PTFE guide for rollers
X
Edition
0
Sheet
1/1

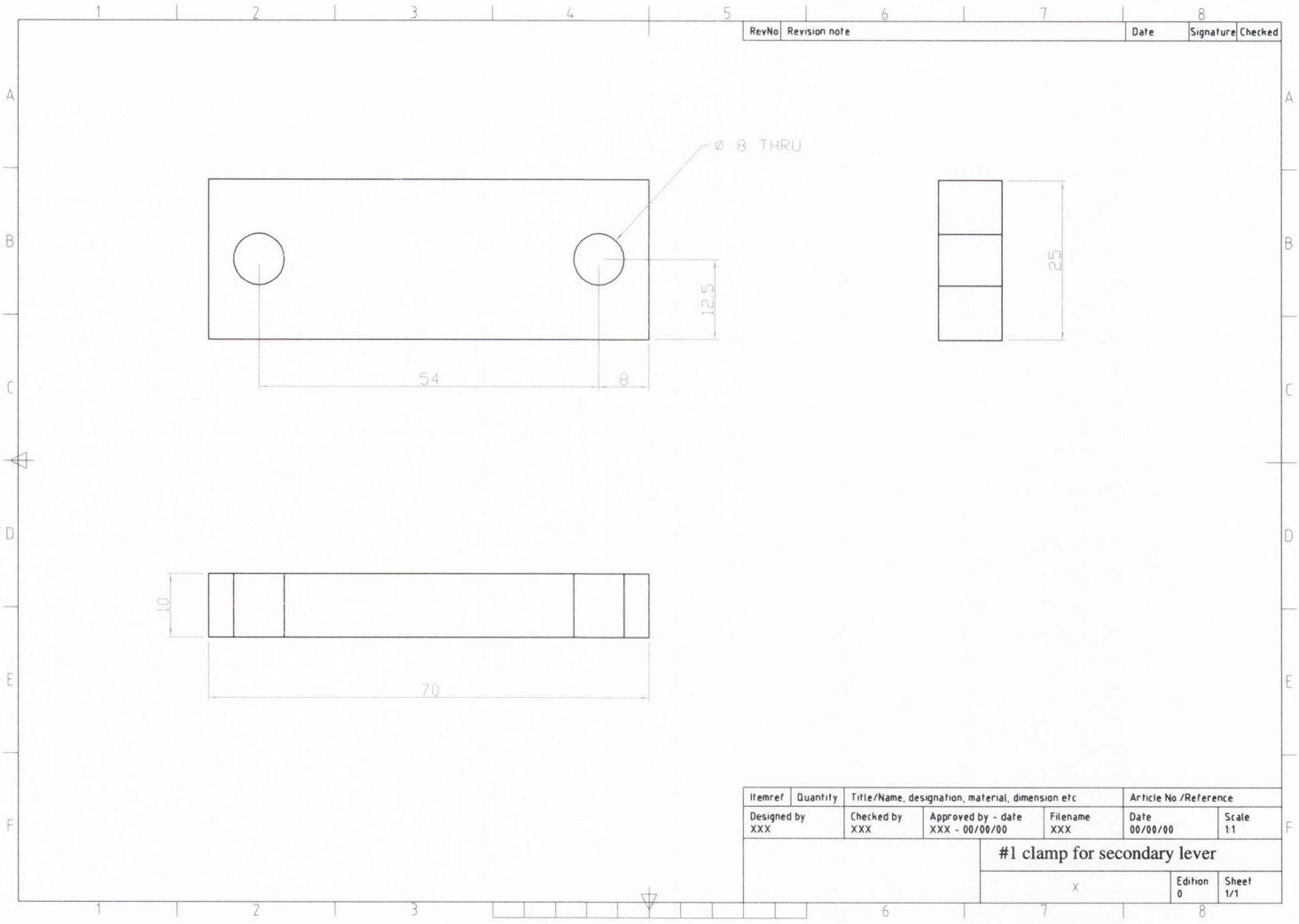
RevNo
Revision note
Date
Signature
Checked
Ø 8 THRU
12.5
54
8
25
10
70
Itemref
Quantity
Title/Name, designation, material, dimension etc
Article No./Reference
Designed by
XXX
Checked by
XXX
Approved by - date
XXX - 00/00/00
Filename
XXX
Date
00/00/00
Scale
1:1
#1 clamp for secondary lever
X
Edition
0
Sheet
1/1

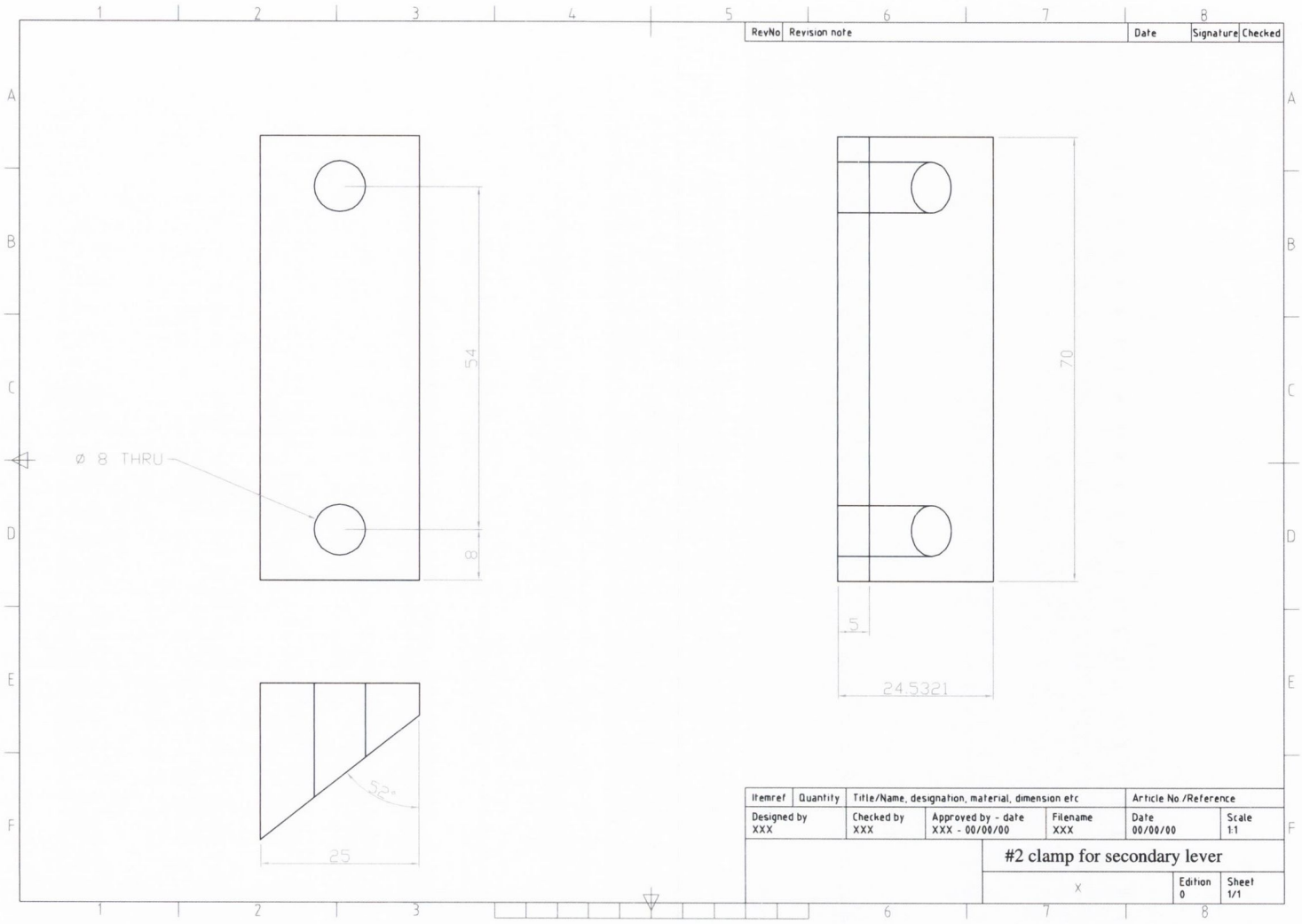
RevNo
Revision note
Date
Signature
Checked
ø 8 THRU
54
8
70
5
24.5321
52°
25
Itemref
Quantity
Title/Name, designation, material, dimension etc
Article No./Reference
Designed by
XXX
Checked by
XXX
Approved by - date
XXX - 00/00/00
Filename
XXX
Date
00/00/00
Scale
1:1
#2 clamp for secondary lever
x
Edition
0
Sheet
1/1

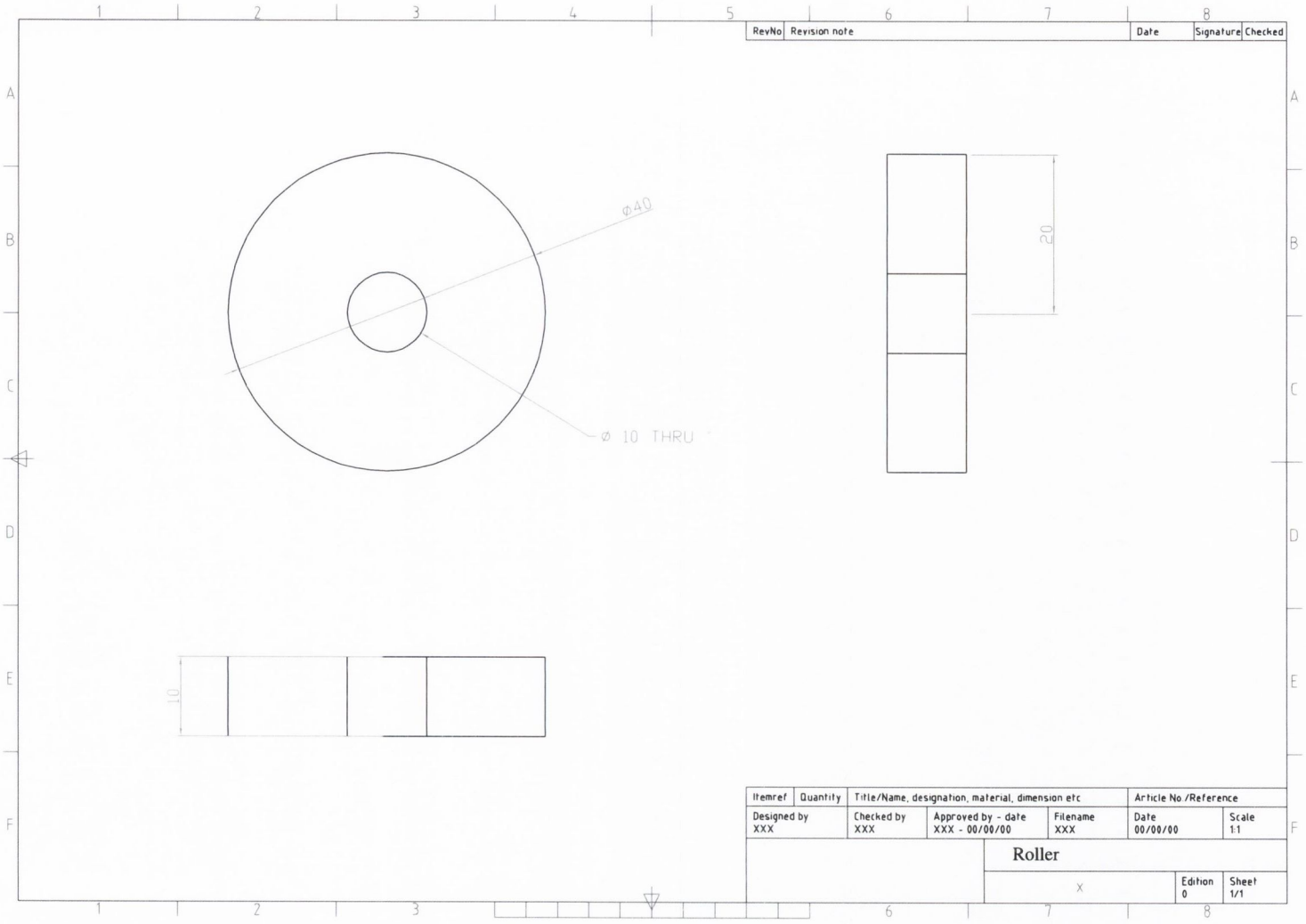
RevNo
Revision note
Date
Signature
Checked
φ40
ø 10 THRU
20
10
Itemref
Quantity
Title/Name, designation, material, dimension etc
Article No./Reference
Designed by
XXX
Checked by
XXX
Approved by - date
XXX - 00/00/00
Filename
XXX
Date
00/00/00
Scale
1:1
Roller
X
Edition
0
Sheet
1/1

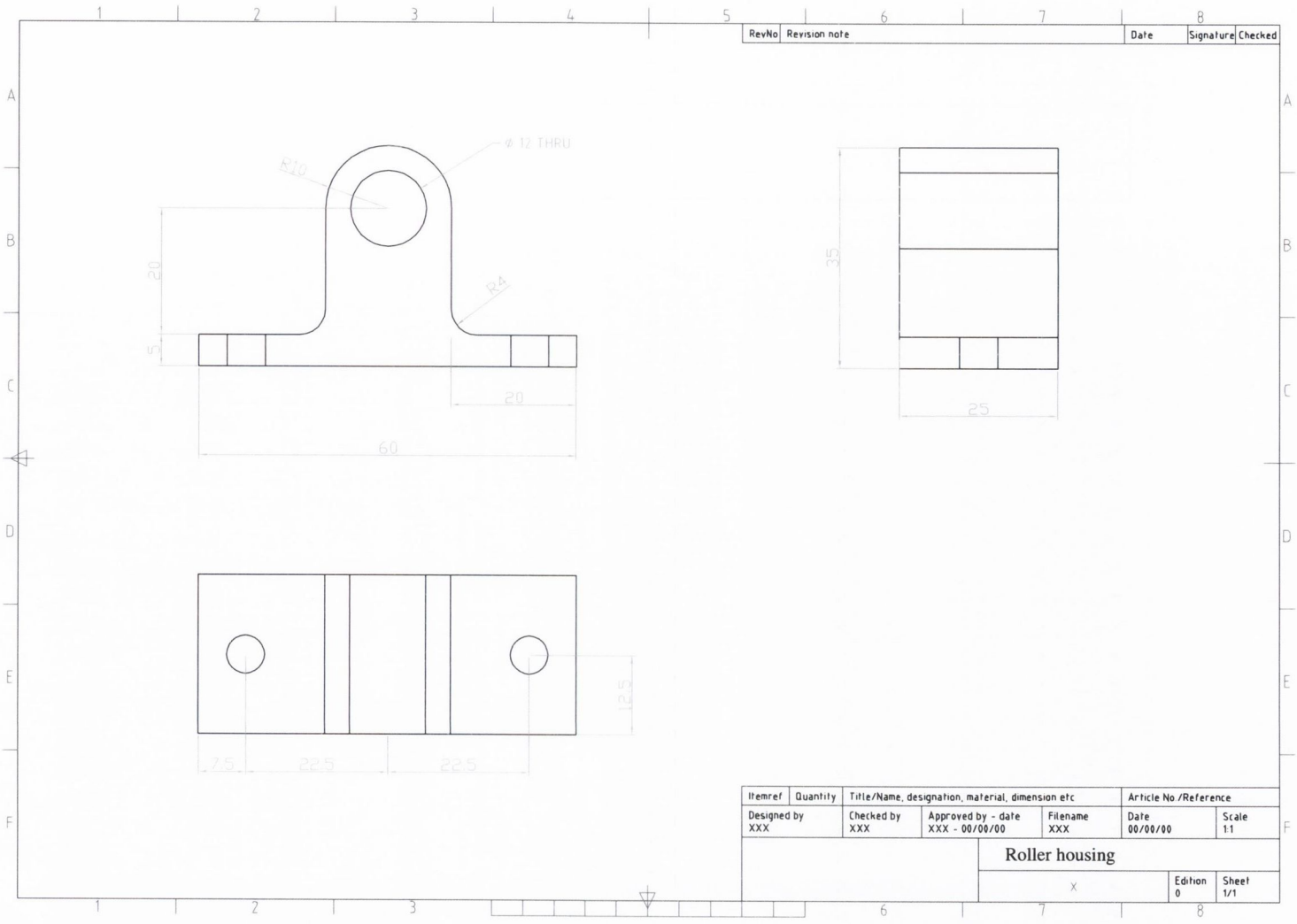
RevNo
Revision note
Date
Signature
Checked
Ø 12 THRU
R10
R4
20
5
60
35
25
12.5
7.5
22.5
22.5
Itemref
Quantity
Title/Name, designation, material, dimension etc
Article No /Reference
Designed by
XXX
Checked by
XXX
Approved by - date
XXX - 00/00/00
Filename
XXX
Date
00/00/00
Scale
1:1
Roller housing
X
Edition
0
Sheet
1/1

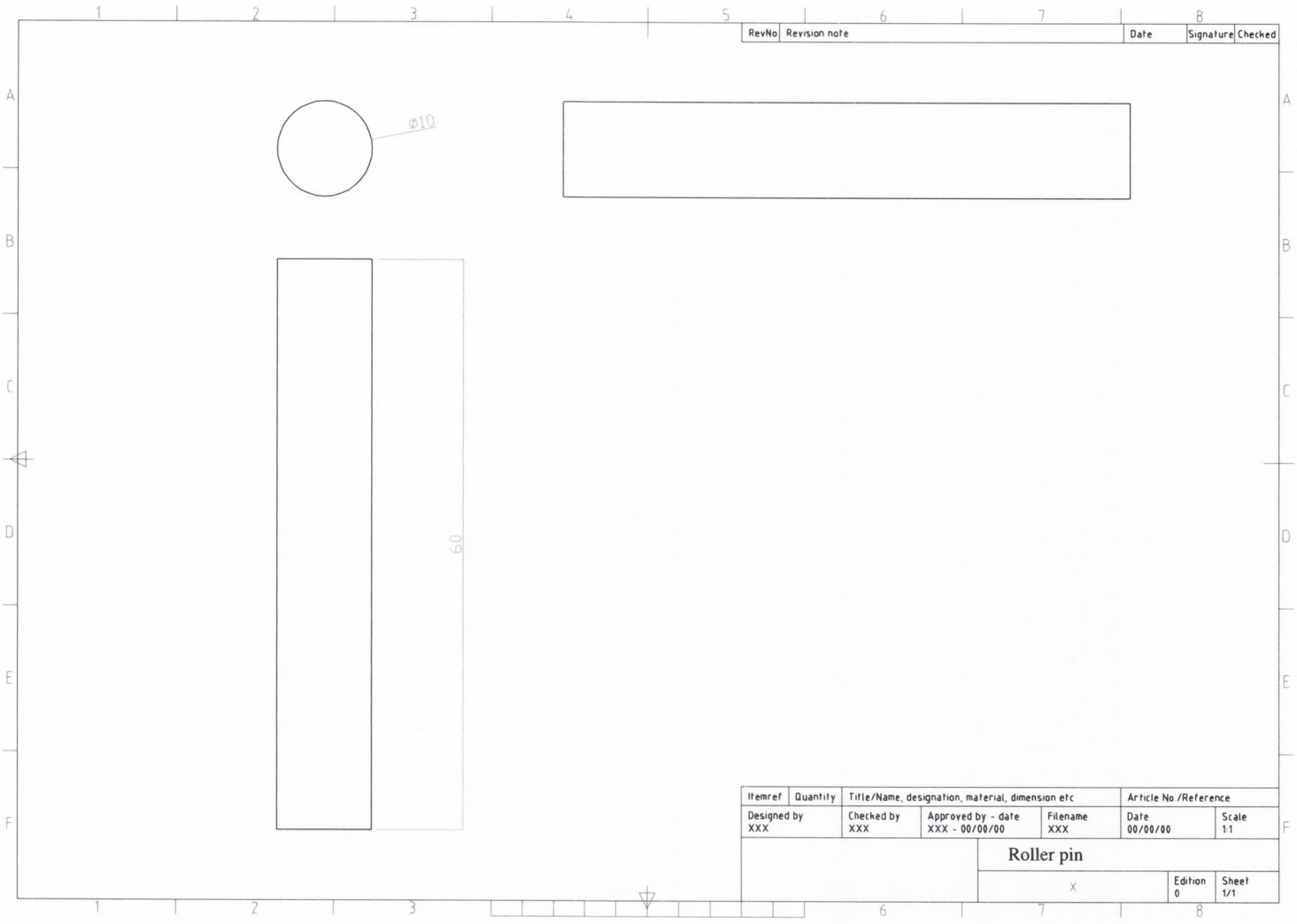
RevNo
Revision note
Date
Signature
Checked
ø10
60
Itemref
Quantity
Title/Name, designation, material, dimension etc
Article No /Reference
Designed by
XXX
Checked by
XXX
Approved by - date
XXX - 00/00/00
Filename
XXX
Date
00/00/00
Scale
1:1
Roller pin
X
Edition
0
Sheet
1/1

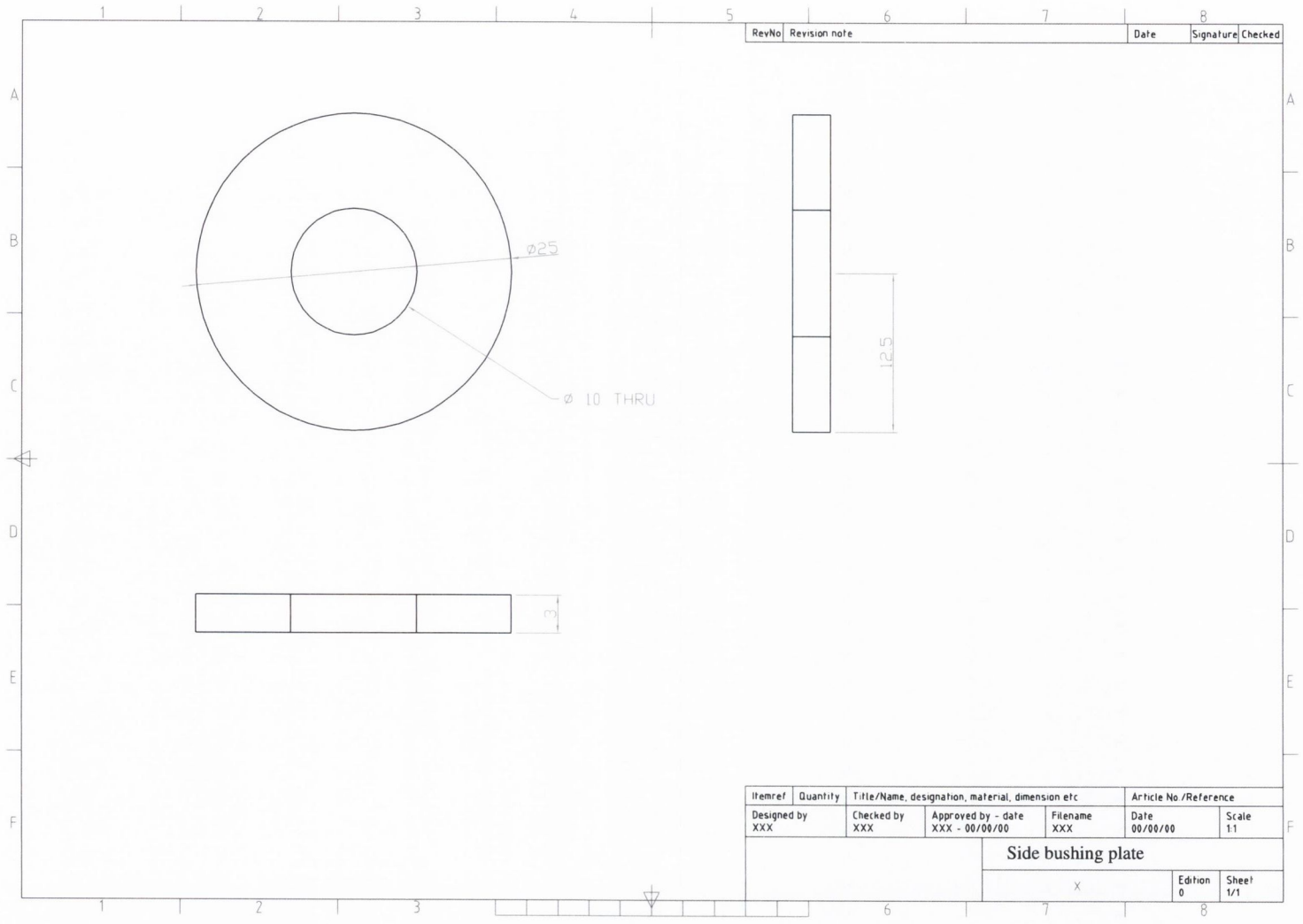
RevNo
Revision note
Date
Signature
Checked
ø25
ø 10 THRU
12.5
3
Itemref
Quantity
Title/Name, designation, material, dimension etc
Article No /Reference
Designed by
XXX
Checked by
XXX
Approved by - date
XXX - 00/00/00
Filename
XXX
Date
00/00/00
Scale
1:1
Side bushing plate
X
Edition
0
Sheet
1/1

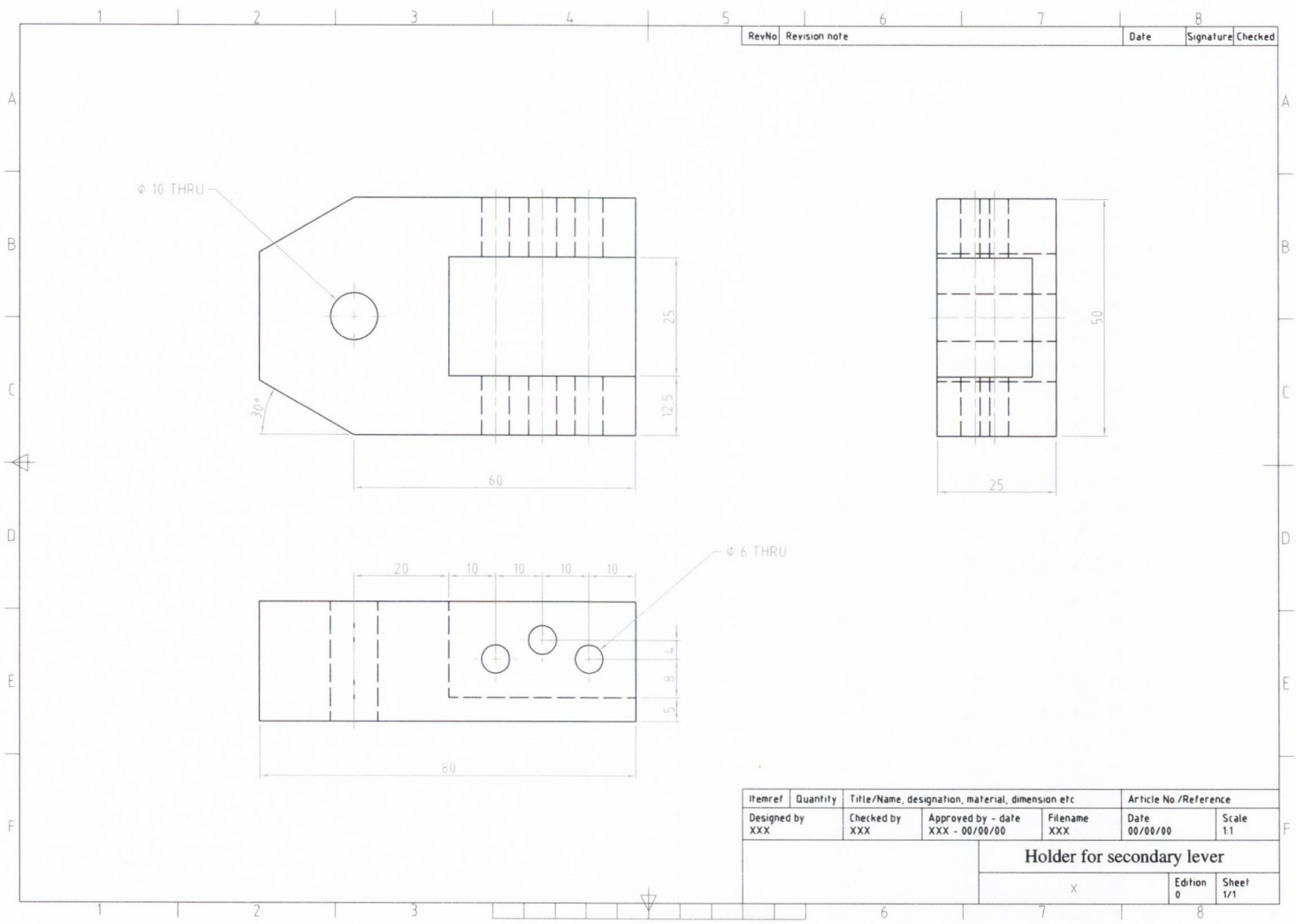
RevNo
Revision note
Date
Signature
Checked
ϕ 10 THRU
25
12.5
30°
60
50
25
ϕ 6 THRU
20
10
10
10
10
14
8
5
80
Itemref
Quantity
Title/Name, designation, material, dimension etc
Article No./Reference
Designed by
XXX
Checked by
XXX
Approved by - date
XXX - 00/00/00
Filename
XXX
Date
00/00/00
Scale
1:1
Holder for secondary lever
X
Edition
0
Sheet
1/1

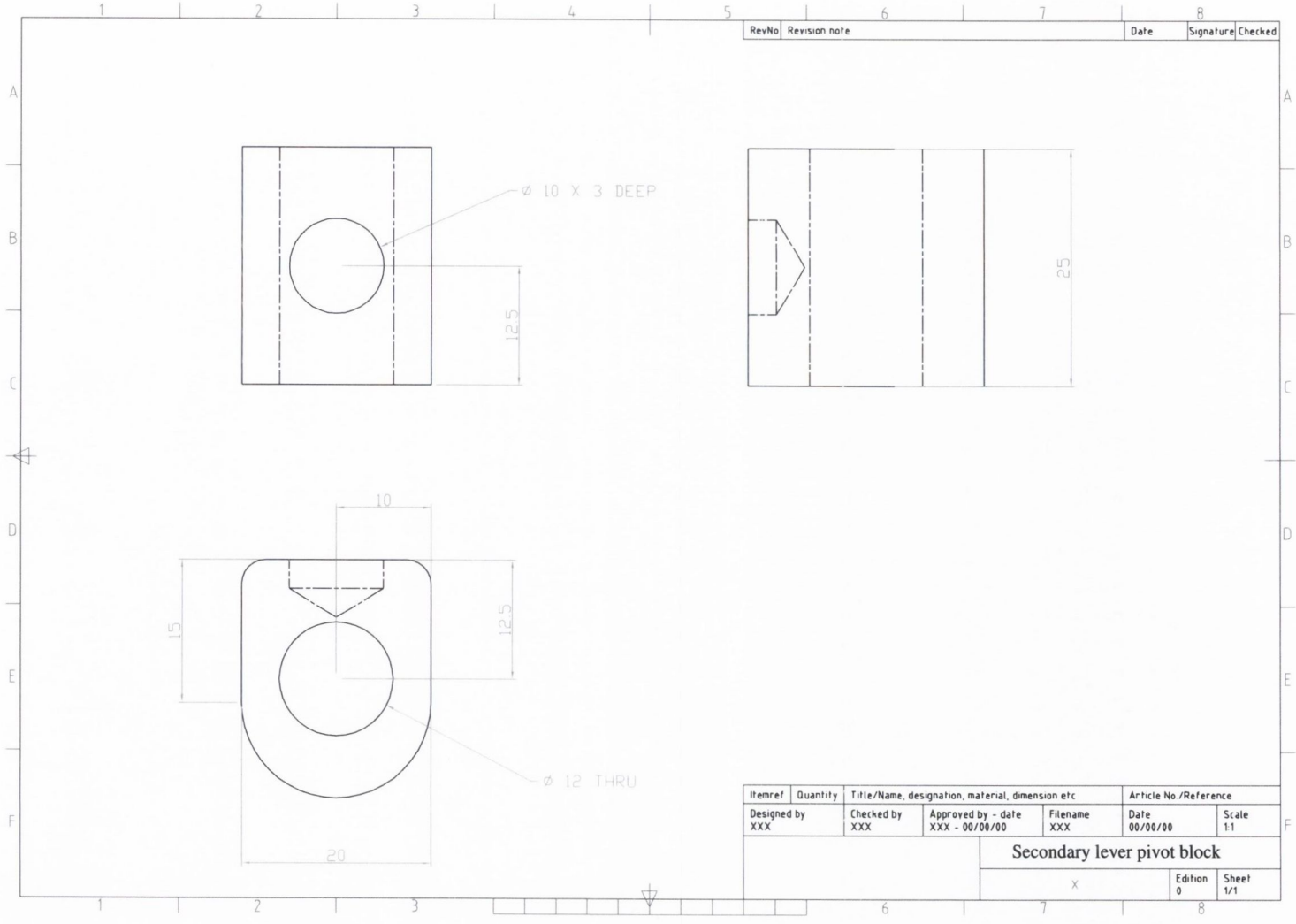
RevNo
Revision note
Date
Signature
Checked
Ø 10 X 3 DEEP
12.5
25
10
15
12.5
Ø 12 THRU
20
Itemref
Quantity
Title/Name, designation, material, dimension etc
Article No /Reference
Designed by
XXX
Checked by
XXX
Approved by - date
XXX - 00/00/00
Filename
XXX
Date
00/00/00
Scale
1:1
Secondary lever pivot block
x
Edition
0
Sheet
1/1